Universidade Federal do Rio Grande – FURG

Instituto de Oceanografia

Programa de Pós-Graduação em Oceanologia

VIABILIDADE OPERACIONAL DA INSTALAÇÃO DE USINAS DE CONVERSÃO DE ENERGIA TÉRMICA EM ELÉTRICA NA AMAZÔNIA AZUL BRASILEIRA

Roberto Valente de Souza

Tese apresentada a Coordenação do Programa de Pós-Graduação em Oceanologia como requisito parcial para a obtenção do título de Doutor

Orientadora: *Profª. Drª.* ELISA HELENA FERNANDES
Universidade Federal do Rio Grande (FURG), Brasil

Coorientador: *Prof. Dr.* JOSÉ LUIZ DIAS AZEVEDO
Universidade Federal do Rio Grande (FURG), Brasil

Rio Grande, RS, Brasil

Junho, 2019.

VIABILIDADE OPERACIONAL DA INSTALAÇÃO DE USINAS DE CONVERSÃO DE ENERGIA TÉRMICA EM ELÉTRICA NA AMAZÔNIA AZUL BRASILEIRA

Tese apresentada ao Programa de Pós-Graduação em Oceanologia, como parte dos requisitos para a obtenção do Título de Doutor

por

ROBERTO VALENTE DE SOUZA

Rio Grande, RS, Brasil

Junho, 2019.

VALENTE, ROBERTO DE SOUZA

Viabilidade de conversão de energia térmica em elétrica na Amazônia Azul Brasileira/ Roberto Valente de Souza. – Rio Grande: FURG, 2019.

Número de páginas 122p.

Tese (Doutorado) – Universidade Federal do Rio Grande. Mestrado/Doutorado em Oceanologia. Área de Concentração: Física dos Oceanos e Clima.

Palavra-chave 1. Energia Renovável. 2.Energia térmica. 3.HYCOM 4. Amazônia Azul 5. Viabilidade 6. OTEC 7. OTEP 8.IAE

ATA DE DEFESA

Agradecimentos

Primeiramente, gostaria de ressaltar minha mãe, Maria Helena Valente de Souza por todo amor, paciência, confiança, suporte e exemplo de vida. Em especial, gostaria de agradecer à minha mulher, Mariana dos Santos Passos, por todo amor e perseverança, sempre me puxando para frente e nunca me deixando desistir dos meus objetivos e coautora do meu segundo artigo. Destacando ambas como estrelas que me iluminam nos momentos de escuridão.

A todos os meus irmãos, que mesmo com os contratempos e brigas, me mandaram energia positiva e nunca desistiram de mim. Ao meu Padrasto, Sogro e Sogra, por todos os carinhos, cuidados, amizade e querer bem para comigo. Aos meus afilhados, Nicolas Francisco de Souza, Sophia Esquerdo Passos e Otávio Furtado de Souza, por todo amor, alegria e de ver meu caminho de estudos como exemplo. Todos vocês são aqueles que fazem parte deste ciclo, mas não foram citados, tem uma parcela significativa nessa conquista.

À minha Orientadora, a Dr(a) Elisa Fernandes, por ter tido papel importantíssimo em um momento delicado, que poderia ter me afastado da Academia, a oportunidade de dar sequência ao meu trabalho e permitir que ele alcance maiores patamares, além da ajuda mutua em finalizar etapas, desafios e dos momentos de descontração com o pessoal do laboratório. Ao meu coorientador, Dr. José Luiz Azevedo, pelo os momentos de discussão científica, construção de pensamento e pela acessibilidade como professor, pesquisador, incentivador e amizade. Aos meus grandes amigos Pablo e Daniel, incluídos no parágrafo anterior, mas que me fazem sentir em família longe de casa. E também aos meus companheiros do LOCOSTE, submetidos a este louco, de bom coração, humor estranho e comunicação contundente, pelos ouvidos por todos esses anos, e pela possibilidade de fazer parte de um verdadeiro e digno, grupo de amigos pesquisadores com ótimo ambiente de laboratório.

A todos os meus amigos, que por mais tempo ou distância que estiveram,

representam uma fagulha da construção da fogueira do meu ser, através de amor, companheirismo e suporte ao longo da minha longa jornada acadêmica, em especial para a minha turma da física, eternos camaradas de alma pura.

À toda Coordenação de Aperfeiçoamento de Pessoal de Ensino Superior (CAPES) pelo apoio, bolsa de estudos concedida e ao incentivo da educação de qualidade no Brasil .

Índice

Lista de Figuras

ARTIGO I

ARTIGO II

Lista de Tabelas

Lista de Acrônimos e Abreviaturas

A

AA - Azul (Blue Amazon)

ACAS - Água Central do Atlântico Sul (South Atlantic Central Water)

AIA - Água Intermediária Antártica (Intermediate Water Antarctica)

AL- Alagoas

APAN - Água Profunda do Atlântico Norte (Deep North Atlantic Water)

AS - Atlântico Sul (South Atlantic)

AT - Água Tropical (Tropical Water)

B

BA - Bahia

BT - Bati-Termógrafos

C

CB - Corrente do Brasil (Brazilian Current).

CE - Ceará (CE).

CNB - Corrente Norte do Brasil (Brazil's North Current)

CWP - Cold Water Pipe (tubo de água fria)

CSE - Corrente Sul Equatorial ()

CTD - Conductivity, Temperature and Depth (Condutividade, Temperatura e Profundidade)

E

EIA - Efeito Antropogênico Inverso (Inverse Anthrogenic Effect)

G.

GODAE - Global Ocean Data Assimilation Experiment (Experiência Global de Assimilação de Dados do Oceano)

H

HWP - Hot Water Pipe (tubulação de água quente),

HYCOM - hybrid Coordinated Ocean Model (Modelo Oceânico de Coordenadas Hibridas),

I

IPCC – Intergovernmental Panel on Climate Change **(**Painel Intergovernamental de Mudanças Climáticas)

J

JC - Julian Climatology (Climatogia Juliana)

M.

MA - Maranhão

N

NACW - North Atlantic Central Water (Àgua Central do Atlântico Norte)

NOPP - National Oceanographic Partnership Program (Programa de Parceria Oceanográfica Nacional),

NE - Northeast (Nordeste)

O

OEMT – OTEC Energy Module Theoretical (Módulo de Energia OTEC Teórica)

ONU - Organização das Nações Unidas (United Nations Organization)

OTEC - Ocean Thermal Energy Conversion (Conversão de Energia Térmica Oceânica)

OTEP - Ocean Thermal Energy Park (Parque de Energia Térmica Oceânica)

P

PI - Piauí

PE - Pernambuco

PB - Paraíba

R

RN - Rio Grande do Norte

S

SE - Sergipe

SST - Sea Surface Temperature (Temperatura da Superfície do Mar)

U

UNCLS - United Nations Convention on the Law of the Sea (Convenção das Nações Unidas sobre o Direito do Mar)

Resumo

A busca por alternativas energéticas de alta tecnologia que causem menor impacto ambiental é cada vez mais presente no plano estratégico de desenvolvimento de diversos países, pois o acelerado crescimento econômico e populacional mundial tem pressionado significativamente a demanda por energia em escala global. Atualmente existe uma grande diversidade de conceitos e tecnologias em competição no campo da conversão da energia dos oceanos em energia elétrica. Destaque deste trabalho foi dado para a energia dos gradientes térmicos, a qual possui o maior potencial de exploração nos oceanos, com cerca de 40 bilhões de MW. Uma das principais vantagens desse tipo de usina é que sua fonte de energia é vasta, naturalmente renovável e não poluente. Neste estudo os resultados obtidos indicam a variabilidade espacial e temporal do gradiente térmico vertical no Atlântico Sul e em especial na Amazônia Azul, a definição de uma Parque de Energia Térmica oceânica (PETO) Brasileira, a variabilidade do parque nos seus parâmetros de controle e a produção de energia elétrica de usinas de conversão de energia térmica oceânica e sua possibilidade de realizar o Efeito Antropogênico Inverso (EIA); na forma matricial para o oceano Atlântico Sul. Além disso, foi aplicada a usina OTEC de forma pontual, verificando-se os mesmos itens listados para os principais sítios energéticos do parque (regiões de maior potência) em relação a sua viabilidade operacional (relação entre superfície e as profundidades que podem configurar o gradiente térmico vertical)

Palavras-chave*:* Energia Renovável, Energia térmica, Hycom, Viabilidade, Amazônia Azul, OTEC, PETO, EIA.

Abstract

The search for high-tech energy alternatives that cause less environmental impact is increasingly present in the strategic development plan of several countries, as the rapid economic and population growth in the world has significantly pressured the demand for energy on a global scale. Currently there is a great diversity of competing concepts and technologies in the field of converting ocean energy into electricity. Highlight of this work was given to thermal gradient energy, which has the highest exploration potential in the oceans, with about 40 billion MW. One of the main advantages of this type of power plant is that its energy source is vast, naturally renewable and non-polluting. In this study the results indicate the spatial and temporal variability of the vertical thermal gradient in the South Atlantic and especially in the Blue Amazon, the definition of a Brazilian Ocean Thermal Energy Park (OTEP), the variability of the park in its control parameters and the production of electric power from ocean thermal energy conversion plants and their possibility to perform the Inverse Anthropogenic Effect (IAE); in the matrix form for the South Atlantic Ocean. In addition, the OTEC plant was applied in a timely manner, with the same items listed for the main energy sites of the park (higher power regions) in relation to their operational viability (relationship between surface and depths that can configure the vertical thermal gradient)

Keywords: Renewable Energy, Thermal Energy, Hycom, Viability, Blue Amazon, OTEC, OTEP, IAE.

I. Capítulo: Introdução

Com demasiada frequência, quando as sociedades enfrentam crises envolvendo a população, energia, recursos ou meio ambiente, elas procrastinam até que o problema não possa mais ser ignorado. Esta fase é seguida por um período em que a sociedade se volta a aplicações de soluções paliativas e pouco eficazes. Essas soluções cosméticas mascaram e adiam o problema até que uma nova crise com potencial elevado de catástrofe. Felizmente, algumas soluções reais para os problemas surgiram ao longo das últimas décadas. Essas soluções resultaram do trabalho e esforço, de pesquisadores que reconheceram que não havia respostas de curto prazo.

A crise energético-ambiental com a qual o mundo está lutando, quando associada à demanda populacional, falta de consciência no consumo, nos levará a mais crônica e crucial de todas as crises mundiais, aquela que ameaça o ecossistema como conhecemos. Agora sabemos que as técnicas de conversão solar direta e não renovável, da energia nuclear e do gás natural, mesmo com os paliativos os conceitos de conservação de energia, são soluções ineficazes para o combate do aquecimento global e de alto impacto ao equilíbrio do ecossistema. A competição mundial atual envolve as reservas de petróleo quase esgotadas, demonstra mais uma vez, que o maquinário de criação, com ressalvas de algumas nações que estão alinhadas com a evolução tecnológica, está se movimentando para impulsionar uma nova

geração de soluções de curto prazo e de alto impacto ambiental.

Os leitores deste trabalho reconhecerão que as soluções de longo prazo são uma necessidade absoluta, sendo o foco destas práticas o desenvolvimento sustentável e as energias renováveis pelo sol, em suas diversas formas. Uma dessas soluções está nas energias renováveis do mar, mais especificamente o desenvolvimento da energia térmica oceânica e os seus subprodutos de alto valor. Com destaque, no maior potencial de conversão de energia dos oceanos e sua capacidade de realizar atenuações do aquecimento global.

O autor e os outros integrantes do estudo, se fizeram a pergunta científica de como seria melhor foram de mudar de matriz energética, e inverter a lógica do aquecimento global e das mudanças climáticas. Foi quando ao lembrar da sua trajetória acadêmica, de seus trabalhos anteriores, e da sua fonte de inspiração, o pesquisador Almirante Paulo Castro Moreira da Sila da Marinha do Brasil, autor de vários livros, sendo dois em destaque, (i) Oceanografia Física: O sol e mar [1975] e (ii) Os usos do mar [1978], tornou-os familiarizados com a abordagem científica da inovação, e levando este questionamento a redução do problema a uma questão de física e geofísica fundamental.

Essa abordagem levou à identificação dos “Usos do Mar”, como a palavra chave para responder aos questionamentos científicos realizados, nos levando a conversão de energia térmica oceânica como uma maneira prática e abundante de aliviar as necessidades energéticas nos dois sentidos, geração de energia elétrica limpa e retirada de calor dos oceanos e CO2 da atmosfera, atenuações do aquecimento global denominadas neste estudo de efeito

antropogênico inverso. Invertendo a lógica das aplicações de curto prazo de resposta, se utilizando dos gradientes térmicos verticais, oriundos da energia solar armazenada nos oceanos tropicais, que estão disponíveis dia e noite, durante todo o ano.

Uma vez identificada, havia a documentação analítica e experimental de formas práticas de transferir essa energia térmica em energia elétrica, se utilizando do processo de conversão para a geração de uma gama de subprodutos, de alto valor comercial, social e de reverter o impacto geofísico da nossa atividade. Onde cada passo, desse processo de longo prazo, exige a consideração da economia atual, problemas ambientais, das tecnologias nacionais, enquadramento institucional e nacional do estudo, mapeamento do recurso e da viabilidade da idealização aqui apresentada.

O autor deste estudo, proferiu a leitura dos dois livros citados do Almirante, no início do curso de Bacharel em Física dos Oceanos e Atmosfera, e começou sua trajetória de pesquisa, onde deparou-se com o conceito de uma usina de Ocean Thermal Energy Conversion (OTEC), unindo algumas áreas de sua predileção (Oceanografia Física e termodinâmica). Sendo a primeira parte trabalho, uma singela homenagem a um desbravador da educação, pesquisa e extensão, tripé educacional, inovação cientifica e ressaltando sempre a soberania nacional do mar.

Ressalto que mesmo suas obras sendo uma referência antiga, associada a outros autores de renome, explica de forma introdutória os principais aspectos do caminho da energia desde a reação nuclear no interior do sol, sua passagem pela atmosfera, até chegar ao foco deste estudo, a configuração da

reserva de energia térmica estocada nos gradientes térmicos verticais do mar.

I.I O sol e sua cascata energética até o mar

Este trabalho se alimenta da necessidade de, através de estudos, quantificar a energia armazenada em dos reservatórios geofísicos do nosso planeta e também aquela que circula entre eles. Sendo o mar a próxima fronteira energética que iremos cruzar [Neshyba. 1987, Skinner and Tukerian. 1988; Avery and Wu. 1994, Thurman and Trujillo. 2004], nossa fonte de informação para se medir a energia do mar é o sol. Onde sua capacidade como fonte energética, é representada pelas reações nucleares que mantém sua superfície a uma temperatura de 6.000°K, irradiando $36{,}28 \times 10^{22}$ J/s, em um espectro característico de ondas curtas, sendo que metade se constitui de luz. Devido a estas altas taxas de radiação, necessitamos estabelecer a interação destes pacotes energéticos com os compartimentos fluídicos do sistema geofísico, de forma a entender a cascata energética e sua distribuição energética até o mar.

Ao entrar na Termosfera (camada atmosférica mais extensa) que fica entre 80 km a 500 km de distância da superfície da terra, chega parte de meio bilionésimo da energia, que cada cm² que o topo recebe, raios perpendiculares à superfície, a constante solar é de 8368 J/cm².min ou 1360 W/m² (Figura 1). Na travessia da atmosfera a dose é atenuada por absorção e difusão ao passar pelas demais camadas atmosféricas [Silva. 1975, Iqbal. 1983, Frölich. and Lean. 1998, Liou. 2002].

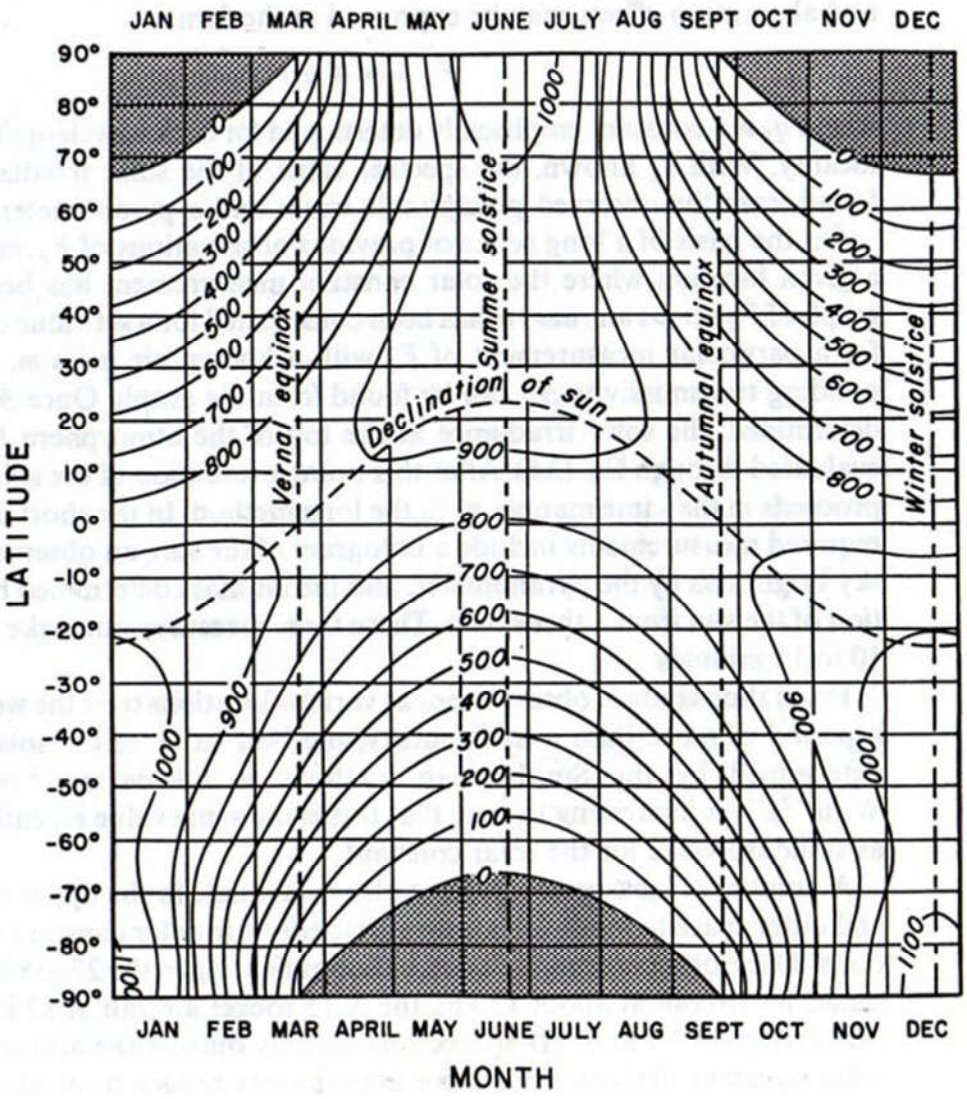

Figura 1: Distribuição da incidência de radiação média ao das faixas latitudinais e meses do ano, além da declinação do sol e dos solstícios e equinócios. (Fonte: Christopherson et al. [2009])

É necessário considerar, entretanto, que estes raios solares possuem uma angulação diferente, ou seja, o cm^2 do teto da atmosfera não recebe a mesma constante solar (Figura 1), e o cm^2 do solo receberá apenas parte desta energia. Como a incidência solar sobre a superfície do mar não é perpendicular, uma parte é refletida e apenas o restante penetra, porém de forma refratada.

Em consequência da absorção da energia solar o mar pode assumir temperaturas entre -1° e 29° (extremos explicados pela estratificação térmica e suas camadas da superfície até o fundo). As temperaturas, emissão de energia radiante ocorre sempre do comprimento de onda proporcional à quarta potência da temperatura (Lei de Stefan-Boltzman), e, naturalmente, valores muito inferiores, aos da radiação solar

Segundo Silva. [1975] e Liou. [2002], o anidrido carbônico e o vapor d'água da atmosfera são virtualmente transparentes à irradiação entre 8 e 14μ (janela de Simpson), e, assim, à falta de nuvens, uma parte importante da radiação terrestre se perde para o espaço. No restante do espectro, o vapor d'água e o anidrido carbônico são grande absorvedores, normalmente se a atmosfera é densa deles, isto é, muito úmida e poluída, as nuvens absorvem em todo o espectro, inclusive na janela de Simpson.

Conforme Silva. [1975], o que acontece é que, à medida que o mar se aquece por efeito do sol, passa a irradiar mais energia na faixa da janela de Simpson, perdendo, assim, mais energia para o espaço. O importante no que tange o equilíbrio geotérmico é o balanço, isto é, a irradiação terrestre efetivamente perdida, que é igual à irradiada menos a devolução da atmosfera e das nuvens, também, evidentemente, em onda longa, para o globo inteiro, onde balanço deve ser nulo,

Com base em Silva. [1975], Kennett. [1983], Neshyba. [1987], Brown et al. [1995], Liou. [2002], Thurman and Trujillo. [2004] e outros tantos, as regiões tropicais recebem certamente um excesso de radiação (pois o sol se mantém longamente alto no céu), e as perdas são atenuadas pela maior nebulosidade;

as regiões polares são deficitárias (Figura 1). Isto obriga a uma redistribuição de energia, realizada por diversos processos geofísicos naturais.

Tanto a evaporação (que transfere calor do mar ao ar), como a condensação (que transfere calor do ar ao mar), o calor latente e a condução (em que o ar, se mais quente, aquece o mar mais frio), são complexos processos de interface na qual a definição pura de calor acontece, transmissão de energia.

A perda por evaporação a maior perda potencial; cerca de metade da energia absorvida pelas águas do oceano é devolvida à atmosfera pelo processo de evaporação. A radiação da terra perdida é virtualmente a mesma em todas as latitudes. O calor perdido por evaporação, grande na zona tropical, declina a zero na zona polar. O calor ganho da atmosfera por condução, é pequeno, e praticamente constante em todas as latitudes. O balanço de calor é positivo no mar até a latitude de 30°, e a partir de então até o polo se torna deficitário (Figura 2) [Silva. 1975, Kennett. 1983, Neshyba. 1987, Brown et al. 1995; Thurman and Trujillo. 2004]

.

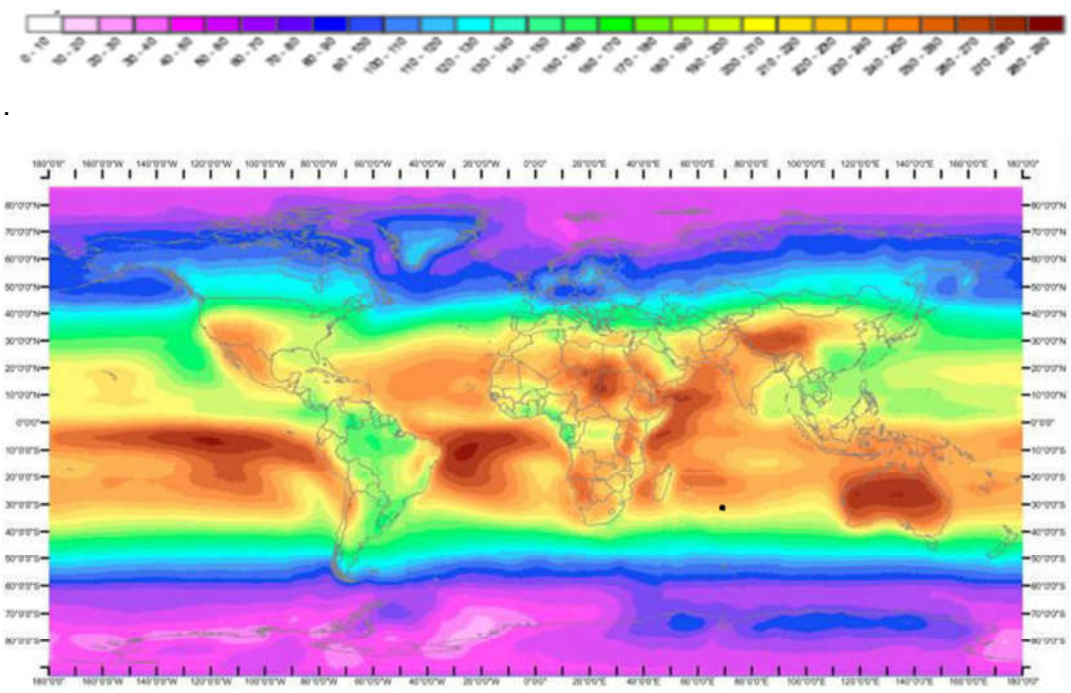

Figura 2: Irradiação solar média anual da superfície (W/m 2) observada por satélite durante o período de 1990-2004, onde a escala de cores varia de forma linear entre 0 W/m2 (branco) e 300 w/m2 (vermelho escuro) (Fonte : adaptado de École des Mines de Paris, Armines. [2006])

Com base no estudo clássico Sverdrup et al. [1942], são classificadas três tipos de água, oceânica clara, oceânica média e costeira média, calculou-se um fator que deve multiplicar o saldo de radiação para se obter o número de graus de aquecimento de cada camada (A percentagem de radiação absorvida é dividida pelo produto do volume da camada em cm³ e pelo calor específico).

As estruturas térmicas do oceano, são sobreposições de isotermas, entretanto com a evaporação, irradiação e condução, somente afetam a película superficial. Sendo assim, o resfriamento também ocorre nesta micro camada da superfície; mas as partículas e as adjacências tornam-se imediatamente mais densas. Percorrendo um caminho vertical até onde encontram a sua densidade, quando novamente sobem, e este movimento

convectivo dá a camada de mistura uma temperatura homogênea (perfis de temperatura Figura 3).

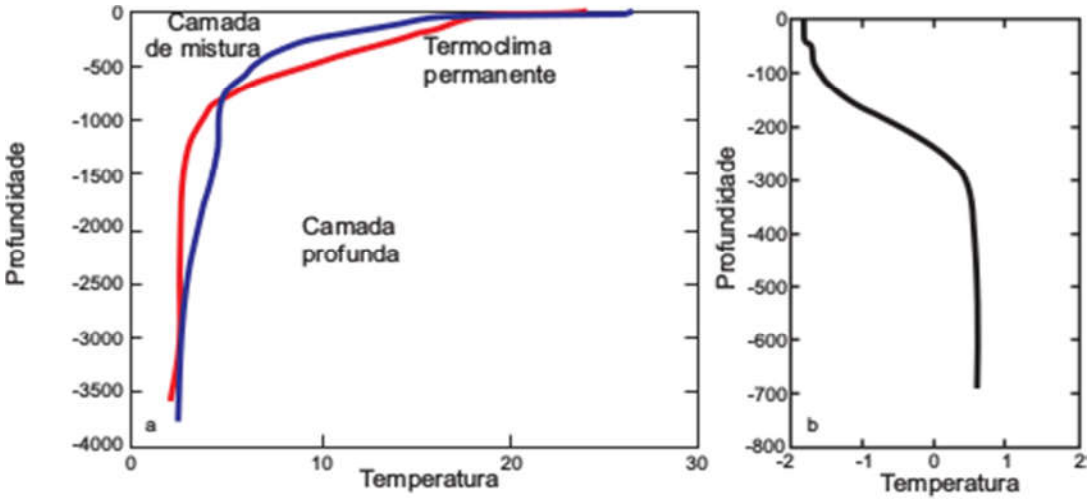

Figura 3: Distribuição vertical de temperatura (ºC), para Oceano Atlântico Sul em baixas (azul), médias (vermelho) e altas (preto) latitudes e suas variações em diferentes faixas latitudinais no Atlântico Sul (Fonte: adaptado de Castell and Krug. [2015]).

Do comportamento dos perfis clássicos da temperatura, Figura 3, nas três faixas do Atlântico Sul, existe uma semelhança correlata que as afeta, é a profundidade do giro convectivo, por alterar a densidade, varia a profundidade da camada de mistura e a inclinação da termoclina. Consideramos, no momento, um modelo teórico exclusivamente para mostrar como os processos de radiação e mecanismos de transferência, afetam a estrutura térmica do oceano e sua configuração ao longo da vertical. Cabe dizer também que outros processos interferem na camada de mistura, mais eficazes que o giro da convecção, distribuindo melhor que o aquecimento e resfriamento. Este processo é a agitação mecânica produzida pelas ondas de vento.

Vemos então que as identidades dos efeitos radiativos sobre o mar, os processos de troca e a estratificação térmica, desde de a superfície livre do

mar até a base do assoalho oceânico, dependem da variável temperatura. Onde no caso da transferência da energia térmica em elétrica, será a variável de controle dos conteúdos térmicos verticais a serem convertidos.

I.II Temperatura a variável mais coletada história da Oceanografia e sua importância cientifica

A água do mar funciona como um fluido de trabalho de máquina térmica geofísica, o que possibilita a interação entre os compartimentos de maior escala do ecossistema (oceano-atmosfera-continente). Temos que ressaltar, se o foco é verificar o fluxo dessa energia térmica oceânica, a pequena amplitude no que se refere a salinidade nas faixas latitudinais termicamente energéticas, ou seja, a temperatura se torna a variável oceanográfica mais importante de todas.

A temperatura é a variável mais medida nos oceanos, existe um grande banco de dados gerado a partir do controle de resfriamento de motores de navios mercantes e do desenvolvimento de satélites meteorológicos que medem a radiação emitida pela superfície terrestre na faixa do infravermelho (algoritmos baseados na lei de Stefan). Nestes dois casos, os dados limitam-se à camada mais superficial dos oceanos.

Em profundidade, existe todo um desenvolvimento de equipamentos como garrafas de coleta de água que serviram de suporte para termômetros de diversos tipos até chegarmos naqueles que foram mais utilizados, os chamados termômetros de inversão. Perfiladores em profundidade de temperatura, mecânicos e com formato de torpedo, os chamados bati-

termógrafos (BT) mecânicos também foram desenvolvidos e são considerados os precursores dos sistemas de registros contínuo que existem hoje como: o X-BT, sigla para eXpendable BT ou bati-termógrafos descartáveis; os conductivity, temperature and depth (CTD), as boias ARGO e os modelos numéricos (seja no processamento de modelos de grande escala ou nos algoritmos inseridos nos aparelhos citados) .

A temperatura (T) mede o grau de agitação das moléculas de um corpo e está relacionada, pelas equações termodinâmicas, à outras propriedades como: pressão, energia interna, capacidade calorífica, densidade, condutividade elétrica, velocidade de propagação do som e etc. Além disso, o potencial mecânico do oceano é um subproduto fraco, quando comparado fontes térmicas que são em média quatro ordens de grandezas superiores as mecânicas [Silva. 1978, Neshyba. 1987, Avery e Wu. 1994, Meisen. 2009]. É importante ainda ressaltar que os primeiros metros de camada superficial do oceano armazenam mais energia solar que toda atmosfera, embora mais de 76% das massas oceânicas estarem a uma temperatura inferior a 4^0C [Silva. 1978, Avery e Wu. 1994, Meisen. 2009]

Desta forma, sendo destacado a infinidade de processos relacionados ao aquecimento diferencial e espacial do oceano, demonstramos a abrangência da temperatura como ferramenta para descrever o comportamento de uma ampla gama de fenômenos oceanográficos, climáticos e geofísicos. As características do comportamento da temperatura nos oceanos e sua influência em fenômenos físicos, químicos e biológicos, vêm sendo estudadas ao longo do tempo, segundo artigos [Friedrich et all. 1973; Sears and Merriman. 1980; Thurman. 1986].

A primeira expedição oceanográfica a coletar dados de temperatura foi a Challenger Expedition (1872 – 1876), expedição inglesa sob o comando de Sir Charles Wyville Thompson, circunavegou o mundo. Ao total a expedição teve estudos específicos sobre biologia, física, química e geologia marinha .[Friedrich et all. 1973; Sears and Merriman. 1980; Thurman. 1986; Ross. 1988].

Depois desta expedição, que serviu como um marco oceanográfico, as margens do oceano (mesmo período que as margens do oceano cósmico também se abriram para humanidade) se revelaram para uma série de outras expedições.

A Oceanografia expandiu-se rapidamente, logo após a segunda guerra mundial, como resultado dos avanços tecnológicos e uso militares dos oceanos. Por volta dos anos 1960 e continuando até os 1980, surgiram muitos Centros Oceanográficos, tornando possível a realização de projetos integrados a nível internacional envolvendo vários países.

Projetos internacionais e nacionais, contribuíram para os avanços dos nossos conhecimentos sobre o oceano. As expedições enunciadas acima e o cenário expresso nos últimos parágrafos, demonstram o porquê de a temperatura dos oceanos ser a variável mais coletada, ao longo do tempo, sua vasta publicação e sua correlação direta com segmentos da ciência em destaque nas últimas décadas.

As pesquisas relacionadas a temperatura dos oceanos, assumiram um caráter não apenas de verificar o comportamento e sua variabilidade temporal e espacial, mas sim mensurar e identificar uma gama de processos relacionados a mudança do clima, alteração de fenômenos naturais e sua

correlação com antropogenia. Sua influência direta em uma infinidade de propriedades, forçantes, métodos matemáticos, modelos numéricos, métodos de coleta e de determinações, possibilitando que várias ramificações da oceanografia se usem desta variável para realizar suas pesquisas e obtenção de resultados.

Destacamos desta forma, que mesmo neste estudo sejam utilizados modelos numéricos de circulação global, regional e pontual, e que os instrumentos oceanográficos assumam a forma de linhas de comando, os resultados aqui obtidos exaltam a oceanografia de campo, como o alicerce primordial e contínuo de todas as ramificações da oceanografia, sendo os profissionais de campo da oceanografia física, os grandes responsáveis pelo imenso avanço ao longo das últimas seis décadas e da possibilidade do avanço do campo da modelagem numérica na oceanografia.

De forma que estudos centrais no contexto cientifico mundial, aquecimento do planeta e suas mudanças climáticas, estão relacionados com este trabalho, na forma que a tecnologia OTEC se embasa em trocas térmicas verticais e possibilita o efeito antropogênico inverso, na tentativa de inverter a lógica do aquecimento global. Exalta-se a vantagem de se utilizar de um modelo numérico de alta confiabilidade, no que tange as interfaces termohalinas, devido a sua validação pela vasta literatura térmica e evolução temporal da modelagem numérica.

I.III O oceano como uma bateria térmica

De posse da teoria apresentada até aqui, explicamos o mar como um grande reservatório térmico, e sua relação direta como o sol, atmosfera e as

massas de terra. Olhando para nosso planeta do espaço, nossa maneira de enxergar o mundo mudou fundamentalmente e podemos ver o mar, como nossa grande “célula fotovoltaica”, ou seja, o meio material capaz de absorver e converter está energia proveniente do sol em várias formas.

Vários autores, como Béguery. [1979]; Neshyba. [1987]; Avery and Wu. [1994]; Brown et al. [1995]; Thurman and Trujillo. [2004]; Da Rosa. [2012] e Twidel and Weir. [2015], relatam a possibilidade de uso de recursos energéticos do oceano, bem como sua utilização como fonte de energia para as sociedades modernas e desenvolvidas. Os autores supracitados destacam a característica da renovação dos recursos energéticos oceânicos, estando todos nós imersos num cenário de aquecimento global, esses recursos seriam obtidos e utilizados sem poluição oceânica e atmosférica relevante, demonstrando que os recursos do mar são cada vez mais relevantes e de cada vez mais destaque. Alguns destes autores ainda apontam que os oceanos, devido suas grandes capacidades térmicas, possuem maior quantidade de energia derivada do sol, estocada em uma coluna d'água de área unitária do que aquela contida numa coluna de área igual na atmosfera ou no continente.

Avery and Wu. [1994] postulam que em média, num dia, o calor absorvido pelas águas superficiais por aproximadamente 2,6 km^2 de área oceânica é maior do que aquele produzido pela queima de 1.113.000 litros de petróleo. Já conforme estimativas de Meisen. [2009], num dia, em média os mares tropicais com área de aproximadamente $60x10^6$ km² absorvem uma quantidade de radiação solar semelhante ao conteúdo de calor da combustão de cerca de $39,75 \times 10^{12}$ litros de petróleo.

Segundo Vega [1999], a quantidade de energia solar anual absorvida

pelos oceanos é equivalente a pelo menos 4000 vezes a taxa de consumo anual de energia no mundo, no período da década de 90. Seguindo a taxa consumo anual de energia, a partir de sistemas OTEC com eficiência de 3%, (eficiência da atingida na usina OTEC deste estudo) – ao utilizar menos de 2% do recurso da energia térmica dos oceanos seria suficiente para suprir toda a demanda energética humana.

O Oceano é como uma grande máquina térmica geofísica, na qual a água do mar funciona como fluido de trabalho, movendo-se entre a camada superficial dos oceanos tropicais (fonte quente) e as regiões polares e subpolares (fonte fria), de onde parte dela afunda e se espalha pelas bacias oceânicas [Neshyba. 1987; Skinner and Turekian. 1988, Avery and Wu. 1994].

I.IV O recurso da Energia Térmica Oceânica no Atlântico Sul (AS)

De acordo com Crews. [1997], metade da água do oceano Atlântico Sul (AS) possui um vasto conteúdo térmico vertical, pois os gradientes térmicos verticais são aproximadamente iguais ou superiores a 20°C. Portanto, as condições brasileiras são muito favoráveis ao aproveitamento da energia dos gradientes térmicos, especialmente pela vasta extensão da região de mar territorial nas regiões de latitudes inferiores a 30ºS (Figura 2).

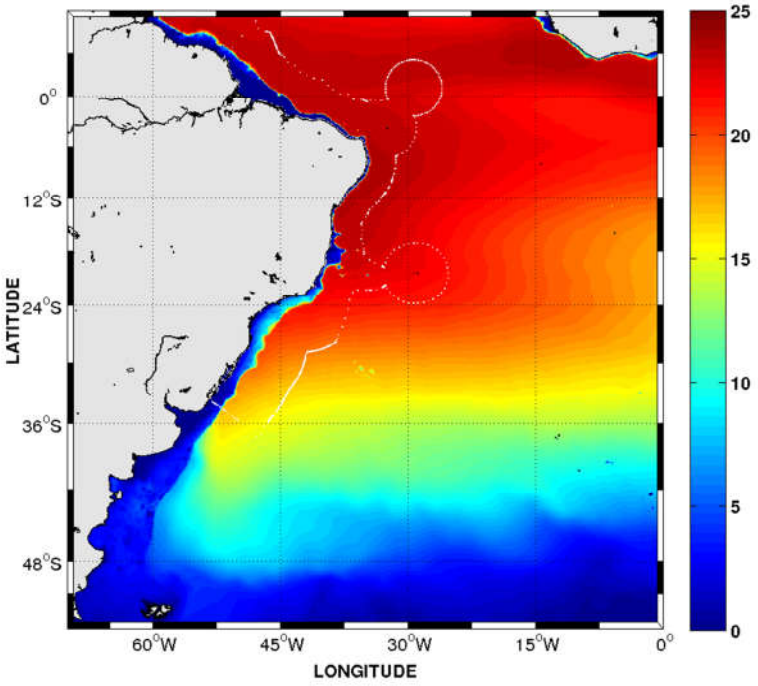

Figura 4: Gradiente térmico, entre a superfície e a profundidade de 1000m, médio anual (ºC), média do modelo HYCOM entre o ano de 1993 até 2012, do Atlântico Sul (Fonte: Imagem gerada pelo autor).

Objetivando a explicação da configuração dos gradientes térmicos verticais do oceano AS, Figura 4, existe um grande giro anticiclônico, que de acordo com Stramma and England. [1999] e limitado meridionalmente pela Corrente do Atlântico Sul em seu limite inferior e a Corrente Sul Equatorial (CSE) em seu limite superior. A borda leste desse oceano e ocupada pela Corrente de Benguela. A Corrente de Contorno Oeste que completa o giro é a Corrente do Brasil (CB).

Segundo Cirano et al. [2006], decorrente dos efeitos da CSE, que flui no sentido Leste-Oeste, influenciando a parcela Nordeste (NE) da costa brasileira. Ao sul de 10°S, a CSE se bifurca originando a CB e a Corrente Norte do Brasil (CNB). De forma a simplificar a descrição dos padrões das duas correntes Brasileiras, CB e CBN, além dos extratos abaixo das mesmas, dividiremos a porção do oceano sobre a margem continental brasileira em três camadas

principais, conforme descrito nos esforços de Stramma and England. [1999]. Nos primeiros 150 m de coluna de água; superficial (associada a camada de mistura), entre 150 e 500 m; intermediária, entre 500 até a base do assoalho oceânico, profunda. Estes domínios verticais, estão associadas as principais massas de água do oceano superior no AS, sendo a Água Tropical (AT) na superfície, a Água Central do Atlântico Sul (ACAS) e a Água Intermediária Antártica (AIA) na camada intermediária. A camada profunda, do sopé continental e parte da planície abissal, é composta por três massas de água: a Água Circumpolar Superior, a Água Profunda do Atlântico Norte (APAN) e a Água de Fundo Antártica (AFA [Stramma and England.1999; Mémery et al. 2000].

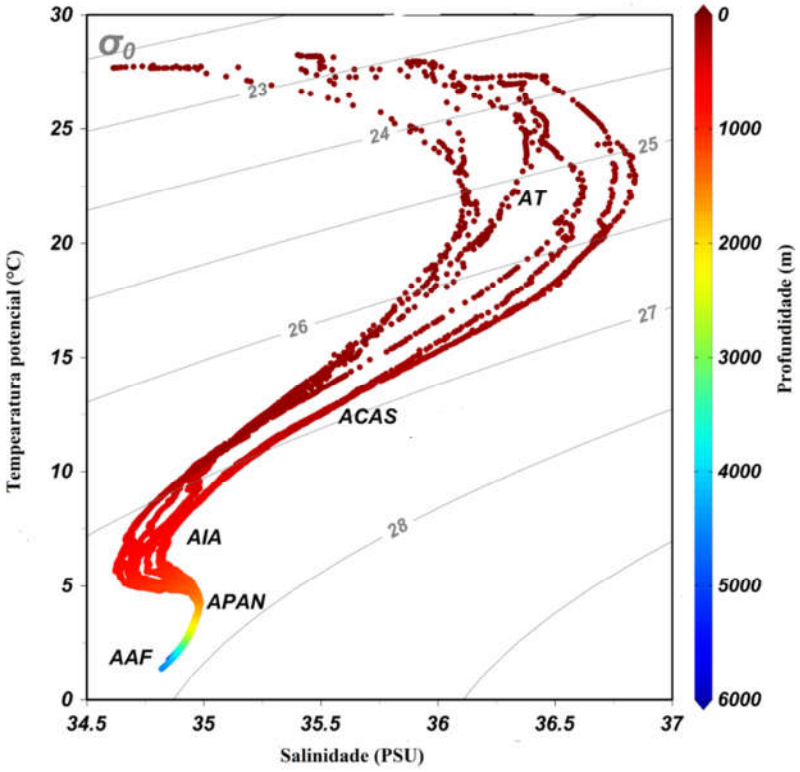

Figura 5: Diagrama TS do AS, entre as latitudes de 6 e 8ºS e ao longo da longitude de 31ºW, referente a figura 3 do máximo gradiente (Fonte; Gráfico obtido pelo autor tendo como base nos dados médios do Hycom no ano de 2009, espelhando os resultados obtidos por Stramma and England. [1999].).

Tabela 1: Limites dos índices térmicos das massas de águas constituintes do diagrama TS apresentada na Figura 4 (Fonte: Retirado de De Souza.[2015])

Massas de água	Intervalor de temperatura (ºC)
AT	>20
ACAS	4-20
AIA	3-6
APAN	1,5-4
AFA	-1,8-(-0,5)

Durante o verão, a contribuição da AT, somada a ressurgência em superfície e sub-superfície (ACAS), pode maximizar o potencial do gradiente térmico. O aparecimento de água fria a menor profundidade, da Plataforma Continental Brasileira, possibilita a maximização dos gradientes térmicos verticais. A combinação de processos de mistura de diferentes massas de água resultam num padrão termohalino homogêneo e espacialmente estável [Castro et al, 2006].

A existência de intensos gradientes térmicos, principalmente em regiões próximas à costa, pode ser um fator determinante na implementação de uma usina de conversão de energia térmica em elétrica, devido ao menor custo de instalação e operação [Valente and Marques. 2016].

O gradiente térmico vertical, é a variação de temperatura ao longo da coluna de água, ou seja, é uma grandeza expressa pela unidade de temperatura. Os campos médios dos gradientes térmicos têm variabilidade temporal e espacial, associados as alterações dos processos meteorológicos e oceanográficos sobre a região. Esta variabilidade está associada a circulação de massas de água, porém, do ponto de vista quantitativo, esta variação não é tão significativa

Para Cirano et al. [2006], a CB e CBN podem ser definidas como um fluxo associado ao movimento da AT, altos conteúdos de calor e é resultante da radiação intensa e da evaporação excessiva em relação à precipitação, características do AS equatorial, sendo transportada para Sul pela CB e ao Norte pela CBN. A ACAS tem sua origem na zona de confluência da CB com a Corrente das Malvinas, ainda segundo autores como Silva. [2006], e sua posição em nível inferior a AT maximiza os conteúdos de calor do gradiente térmico em baixa profundidade.

Na região mais ao norte ocorre uma intrusão em sub-superfície da Água Central do Atlântico Norte (ACAN), ocupando o mesmo extrato indicado no TS para ACAS, na costa norte, em região próxima ao Amapá, que com a contribuição dos altos conteúdos de calor da zona de Convergência intertropical, maximiza os valores do gradiente térmico sobre a região próxima à região norte do mar Brasileiro.

A tecnologia OTEC, então, tem como principal aspecto de viabilidade a configuração de um gradiente térmico, estabelecido entre a superfície e no máximo 1000m de profundidade [Ascari et al, 2012]. Essas características geográficas e assinaturas térmicas oceanográficas, sugerem que uma usina OTEC teria plena capacidade de operação nos limites Brasileiros, operando entre as massas de água AT e ACAS, ao longo do mar da porção sudeste e nordeste, AT e ACAN, ao longo do mar na porção norte da costa do Brasil. [Strama and England. 1999].

Este padrão de distribuição de temperatura é responsável pela estabilidade térmica nos oceanos, onde existe uma massa de água superficial menos densa, continuamente aquecida. Esta camada de água normalmente

tem temperaturas médias superiores de 20 a 29°C (Indices da AT, Tabela 1), onde excluindo as regiões de ressurgência superficial, esta camada não se mistura de maneira efetiva com as águas mais frias em sub-superfície, ACAS e ACAN, que são mais densas, possuindo temperaturas médias de 4 a 6ºC (intervalo da ACAS, Tabela 1). Explicando os valores de gradiente térmicos verticais máximos, entre a superfície e 1000m, de 25ºC, indicados na Figura 4.

Desta forma, podemos reafirmar o papel da água do mar como de fluido de trabalho geofísico do planeta, ou seja, a circulação termohalina, possibilita a essas massas, configurarem um reservatório térmico, que viabiliza a ideia da conversão de energia térmica em elétrica, através de uma máquina térmica adaptada ao ambiente marinho. Assim uma usina OTEC, está se utilizando da segunda lei da termodinâmica, lei que define o comportamento de maquinas térmicas, estabelecida pelos físicos Clausius. [1850], Thomson. [1851], conhecido como Lord Kelvin, aplicada conceitualmente nos oceanos por D'Arsonval. [1881] e seu primeiro aparato operacional realizado pelo engenheiro Claude. [1930].

I.V O conceito OTEC e seus sistemas

Um sistema OTEC é basicamente uma máquina térmica na qual a fonte quente é a água superficial do oceano e a fonte fria é a água mais profunda [Vega,1999]. Existem, basicamente, duas abordagens para a conversão de energia térmica dos oceanos, o primeiro referido como um ciclo fechado (adotado neste estudo) e o segundo como um ciclo aberto.

As águas superficiais de maior temperatura (AT – Figura TS) e as águas mais frias e profundas (ACAS e ACAN, Figura TS), assumindo o limite operacional de captação da agua de fundo de 1000m [Ascari et al, 2012]. O

ciclo termodinâmico, baseado no ciclo de Carnot, vaporiza (via energia térmica da AT) e condensa (via baixa energia térmica da ACAS ou- ACAN) um fluido de trabalho, que à circular entre o dipolo térmico cria momento, que gera energia elétrica pelo acionamento de uma turbina.

Para Avery and Wu. [1994], guia OTEC mais aclamado da literatura mundial um sistema OTEC apresenta os seguintes subsistemas:

• I - Uma máquina térmica ou usina de força, incluindo permutadores de calor, turbinas, geradores elétricos, bombas de água e fluido de trabalho, tubulações associadas e controles;

• II - Um sistema de tubulação de água, que inclui um tubo de água fria, Cold Water Pipe (CWP), através do qual a mesma é trazida de uma grande profundidade (máximo de 1000m) até a superfície. Além de entrada de água quente, Hot Water Pipe (HWP), e tubos de saída e escape dos fluidos utilizados no ciclo;

• III - Um sistema de transferência para carregar energia produzida no oceano para consumidores no continente, tanto na forma de eletricidade, bem como, na forma de combustível;

• IV - Um sistema de controle de posição, incluindo equipamentos de propulsão e ancoramento, controles e sistemas de potência de reserva;

• V - Uma plataforma para sustentar a usina de força, sistemas de tubulações, equipamentos de embarcação auxiliar, acomodações para os técnicos operacionais, junto com equipamentos de segurança e outros requisitos de habitabilidade.

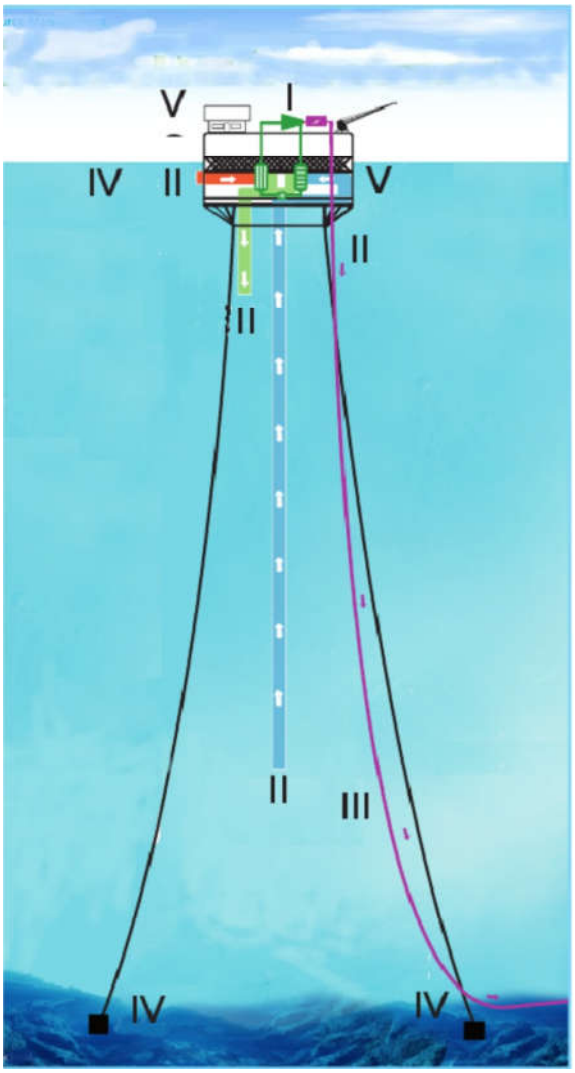

Figura 6: Esquema representativo dos subsistemas de uma usina OTEC (Fonte:Adaptado de http://coastalmanagement.noaa.gov/otec/otecrdda).

Existem, basicamente, duas abordagens para a conversão de energia térmica dos oceanos, o primeiro referido como um "ciclo fechado" e o segundo como um "ciclo aberto". No ciclo fechado, as águas superficiais de maior temperatura e as águas mais frias e profundas são utilizadas para vaporizar e condensar, respectivamente, um fluido de trabalho. Este fluido de trabalho se dirige a uma turbina geradora em um circuito de forma a produzir eletricidade.

No sistema de ciclo aberto, segundo Avery and Wu [1994]. o fluido de trabalho é ventilado após o uso, via aberturas das conforme mostrado na

Figura 7. Neste caso, o fluido de trabalho é vapor de água. A água quente do mar é bombeada para uma câmara na qual a pressão é reduzida por uma bomba de vácuo para um valor baixo o suficiente para fazer com que a água ferva (3% do nominal de uma Atmosfera $1,01x10^5$ N/m^2). O vapor de baixa pressão, depois de passar por uma turbina, é condensado pela água fria em uma câmara semelhante e é então descarregado no oceano. Em vez de ser condensado por contato direto com água fria, o vapor pode ser direcionado para um trocador de calor resfriado pela água do mar fria. Neste caso, o vapor condensado torna-se uma fonte de água doce, no equivalente inverso a água vaporizada pode se obter sal marinho.

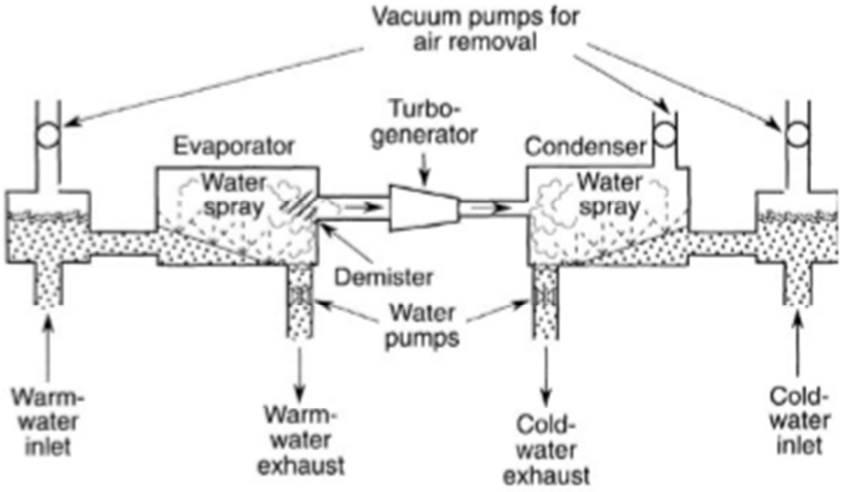

Figura 7: Ciclo aberto ou de Claude (Fonte: Adaptado de Avery and Wu. [1994])

Neste estudo são utilizados os conceitos do ciclo fechado (ver figura 4) (ciclo de Rankine), desta forma será apresentado aqui com mais detalhes, mas de maneira muito sucinta e objetiva. Portanto, uma máquina térmica oceânica que seque a segunda lei da termodinâmica, aplicadas as pequenas diferenças de temperatura (adaptação que deu o nome ao ciclo fechado para o oceano, Ciclo de Rankine).

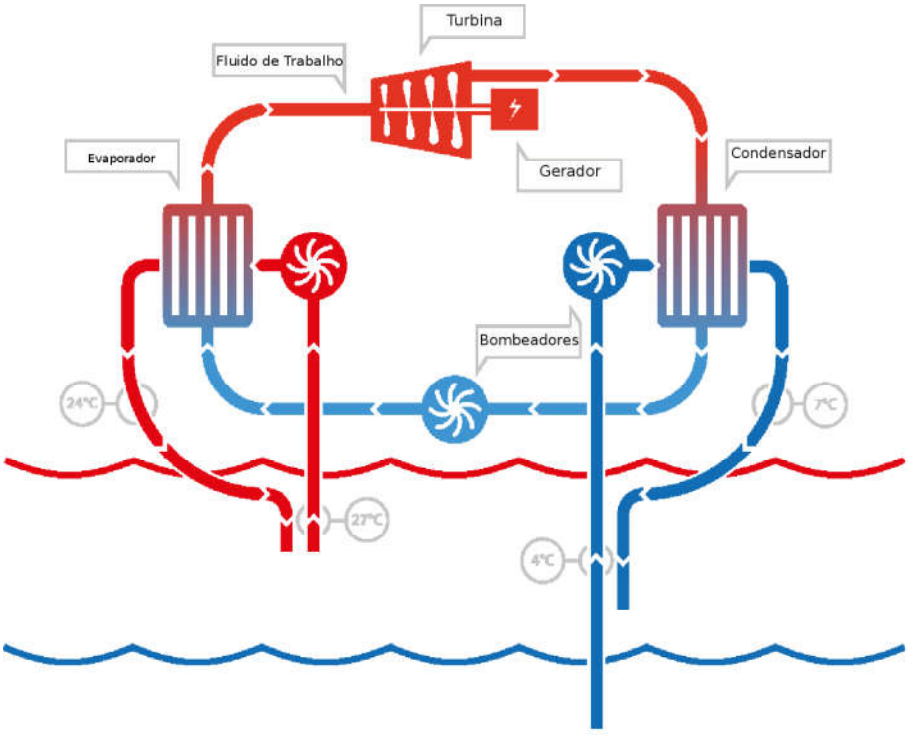

Figura 8 Esquema do Ciclo fechado ou de Rankine (Fonte: Adaptado de http://www.otecnews.org/)

Neste sistema, o fluido operante utilizado para produzir trabalho mecânico percorre um circuito fechado. Neste sistema de acordo com: Avery and Wu, [1994] e Beavis, et al, [1986], um fluido operante de baixo ponto de ebulição, amônia, fréon ou propileno [Bharathan. 2011], é vaporizado pela água do mar de mais alta temperatura (AT), ao passar por um permutador de calor (evaporador). Neste permutador, ocorre uma expansão moderada do vapor, que através do momento gerado aciona uma turbina geradora, produzindo eletricidade.

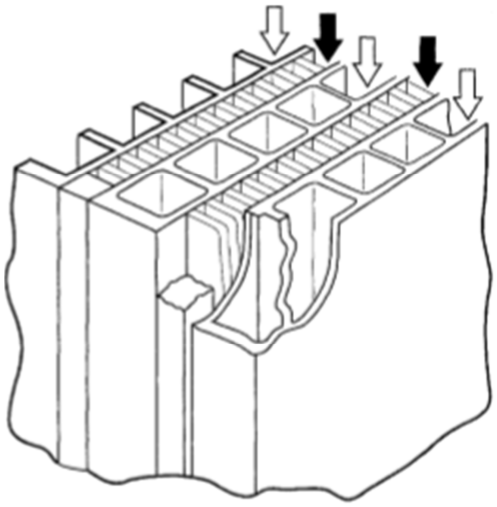

Figura 9:Permutador de calor, indicando pelas setas pretas onde circula o fluido de trabalho (operador do ciclo) e pelas setas brancas onde circula a água do mar (Fonte: Adaptado de Avery and Wu. [1994]

Ao entrar em contato com outro permutador de calor (condensador), o fluido operante é condensado ao ceder calor para o meio, devido à passagem da água fria do mar (ACAS ou ACAN). Esta água profunda é bombeada até este ponto através do CWP.

Tanto no condensador, como no evaporador, não existe contato direto entre o fluido operante e a água do mar. Existe uma troca de calor através dos permutadores de calor. Depois de se mover pelo condensador, o fluido condensado é então bombeado de volta para o evaporador para reiniciar o ciclo. Assim, estabelece-se uma circulação fechada para o fluido de trabalho, que numa situação ideal se movimenta continuamente enquanto a água do mar possuir a diferença de temperatura.

Para Avery and Wu, [1994], dentre os subsistemas presentes num sistema de ciclo fechado, os permutadores de calor têm uma importância considerável. Por causa da pequena diferença de temperatura, estes componentes precisam ser projetados com uma área suficientemente grande para garantir a transferência de calor necessária. Além disso, outra parcela

importante da infraestrutura são as tubulações de HWP e CWP, devido a suas características a semi-adiabáticas.

Destaca-se ainda, segundo, a ressurgência artificial forçada pelas bombas da usina OTEC, via CWP, geram uma infinidade de produtos, que não são a energia elétrica. Elencando suas possibilidades, afirmamos a possibilidade de geração de subprodutos como, produtos químicos com capacidade motriz (Hidrogênio e oxigênio), água potável (produção de água mineral, isotônicos, agricultura diversificada em zonas tropicais), sal marinho, maricultura (proteína animal e vegetal, bio-fármacos, bio-pigmentos, absorve grandes quantidades de CO_2 atmosférico e inúmeras outras possibilidades) e principalmente, viabiliza a retirada de altas taxas de conteúdo de calor do oceano, ou seja, pode inverter a lógica , mesmo em pequena escala, da aceleração do efeito estufa (retira CO2 atmosférico), do aumento da temperatura oceânica (via retirada de calor) e consequentemente do aquecimento global.

I.VI Oceano, Clima e o Efeito Antropogênico Inverso (EAI)

Segundo Cheng et al.[2019] Como consequência do aquecimento global, registra-se uma rápida absorção de calor pelos oceanos nas últimas décadas, sendo a velocidade muito maior do que o estimado no último relatório do Painel Intergovernamental de Mudanças Climáticas (IPCC). O aumento das concentrações atmosféricas de gases de efeito estufa levou ao desequilíbrio energético do sistema climático terrestre. A quantidade de energia absorvida pelo sistema na forma de radiação solar tem sido maior do que a quantidade de energia emitida de volta ao espaço na forma de radiação infravermelha. Ainda segundo o mesmo, aproximadamente 93% da energia adicional acumulada

pelo sistema climático se acumula no oceano na forma de calor. Dessa forma, o aquecimento global leva ao crescimento da quantidade de calor presente no oceano.

O último relatório do Stocker et al. [2013] e Cheng et al. [2019], afirmam que ao contrário do aumento da temperatura média do ar, o crescimento da quantidade de calor do oceano sofre menos interferência da variabilidade interna do sistema climático. Constitui, assim, um indicador mais adequado para detectar os efeitos do aquecimento provocado pelas emissões das atividades humanas, efeito Antrogênico.

Conforme dados de Cheng et al.[2019], as novas estimativas mostram uma tendência de aumento altamente consistentes desde o final da década de 1950. O aquecimento observado entre 1971 e 2010 é maior do que o apresentado no último relatório do IPCC.O monitoramento dos oceanos deu um grande salto a partir do início dos anos 2000, quando foi implantada a rede Argo, com um conjunto de estações de coleta de dados distribuída ao redor do planeta. Apesar de relativamente recente, a rede ampliou a cobertura de observações e diminuiu as incertezas.

Tanto as novas estimativas quanto os dados da rede Argos, apontam para o conservadorismo das estimativas anteriores do IPCC. A absorção de calor pelos oceanos está se acelerando. No entanto, segundo Cheng et al.[2019] algumas incertezas permanecem, em especial para as camadas profundas dos oceanos, as regiões costeiras, e para o período anterior à implantação da rede Argo. Ainda há espaço para aprimoramentos na recuperação e tratamento de dados históricos de monitoramento das águas oceânicas.

O aumento da absorção de calor pelos oceanos é um indicador claro do aquecimento global, afirmaram a comunidade científica em geral. As projeções dos modelos climáticos apontam que a tendência continuará, acompanhando o crescimento das concentrações atmosféricas dos gases de efeito estufa, provocas pelas emissões antropogênicas humanas.

Segundo Cheng et al. [2019], a alteração registrada nos oceanos tem se traduzido em temperaturas da água mais elevadas e no aumento do nível médio do mar. Tais modificações estão associadas a transformações em tempestades, furacões e no ciclo hidrológico, incluindo eventos extremos de precipitação, as mudanças climáticas. A fim de evitar o agravamento das condições atuais, deve-se diminuir ou interromper as emissões, limitando o aquecimento global. Mas impactos das alterações provocadas até o momento ainda ocorrerão e, por isso, as sociedades precisarão também se adaptar.

Neste cenário global, é necessário notar que, em termos globais, a questão ambiental em seu foco, necessita de um novo modelo de organização humana. Ao longa dos últimos quarenta anos o avanço apresentado tem sido muito lento em relação ao efeito danoso que o modelo atual tem perpetuado e até mesmo aumentado. Nesta mudança do modelo, o papel da energia tem caráter central na mudança das práticas e na realidade do ecossistema como um todo. No entanto, fornecer subsídios suficientes para uma reflexão profunda dos impactos é urgente. O conhecimento científico e empirismo proporcionou aos humanos a capacidade de manipular os recursos naturais, essa capacidade trouxe, traz e trará benefícios, mas no atual cenário o cerne é busca de converter nossas necessidades, como energia elétrica, em benefício

da busca pelo equilíbrio natural.

Estamos em pleno século XXI, e os conceitos e tecnologias aplicadas no modelo mundial energético ainda não abandoaram conceitos arcaicos de produção de energia, em contraponto, diversos processos de conversão entre fenômenos de natureza distintas foram descobertos. Para cada uma das formas da natureza, está vinculada um tipo de energia: mecânica, cinética, térmica, química, elétrica, eletromagnética, nuclear e de massa.

A energia renovável térmica é proveniente de ciclos naturais de conversão da radiação solar e, por isso, são praticamente inesgotáveis, tendo em vista que no cenário atual mundial existem várias tecnologias, que geram energia com impactos inerentes a sua forma de converter energia. Porém, entretanto, vemos que na atual configuração além da produção de energia amigável ao meio ambiente, existe a necessidade de atuar na tentativa de mitigar nosso efeito antropogênico histórico, que pressiona os índices do aquecimento global e do cenário das mudanças climáticas, indicados por Cheng et al. [2019] .

Os subprodutos OTEC, demonstram a possibilidade de aplicação do conceito de antropogenia inversa, ou seja, da capacidade da tecnologia OTEC retirar, via sua operação com fluxo de calor entre os compartimentos termodinâmicos do sistema (evaporador e condensador), grandes quantidades de calor do oceano, onde os converte em energia elétrica limpa e renovável. Além disso, foi abordado a capacidade de o sistema possibilitar a operação de fazendas de maricultura no entorno da usina, via ressurgência artificial, possibilitando a fertilidade dos oceanos e a retirara de altos conteúdos valores de co_2 atmosférico [Rau and Baird, 2018].

Ao mudar a lógica das práticas de planejamento de curto prazo, alterar nosso sistema de desenvolvimento para uma matriz renovável, poderíamos dar início a um efeito antropogênico inverso em domino, como exemplo, ao diluirmos a temperatura do oceanos, o mesmo acontece com a atmosfera, e ao retirar CO_2 da mesma reabrimos a janela de Simpson, diminuindo a radiação retida, ou seja, uma sequência de efeitos, subestimados, que mitigariam o efeito estufa, as mudanças climáticas e consequentemente o aquecimento global.

Da Rosa [2012] e Twidel and Weir. [2015], indicam que o futuro está na engenharia geofísica aplicada ao uso do mar, exalta em ainda o alcance do potencial econômico e energético da OTEC em nível global. Os cenários apresentados nesta seção provam que a tecnologia OTEC, pode ser um alicerce firme de um futuro necessário, requerendo um crescimento rápido da instalação e fortes efeitos de aprendizado para tornar a tecnologia uma das principais matrizes energéticas, de forma lucrativa, sustentável, socialmente impactante e alinhada com as necessidades de uma nova era da relação humana com o planeta, onde nossas atividades geram antropogenia inversa. Esta tese contribui para o campo de pesquisa da OTEC, abordando várias lacunas de conhecimento na literatura e, na forma de seus artigos, em contrapartida, oferece muitas oportunidades para prosseguir investigações. No entanto, além de um escopo mais local de investigações e de idealizações, argumenta-se que os protótipos de escala comercial são o que a OTEC mais precisa.

II. **Capítulo:** Hipótese

Hipótese

A Amazônia Azul Brasileira apresenta condições operacionais para a implementação de usinas de conversão de energia térmica oceânica em elétrica.

III. **Capítulo:** Objetivos

GERAL

Estudo da viabilidade operacional de instalação de usinas de geração de energia elétrica a partir de gradientes térmicos verticais na região da Amazônia Azul Brasileira

Específicos

I. Avaliar a variabilidade espacial e temporal dos gradientes térmicos verticais no Atlântico Sul, na Amazônia Azul e definir os sítios energéticos;

II. Avaliar a sensibilidade dos gradientes térmicos verticais a passagem do

calendário juliano, nos sítios energéticos, ao longo das profundidades operacionais da usina OTEC;

III. Definir o Parque de energia térmica Oceânica Brasileira e avaliar as variáveis de entrada e saída relativas a uma usina OTEC teórica, na forma matricial;

IV. Determinação das áreas de cobertura das faixas de potência, o número de usinas OTEC possível de operar e os melhores locais para sua instalação;

V. Verificar as capacidades subestimadas de produção de energia elétrica, retirada de calor dos oceanos e co_2 da atmosfera (efeito antropogênico inverso), no parque;

VI. Demonstrar o gradiente térmico vertical de melhor viabilidade operacional, sua variabilidade ao longo do calendário juliano e as variáveis de maior relevância da usina OETC nos sítios de maior potência do parque;

IV. **Capítulo:** Artigos Científicos

Para a obtenção do título de Doutor pelo Programa de Pós-Graduação em Oceanografia Física, Química e Geológica, é requerido que o discente realize a submissão de pelo menos dois artigos científico como primeiro autor em periódico com corpo indexado. Desse modo, os resultados da pesquisa desenvolvida durante o período do doutorado e a discussão dos resultados serão apresentados em forma de artigos neste Capítulo. O primeiro manuscrito, de autoria de Roberto Valente de Souza, Elisa Helena Fernandes, José Luiz Lima de Azevedo e Rafaela Martins Corrêa, é intitulado "**Thermal energy sites in the south Atlantic**

Ocean: The potenctial of the Brazilian Blue Amazon". O segundo manuscrito de autoria de Roberto Valente de Souza, Elisa Helena Fernandes, José Luiz Lima de Azevedo, Mariana dos Santos Passos e Rafaela Martins Corrêa, é intitulado "**Potential for Conversion of Thermal Energy in Eletrical: Highlighting the Brazilian Ocean Thermal Energy Park and the Inverse Anthropogenic**", sendo ambos submetidos para publicação no periódico "Renewable Energy*"*.

IV.I Artigo I

THERMAL ENERGY SITES IN THE SOUTH ATLANTIC OCEAN: THE POTENTIAL OF THE BRAZILIAN BLUE AMAZON

Roberto Valente de Souza[a,*], Elisa Helena Leão Fernandes[a,**], José Luiz Lima de Azevedo[b], Rafaela Martins Corrêa[a]

[a] *Institute of Oceanography, Laboratory of Coastal and Estuarine Oceanography (LOCOSTE). Federal University of Rio Grande, Carreiros Campus, Av. Itália without number Km 8, CEP 96201-900, Brasil*
[b] *Institute of Oceanography, Laboratory of Ocean Studies and Climate (LEOC) . Federal University of Rio Grande Carreiros Campus, Av. Itália without number Km 8, CEP 96201-900, Brasil*

Abstract

The search for high-tech energy alternatives that result in lower environmental impacts is increasingly important in the strategic development of countries, as rapid world growth has significantly pressured energy demand. Especially the thermal energy in the oceans, which has the highest exploitation potential of about 40 billion MW, is renewable and has the capacity to remove heat from the oceans and CO_2 from the atmosphere. In this study, we used the temperature results of one numéric model (hybrid Coordinated Ocean Model - HYCOM), which allows a more robust representation of the structure of the ocean temperature, which is important in the evaluation of oceanic thermal energy conversion (OTEC). Based on these data, daily, monthly, seasonal and annual averages of Julian were calculated, allowing to evaluate the variabilities in the thermal gradient of mainly in the Blue Amazon. The definition of three thermal energy sites and their viability were obtained, and their thermal gradients could be converted by a power plant OTEC, being fully operational throughout the period of the Julian average. This realization allows confidence in the viability of the long-term exploitation of thermal energy, with the real possibility of installing a future OTEC park and its benefits.

Keywords: Renewable energy, thermal energy, OTEC, south Atlantic Ocean, Blue Amazon.

1. Introduction

Since first viewing the Earth from space, our way of seeing the world has fundamentally changed: we now enjoy our beautiful and fragile blue planet, which is our life support, as the planet floats in a hostile space, poorly balanced in an orbit around the sun. The energy of the sun is the main source of energy for the Earth, which enables the presence of terrestrial and most

*Corresponding Author
**Corresponding Author
Email addresses: robertovalente@furg.br (Roberto Valente de Souza), fernandes.elisa@gmail.com (Elisa Helena Leão Fernandes), joseazevedo@furg.br (José Luiz Lima de Azevedo), rafsmcorreay@gmail.com (Rafaela Martins Corrêa)

Submitted to Renewable Energy

of marine lives. The sun is responsible for moving the large energy reservoirs of the oceans, atmosphere, terrestrial layers and other forms not yet fully realized. The immense energies of rivers and waterfalls, for example, are associated with the great evaporation cycle, which includes the formation of rain clouds. These clouds are carried by winds, which are driven by differential heating of the planet's surface, and clouds generate surface current systems (including subtropical and subpolar circulations), and thermohaline circulation driven by deep ocean density represents the energy cascade from solar activity.

The sun supplies $1.5x10^{18}kWh$ of radiant energy to the atmosphere annually, which corresponds of 10.000 times the world's energy consumption over the same time period, highlighting the short renewal cycle, spectrum of distribution through physical phenomena and the absence of waste generation at both micro and macro scales. The urgent challenge of humanity is to stop wasting the solar energy received by the planet.

Throughout the ages, the human race has lived following the daily rhythm of the sun. However, the discovery of fire brought a revolutionary way to use the sun's stored energy in wood, with medium-lasting (8-year) solar energy storage cycles. The beginning of the industrial revolution was marked by the use of solar energy in the form of mechanical energy from windmills and water wheels, which was later replaced by wood-fired steam engines. Today, for many developing countries, these energies are the major forms of solar energy being used, which have been conveniently concentrated.

Coal, oil, and gas have been the primary energy sources during the last century, and these energy sources are also considered to be concentrated forms of solar energy that have been stored over 500 million years. Therefore, the production of coal, oil, and gas is a conceptual error once these finite resources are not produced by us. On the other hand, it takes only about a century to exhaust the readily accessible reserves of these finite long regeneration cycle resources.

The technology to exploit these resources has become less expensive over the last century through economies of scale financed by government protection and investment infrastructure, which is geared towards the interests of corporations who own the technology and resource. The major concern is the perception that these materials, which are produced from extensive cycles of degradation and product generators that have decomposition cycles greater than several human life cycles, are becoming a problem for the planet. This problem is demonstrated by the high rate of species annihilation, contaminations of soil, atmosphere, and water resources, and the imbalance of imprisoned heat contents.

On the other hand, the sun's short-cycle energy sources are diffuse natural resources in their various forms. These energy sources are distributed uniformly throughout the world and freely available to all. These sources are ecologically friendly and characteristically work against anthropogenic activity effects. However, the capital costs of developing technologies to use the energy sources that are quickly renewed by the sun are currently a barrier, because scale economies have not considered the effects and returns over a long period.

According to Neshyba [12], the premise for the next century is the expansion of energetic boundaries to the sea, where on a global scale, the oceans occupy approximately 75 % of the total surface area of the Earth, assuming the important role of our large solar cell. Thus, of the $2.1606ZW$ (600 million of MWh) of solar energy that reaches the planet annually, only $0.4321ZW$ (120 million MWh) is absorbed by the oceans and converted into thermal, chemical, mechanical, and biochemical energy. The theoretical potential of energy accumulated in the oceans can be converted into electrical energy and the various forms include the following (Figure 1): 1) thermal gradient 40 $40PW$; 2) salinity gradient $1.4PW$; 3) marine current $5TW$; 4) tidal $2.7TW$; and 5) wave $2.5TW$ [18].

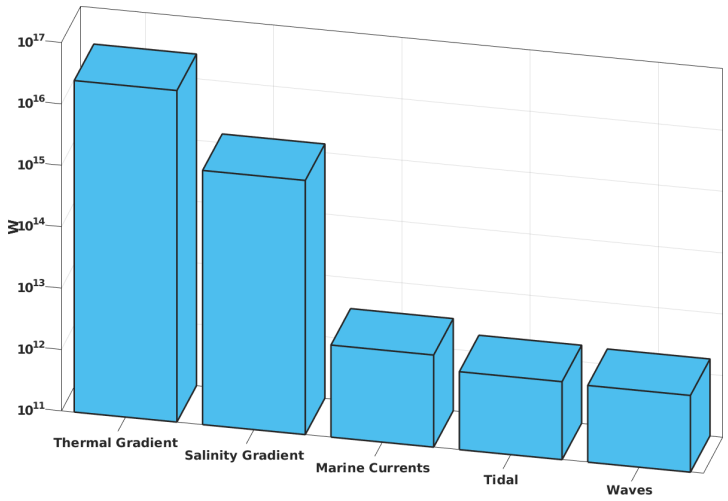

Figure 1: *Theoretical potential of the renewable energy forms in the oceans to be converted into electrical energy, adapted from Silva [18].*

Tropical countries are favourable sites for renewable technologies due to their geographic positions, as these areas are directly affected by high radiation rates. A large portion of the south Atlantic Ocean and Blue Amazon receive high insolation in this equatorial range, which increases the sea surface temperature (SST). The energy is captured in the mixing layer at values close to 28^0C. The average annual temperature of the mixing layer throughout the region, excluding upwelling sites and entry of the coastal current within this domain, ranges from nearly 25^0C to approximately 29^0C. Depending on the latitude of a site, the wind and wave regime and current forcing of the vertical distribution (order of tens of metres deep) of the thermal properties, the mixing layer may have different characteristics.

Below the mixing layer, the water becomes colder with increasing depth, with temperatures around 4^0C. In deeper regions, the soil temperature falls only a few tenths of a degree. This cold water is the result of melted ice water accumulation from the polar regions. Due to the higher density and minimal mixing with the upper waters, the cold water flows along the ocean floor from the poles towards the lower latitudes, following the momentum flow, density adjustment, and thermohaline circulation. The result of these physical processes is the creation of an oceanic structure in the form of a large thermal reservoir, where warm water is compartmentalized on the surface and cold water is deeper, and the temperature difference is maintained, with seasonal and climatic variations, throughout the year.

A potential thermal gradient energy site can be evaluated by using an energy conversion module based on a large OTEC ($100MW$) plant [23]. In the work of de Souza and Marques [20], the physical equations that constitute the numerical model, implemented in the form of a high-capacity algorithm indexed in a programming script, are presented in a synthetic form. The results obtained in this study will be applied to an updated version of this numerical model, simulating the output of a theoretical OTEC plant.

Considering the economic, energy and planning importance of policies in encouraging the use of renewable energies worldwide and the exploration rights issues of the Blue Amazon and south Atlantic Ocean, the scope of this work includes mapping of the thermal gradient in the

south Atlantic Ocean, highlighting the Blue Amazon, and the identification of possible sites that could receive an OTEC plant near the coast to be fully operational throughout the Julian calendar cycles.

2. Ocean Thermal Energy Conversion (OTEC)

According to the most widely used guide to this technology by **?**], the process of converting ocean thermal energy into electrical energy is globally known as Ocean Thermal Energy Conversion (OTEC). During this process, the temperature difference will operate on a thermodynamic cycle (closed, open or hybrid), which produces electricity. Systems in global operation use the Second Law of Thermodynamics applied to the ocean's thermal reservoir, known as the Rankine Cycle (Figure 2)), which is based on the Carnot Cycle.

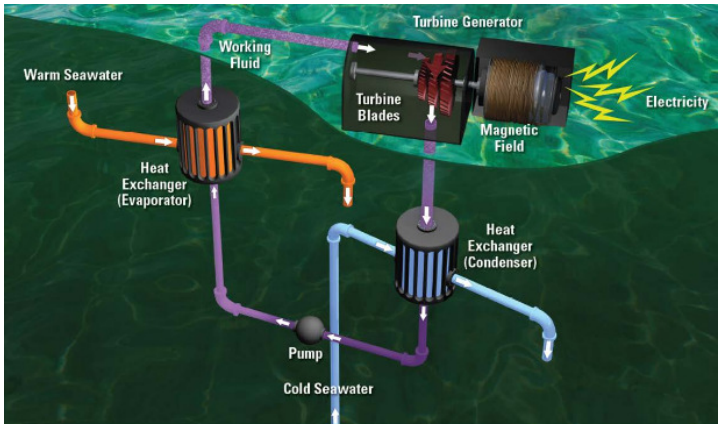

Figure 2: *A thermodynamic cycle adapted to the ocean Rankine Cycle in its closed form, demonstrating all the basic apparatus and structures involved in OTEC plant operation, adapted from Ascari et al. [2].*

In Figure 2, the cycle shown is large plants offering high energy return ($100MW$) [23]. According to the Technical Report by Ascari et al. [2], the maximum depth of the cold water collection pipeline should not be greater than $1000m$, i.e. pressure of approximately 100 atmospheres ($1.01x107P_a$). According to Crews [8], in the operation of an OTEC plant (Figure 2), the correct efficiency of the Rankine Cycle appropriately establishes a temperature difference equal to or greater than 20^0C between the hot and cold water collection pipes. The OTEC technology is mainly viable in the configuration of an established thermal gradient, which is equal to or greater than 20^0C between the surface and a maximum of 1000 m depth. The geographic characteristics, oceanographic thermal signatures and technical limitations of the literature suggest that an OTEC plant would have full operating capacity within the limits of the Brazilian Blue Amazon.

In a region of low latitudes, such as the equatorial region of the Blue Amazon, the cold water obtained by the OTEC plant's pump system (Figure 2), located at the base of the thermocline, has a thermal signature of approximately 4.4^0C. After passage through the condenser [23], this water has a temperature gain of 23.6%, i.e., reaches the signature surface of 7^0C, creating an artificial upwelling (deep, cooler vertical water flow charged to the surface carrying a large amount of nutrients). Considering this information as a starting point, it is possible to consider the use of this upwelling in the cultivation of species adapted to low temperature waters. The main species

for mariculture in the Brazilian scenario would be Atlantic Salmon, Brown Trout, shrimp, crabs, oysters and macroalgae.

The OTEC system also offers other benefits, such as negative feedback on ocean acidification (releases CO_2 to the atmosphere via artificial upwelling) and global warming (removal of heat content from the ocean). In addition, an OTEC plant can generate climatic conditioning, from buildings (inshore OTEC plant) and from a platform (offshore OTEC plant), by directing the bottom water, desalinating sea water and sea salt (via use of seawater as a working fluid in the open thermodynamic cycle).

3. Blue Amazon

The shores of the Brazilian coast are some of the most dynamic regions of the global ocean [7]; [15]. The south Atlantic Ocean is characterized by large thermohaline contrasts, which is an ideal scenario for the extraction of thermal energy from the oceans and intense mesoscale activity [9]. This scenario is due to the various water masses found in the region, which generate high spatial and temporal variability [6]. Additionally, Brazil has the Blue Amazon with an area of 4.4 million km^2 (Exclusive Economic Zone - 3.5 million km^2 + the extended continental shelf - 911 thousand km^2),(Figure 3), and the Blue Amazon is an average of 200 nautical miles from the coast, which constitutes the concept of maritime space introduced by the United Nations Convention on the Law of the Sea (UNCLS).

In the Blue Amazon, Brazil has sovereign rights for exploration, exploitation, conservation and management of living and nonliving natural resources of the waters overlying the seabed, soil and subsoil, as well as exploitation consideration for economic purposes and the sovereignty production of electric energy from the thermal gradient. However, the country lacks studies on renewable marine energy, which will consolidate a sustainable strategic reserve for the Brazilian energy matrix in the near future.

Among all forms of renewable energy from the sea, the main goal of the present study is to map the resources associated with the thermal gradient, which is the largest solar energy well stored in the oceans. The region addressed in this analysis covers from 10^oN-36^oS to 24^oW-60^oW,(Figure 3), with a focus on the Blue Amazon.

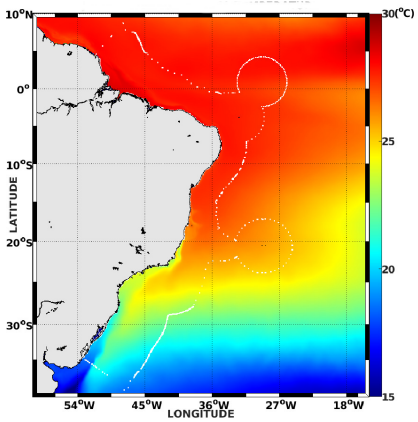

Figure 3: *The first vertical level of SST calculated by the hydrodynamic model, which covers a large part of the south Atlantic Ocean and the entire Blue Amazon.*

3.1. Forcing

3.1.1. Equatorial portion

The energy balance of the ocean-atmosphere system in the study region is characterized by heat gain through radiative processes. Short-wave radiation (i.e., ocean gains energy) and latent heat flux (i.e., loss of heat through evaporation) are the most relevant components of the tropical Atlantic heat balance. On the other hand, the equatorial ocean is distinct from other oceanic regions due to the dynamic and thermodynamic particularities of the equatorial ocean. The geostrophic balance near the equatorial region decreases in such a way that the Ekman transport disappears, and the surface currents are driven by the easterly winds [14].

Regarding the energy balance in the ocean-atmosphere system over equatorial regions, the annual variations in SST are more dependent on the interactions between the two compartments than on the annual cycle of surface heat flows into the Atlantic Ocean Tropical [5]; [25]. Vertical mix variations are induced by wind, vertical and horizontal heat advection and cooling due to evaporation, which is related to ocean-atmosphere feedback processes. All these processes are directly or indirectly associated with the reduction or intensification of surface wind, which is largely determined by intertropical convergence zone displacement [4]; [24].

The intertropical convergence zone (ICZ) is situated in warm water regions, where convection and consequent intense cloudiness and precipitation exist [10]. When the intertropical convergence zone is situated over a given region, the horizontal wind intensity weakens and the main components of the surface radiation balance decrease [19]. Despite the reduction in surface incident solar radiation, previous studies have identified the role of wind reduction in promoting SST increase as a result of two main factors: decrease in latent heat loss induced by wind and thermocline increase [19].

Precipitation in the equatorial Atlantic is related to movement of the intertropical convergence zone due to the amount of clouds and evaporation. Precipitation rates are higher in the tropics than in subtropical regions, and the daytime precipitation regime in Ecuador is characterized by a maximum at night and in the early morning [11]. Precipitation in the equatorial Atlantic is closely related to longwave radiation rates, since the annual SST cycle varies modestly in the equatorial region. The greatest variability of longwave radiation is a result of the cloud quantity and their height variations [3].

This equatorial portion of the south Atlantic Ocean includes the upper part of the great anticyclonic gyre. According to Stramma and England Stramma and England [21], this gyre is meridionally bounded by the South Atlantic Current at the lower boundary and the South Equatorial Current at the upper boundary. The eastern edge of this ocean is occupied by the Benguela Current. The Western Boundary Current that completes the gyre is the Brazil Current. Although it seems like a simple flow pattern, the flow of the South Equatorial Current into the Brazilian continental margin is complex. Upon reaching the continental margin (about 24^0S), this stream is forced to bifurcate. The South Equatorial Current is described as a horizontally extensive westward flow, which crosses the Atlantic Ocean to the Brazilian coast. The Brazilian Current and Northern Brazil Current, Tropical Water, South Atlantic Central Water, and Antarctic Intermediate Water constitute the upper circulation portion of the equatorial south Atlantic Ocean [21]; [26] within the vertical range of interest.

Considering the stability of the SST values along the annual signal, the minimum variation amplitudes and the water masses constituting the vertical profile (from 0 to $1000m$) at this equatorial range, we can expect intense thermal gradients and a small temporal variability.

3.1.2. Southeast-south Portion

The characteristics of the southeast-south portion of the Atlantic Ocean are directly related to the characteristics of the equatorial range of the domain. The most pronounced from the thermal point standpoint is the Brazilian Current, which carries the heat absorbed in the equatorial portion towards the greater latitudes, bordering the coast and the continental shelf (zones contained within the Blue Amazon). The classic definition of the Brazil Current according to Podestá et al. [16] and Olson et al. [13] is that of a high temperature salinity tongue flowing south along the continental margin, and the current's seasonality is marked by the advance and retreat modulated by the ICZ movement.

Considering the seasonally pronounced characteristics, the average thermal gradient fields in the southeast-south portion are highlighted in the winter by the large variability in surface spatial distribution. These characteristics may be associated with the hydrodynamic processes that reconfigure in an abrupt and concomitant way: the Brazil Current retreat, the sub-Antarctic water advancement, the Brazil Current displacement, the La Plata River front advancement and the Coastal Counter Current flowing north.

Therefore, a more homogeneous condition is observed during the summer, which alternates shape with more apparent features during the winter. According to Acha et al. [1], another important aspect for the thermal gradient is the upwelling conditions that predominantly occur during the summer and spring months, when the N-NE wind regimes are observed, which favours penetration of the South Atlantic Central Water and the Antarctic Intermediate Water into the subsurface. In the Cabo de Santa Marta (SC) and Cabo Frio (RJ) regions [17], surface water with a similar signature to that of the Southern Atlantic Central Water during the summer period maximizes the vertical thermal gradient at lower depths but at restricted time intervals. The vertical distribution of water bodies is mainly the same as that of the equatorial portion.

However, the presence of seasonal SST variability, the seasonal contribution of the Brazilian Current and low radiation rate incidence during winter and spring may result in a lack of OTEC plant operation for a significant number of days annually, which limits full movement towards higher latitudes.

4. Data and Methods

The methodology used in the present study is based on development of computational algorithms used to process the temperature results of a global three-dimensional numerical model. This sum of applied tools will enable mapping, as well as obtaining the spatial (x, y, z) and temporal (daily, monthly, seasonal and annual Julian cycles) variabilities in temperature and the thermal gradient contained in the south Atlantic Ocean and Blue Amazon. This study follows that of Tarbell et al. [22], where the first step in the analysis consists of conducting mapping of available resources. Through an understanding of this mapping, we hope to determine the viability and accessibility of these resources.

4.1. Data - Global Model

The HYCOM (HYbrid Coordinate Ocean Model, `https://hycom.org/`) is a multi-institutional effort sponsored by the National Oceanographic Partnership Program (NOPP), as part of the Global Ocean Data Assimilation Experiment (GODAE), to develop and evaluate the hybrid assimilative data of isoponic-sigma-pressure. The hybrid approach to an ocean of vertical structures allows the model to provide a more robust representation of the effects of surface exchange

processes, advection on isopycnals and flows due to bathymetric features. This representation of the vertical structure improves illustration of the exchanges among model compartments in terms of the numerical interfaces of processing, enabling a more realistic representation of the oceanic temperature structure, which is important in the variable evaluations associated with OTEC technology [2]. The high quality publications from the international scientific community indicate the robustness of this information source and researchers' results on oceanographic parameters. The HYCOM temperatures were collected from the study area in 40 vertical levels (depth of up to 6366m) with a temporal resolution of 3h from 1 January 1993 to 31 December 2012, and the experiments were 19.0 and 19.1, totalling 20 years of results.

4.2. Method - Julian Climatology

From the results mentioned in the previous subsection, averages were calculated based on Julian calendar (Table 1), which include the mean of the daily signal (average of eight data points per day, followed by the average of days over 20 years), monthly (counters for January (1-31), February (32-59), March (60-90), April (91-120), May (121-151), June (152-181), July (182-212), August (213-243), September (244-273), October (274-304), November (305-334), and December (335-365)), seasonal (counters for summer (355-79), autumn (80-171), winter (172-263), and spring (264-354)) and annual (1-365) averages. These results allow for the evaluation of thermal gradient variability in the south Atlantic Ocean and the Blue Amazon. The temperature differences among the vertical levels of the model were calculated by means of Julian climatological averages, which subsequently enabled verification of the behaviour of the various vertical thermal gradient fields along the obtained signals.

Table 1: Julian calendar and its representation of the passage of days in relation to the sun

Date	Jan	Feb	Mar	Apr	May	Jun	Jul	Aug	Sep	Oct	Nov	Dec
1	1	32	60	91	121	152	182	213	244	274	305	335
2	2	33	61	92	122	153	183	214	245	275	306	336
3	3	34	62	93	123	154	184	215	246	276	307	337
4	4	35	63	94	124	155	185	216	247	277	308	338
5	5	36	64	95	125	156	186	217	248	278	309	339
6	6	37	65	96	126	157	187	218	249	279	310	340
7	7	38	66	97	127	158	188	219	250	280	311	341
8	8	39	67	98	128	159	189	220	251	281	312	342
9	9	40	68	99	129	160	190	221	252	282	313	343
10	10	41	69	100	130	161	191	222	253	283	314	344
11	11	42	70	101	131	162	192	223	254	284	315	345
12	12	43	71	102	132	163	193	224	255	285	316	346
13	13	44	72	103	133	164	194	225	256	286	317	347
14	14	45	73	104	134	165	195	226	257	287	318	348
15	15	46	74	105	135	166	196	227	258	288	319	349
16	16	47	75	106	136	167	197	228	259	289	320	350
17	17	48	76	107	137	168	198	229	260	290	321	351
18	18	49	77	108	138	169	199	230	261	291	322	352
19	19	50	78	109	139	170	200	231	262	292	323	353
20	20	51	79	110	140	171	201	232	263	293	324	354
21	21	52	80	111	141	172	202	233	264	294	325	355
22	22	53	81	112	142	173	203	234	265	295	326	356
23	23	54	82	113	143	174	204	235	266	296	327	357
24	24	55	83	114	144	175	205	236	267	297	328	358
25	25	56	84	115	145	176	206	237	268	298	329	359
26	26	57	85	116	146	177	207	238	269	299	330	360
27	27	58	86	117	147	178	208	239	270	300	331	361
28	28	59	87	118	148	179	209	240	271	301	332	362
29	29		88	119	149	180	210	241	272	302	333	363
30	30		89	120	150	181	211	242	273	303	334	364
31	31		90		151		212	243		304		365

4.3. Method - Thermal Gradient

The thermal gradients between the surface and depth were obtained with the aim to select the main variations associated with the vertical temperature profile. Considering the operational limits of the OTEC plant in terms of the cold water collection pipe depth ($1000m$) [2], it was possible to highlight the thermal vertical extract at the thermocline top, as well as its variation and base ranges; below these vertical thermal features, the temperature variation is minimal with depth, and the profile is nearly constant.

4.4. Method - Energy Sites

Based on identification of the most energetic sites in the Blue Amazon (with different thermal signatures), the temporal series of SST and subsequent levels were collected up to 1000-m depth, alternating every 100 m (model depth and subscript of the HYCOM relative level: $0m_1$, 100_{20}, 200_{23}, 300_{25}, 400_{27}, 500_{28}, 600_{29}, 700_{30}, 800_{31}, 900_{32} and 1000_{33}), according to Table 1.

This process allows for verification of the sensitivity and variability of signals obtained from each energetic site, enabling the following: site selection and depth, yield maximization and reduction in costs from the infrastructure standpoint, and the operation of the OTEC plant and its subsystems. According to Crews [8], for the installation of an OTEC plant, a thermal gradient of at least 20^0C is required, and this operational limit was highlighted and considered in the present work.

5. Results and discussion

From the climatic results of the monthly, seasonal and annual average temperatures, thermal gradient maps were obtained for all the cycles cited in the methodology (section 4.2, Figures 4, 5 and 6). These values allowed for verification of the cycle variabilities. Based on the technical report highlighted in section 4.3 and with the aim to provide the maximum thermal gradient in each of the cycles, the thermal gradient between the surface and depth of $1000m$ was selected, since this gradient represents the deeper tubing of cold water collection in the OTEC system (Figure 2).

The results show that the mean Julian thermal gradient fields have temporal and spatial variabilities, which differ from the equatorial and southeastern regions of the south Atlantic Ocean, as indicated in sections 3.1.1 and 3.1.2. The results establish a direct relationship with the limits imposed by the theory, which were observed in the temperatures along the water column, as well as the analysis tools responsible for indicating the maintenance and configuration of the oceanic thermal energy reservoir.

In addition, it was possible to obtain representation of the cycles inserted in the Julian calendar, highlighting the daily cycle that presents the sine of annual variability along its passage, which makes the behaviour of the relevant variables available to the gradient composition and sensitivity of the thermal energy sites highlighted in the Blue Amazon.

5.1. Thermal gradient between the surface and $1000m$ *- cyclic climatology*

5.1.1. Monthly Cycle

The results indicate that there is a region with high thermal gradient values and the largest area delimited by the minimum thermal operating gradient is isolated at 20^oS, which is highlighted in Figures 4 a), b), c) and d) along nearly the entire domain of the Blue Amazon. The highest thermal gradient values in the latitudinal ranged between 0^0 and 20^0S. These results

confirm the previous results listed in section 3.1.1, which mention the occurrence of the highest radiation rates on the south Atlantic Ocean in the maximum thermal gradient zone. Additionally, as discussed by 3.1.2, within the solar activity cycle, the modulations associated with the intertropical convergence zone and the Brazil Current, the SST values and radiation rates decrease moving away from the tropical latitudes, as indicated in Figures 4 (f), (g), (h), (i) and (e) moving towards the lower latitudes of the thermal gradient isolated at 20^oS.

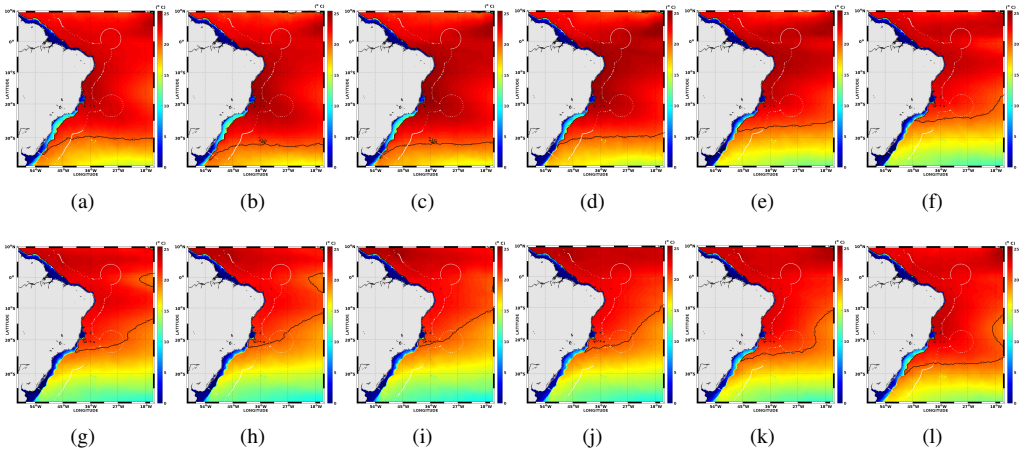

Figure 4: *Thermal gradient averages between the surface and* 1000*m, (levels* 1 *and* 33 *of the HYCOM model), with an emphasis on the thermal gradient isoline of* 20^oC *(in black), operating at the limits of an OTEC plant during a) January, b) February, c) March, d) April, e) May, f) June, g) July, h) August, i) September, j) October, k) November and l) December.*

In July, August, September and October, the thermal gradient isoline boundary shifts, generating a significant reduction in the operational area of the OTEC system in the south Atlantic Ocean. Thus, in addition to the capacity loss of operation in the domain, a robust decrease in the thermal indexes occurs in the region that remains operational. Further details concerning the direct relationship between the thermal gradient and the variations associated with the oceanographic and atmospheric phenomena modulated by the seasonal variability were explored in section 3.1.1.

5.1.2. Seasonal Cycle

Seasonal patterns show uneven features throughout the domain. The behaviour of the thermal gradient changes at nearly all stations by the mechanisms mentioned in section 3.1.2. Thus, the variability is associated with the radiation budget and the movement of the ICZ and consequently, the displacement of the Brazil Current and progression of the Brazil-Malvinas confluence. Therefore, the vertical thermal gradient presents sensitivity to seasonality, showing the peak of the sine cell of the annual signal as well pronounced during the passage of the seasons.

By grouping the stations with similar characteristics together, as shown in Figures 5 (C) winter and (d) spring between Julian calendar days 172 to 263 (spring) and 264 to 354 (winter), the results indicate an operational area loss of the OTEC system with upward movement of the isolated 20^oC area towards the lower latitudes. In addition, Figures 5 a) summer and b) fall

between Julian calendar days 355 to 80 (summer) and 81 to 172 (autumn) illustrate the following: (i) during summer, the largest operating area of the OTEC system is present; and (ii) over autumn, a 10^o latitude loss occurs towards the lower latitudes, indicating thermal gradient field variability and consequently, the operating condition of the OTEC plant. However, we can highlight that there is a vast area that includes all stations in the south Atlantic Ocean and Blue Amazon that have high thermal energy contents, and consequently, there are viable areas for an OTEC plant operation.

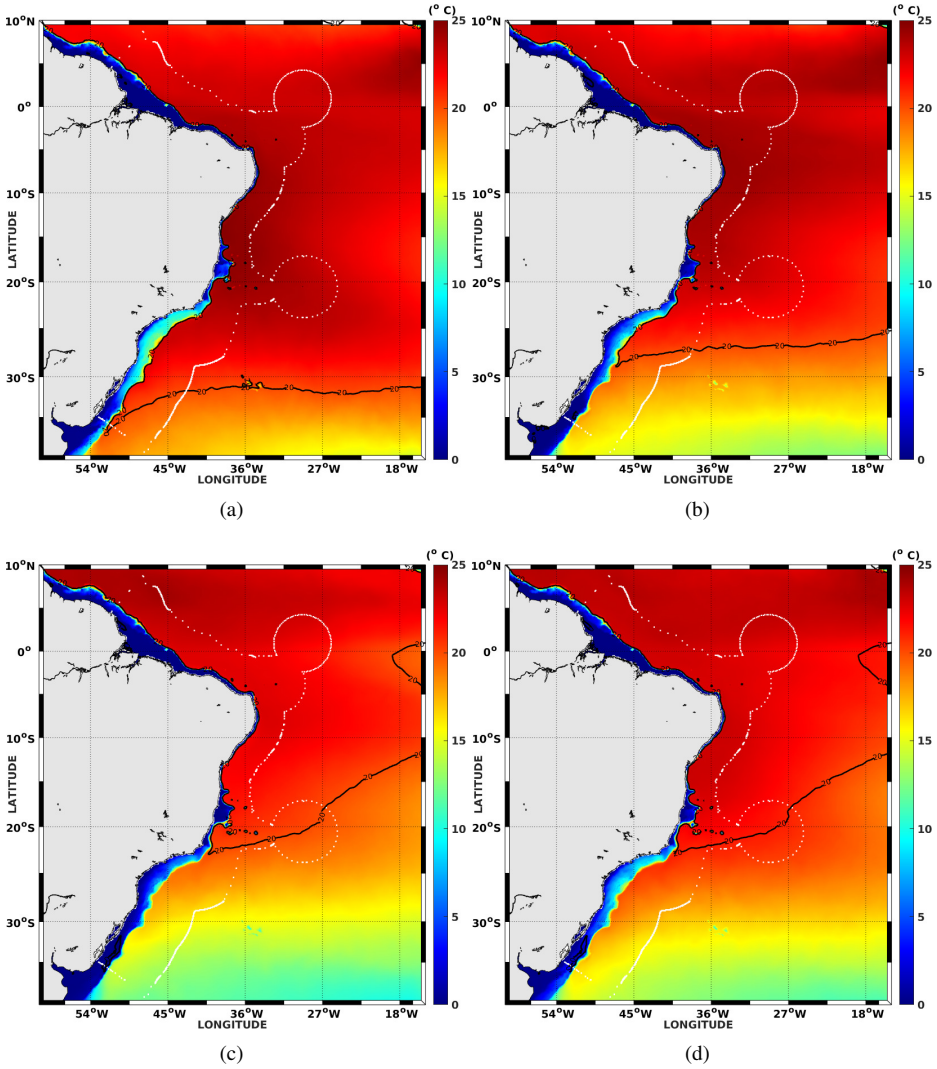

Figure 5: *Thermal gradient averages between the surface and* 1000*m, (levels* 1 *and* 33 *of the HYCOM model), with an emphasis on the thermal gradient isoline of* 20^oC *(in black) and the OTEC plant operating limits in a) summer, b) autumn, c) winter and d) spring.*

5.2. Annual Cycle - Thermal energy sites

As observed in the previous section, there is a wide area of thermal gradient that is considered operational for an OTEC system in the Blue Amazon. According to Ascari et al. [2], the maximum depth value for an operational OTEC system is $1000m$, and the temperature difference between vertical ocean levels must be equal to or greater than $20^{O}c$ (as the thermodynamic operational system mutt adapt to the oceanic Rankine Cycle) [8]. Thus, eight bands of variation were identified in the annual mean of the vertical thermal gradient (depths between 0 and $1000m$) with the following points: (1) $23.5^{o}C$, (2) $23^{o}C$, (3) $22.5^{o}C$, (4) $22^{o}C$, (5) $21.5^{o}C$, (6) $21^{o}C$, (7) $20.5^{o}C$, and (8) $20^{o}C$, as shown in Figure 6.

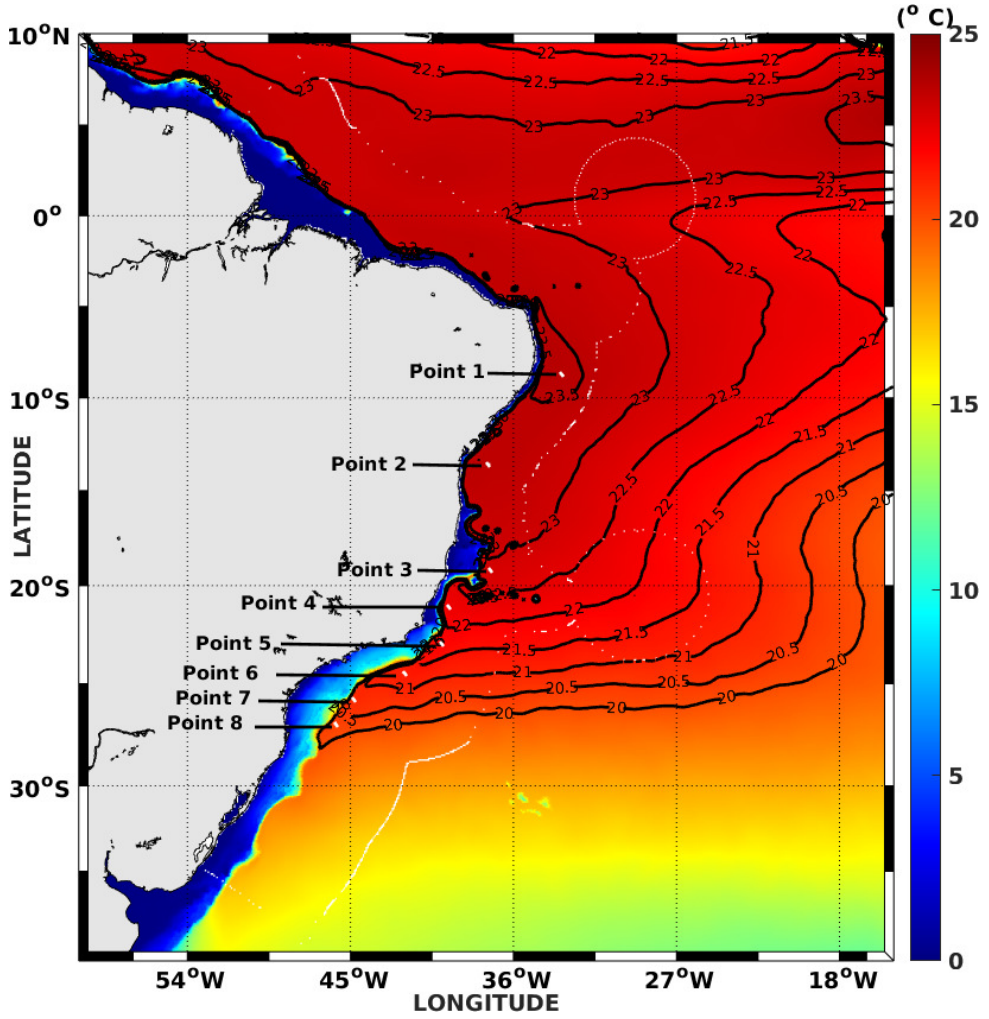

Figure 6: *Annual average of Thermal Gradient between the surface and* 1000*m, (levels* 1 *and* 33 *of the HYCOM model). The area delimited (white dots) represents the Blue Amazon. Highlighted isotherms of* $20^{o}C$, $20.5^{o}C$, $21^{o}C$, $21.5^{o}C$, $22^{o}C$, $22.5^{o}C$, $23^{o}C$, $23.5^{o}C$, *where eight data points were extracted, respectively connected to the thermal gradient isolines.*

Based on this information, temperature time series were extracted, then transformed into thermal gradients at defined points, maintaining the value defined by Crews [8] for an operational thermal gradient along the daily Julian calendar. Based on these results, the sites and their depth levels, which have operational viability, will be highlighted. Additionally, locations that have the yield maximization and minimization of the OTEC plant operating costs (reduction in the semiadiabatic pipeline depth) can be evaluated, advancing the state-of-the-art resource mapping.

5.2.1. Temperature vertical profile in the energy sites

In this study, the maximum thermal gradient was always calculated between the surface and 1000m; these interval depth extracts indicated in section 4.4 were selected, highlighting the most pronounced oceanographic features along the vertical profile, such as the mixing layer, the thermocline top, and the thermocline base.

As we have a significant amount of results regarding the daily Julian temperature climatology over 365 days, visualization of the thermal profiles throughout the entire Julian calendar would be difficult. Thus, the results of the averages processed in the annual signal in the eight points presented in the Blue Amazon (Figure 6) were considered with the aim of identifying the most important variation ranges within the vertical profiles, as well as the configurations of the mixing layer, thermocline top and base. Based on these results, it will be possible to identify the depth ranges where the hot and cold water collection pipes can be installed. The higher thermal gradient values are expected to be present between the thermocline and the thermocline base layer, and due to the stability condition of the vertical distribution, variations in the thermocline base of up to 1000m depth are small. The verification of this hypothesis and the characterization of the vertical temperature profile, shown in Figure 7, will be confirmed during the results discussion (Figura 8).

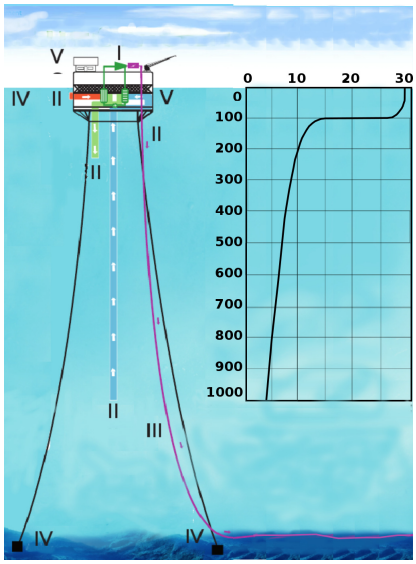

Figure 7: *Representative scheme of the subsystems of an OTEC plant: I - thermodynamic closed circuit (Rankine), II - hot and cold water collection pipes (input and output), III - power transmission cable, IV - mooring system of stability, and V - the typical temperature profile along the operating depth.*

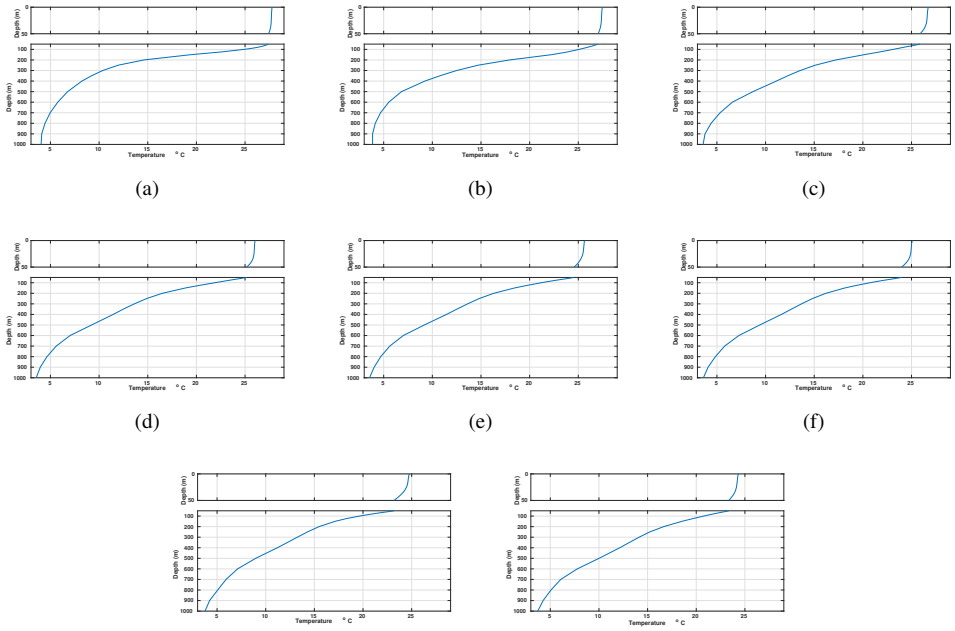

Figure 8: *Temperature vertical profiles of points: 1 (a), 2 (b), 3 (c), 4 (d), 5 (e), 6 (f), 7 (g), and 8 (h), referring to the thermal gradient isolines indicated in Figure 6, which are contained in the Blue Amazon and separate the mixing layer and remainder of the profile up to* 1000*m in each graph.*

In Figure 8, it is possible to evaluate the characteristics of the selected points due to their similarities along the vertical structure, with slight variations in temperature and depth values in the mixing layer, thermocline top and base. These variations mainly originate in latitudinal temperature variations, since the temperature vertical profile inclination along the water column has characteristic intervals of thermal and depth variations between the top and base of the thermocline. On the other hand, it is possible to identify a characteristic change in the mixing layer slopes and in the vertical profile after the thermocline base, which occurs when there is still a sufficient inclination rate for thermal gradient signal perturbation as a function of the small depth variation.

As shown in Figure 8 a) point 1, b) point 2 and c) point 3, it is possible to realise a mixing layer that is nearly tangent to the depth axis, and by losing this characteristic at a depth of 40m, this slope that can be interpreted as the beginning of the thermocline. Following the five thermal variation bands as a function of depth, which is distinct at the rate of $^oC/m$, the thermocline base at 900m is observed for all three points, and the thermal gradient values below should be similar, which corroborates with the typical profile presented in Figure 7.

As shown in Figure 8 d) point 4, e) point 5, f) point 6, g) point 7, and h) point 8, it is possible to evaluate a set of characteristics for all points as a consequence of the same patterns observed along the vertical structure, and only the values at the top of thermocline differ. This variation is a result of the lower incident radiation, which is related to the points deviation in the lower latitude regions. Due to these factors, we have an impact on the temperature variation rates with depth

($^oC/m$), which changes the slope of the vertical profile sectors and allows for the perturbation of the thermal gradient signal with small depth differences.

In the 8 d) point 4, e) point 5, f) point 6, g) point 7, and h) point 8, it is possible to evaluate a set of characteristics of all points as a consequence of their same patterns observed along of the vertical structure, differing only the values at the top of thermocline. This variation is a result of the lower incident radiation, which it is related to the points deviation at regions of lower latitudes. Due to these factors, we have a repercussion on the temperature variation rates with the depth ($^oC/m$), changing the slope of the vertical profile sectors, and allowing perturbation of thermal gradient signal in small differences of depth.

5.3. Daily cycle and the annual sine wave - Thermal sensitivity

The variability in the thermal gradient for a cycle less than 24 hours is minimal and normalized due to the processing of the daily Julian mean (absence of the daily variability sine). Figure 6 shows the maximum values of the mean annual thermal gradient over the days to demonstrate the time series that composed the daily mean in Figure 9, which presents the respective surface levels and 1000m along the highlighted gradient isolines and demonstrates the constituents of the mean annual thermal gradient signal.

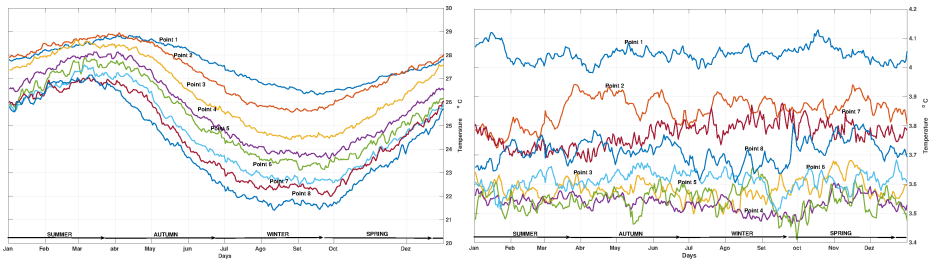

(a) (b)

Figure 9: *Seasonal SST time series (model HYCOM, level 1) a) and 1000 m (model HYCOM, level 33); b) from points 1, 2, 3, 4, 5, 6, 7, and 8 contained in the Blue Amazon, referring to the isolines of the same gradient indicated in Figure 6.*

The results indicate a correlated behaviour between the SST data (Figure 9 a)) and the maximum values of the thermal gradient of the map (Figure 6), i.e., a decrease in the values occurs towards the lower latitudes in the time series at each of the points, illustrating the decrease in thermal gradient values at all points. However, when checking the bottom temperature values (Figure 9 b)), a minimum variation of about 0.6^oC was observed between all points, and there was no correlation between the thermal gradient behaviour and the SST. Therefore, it is possible to confirm that the bottom temperature is part of thermal gradient annual signal, but the behaviour and values of the surface temperature define the bottom temperature amplitude and variation.

5.3.1. Definition and Viability of energy sites

Based on the direct observations in Figures 10, 11, 12, 13, it is possible to highlight that points 1 and 2 (Figure 10) have operational thermal gradients at several depths. Point 3 (Figure 11 a)) is operative between the surface and some depths. On the other hand, from point 4, the plant is no longer operational throughout the period. From point 5 to point 8, none of the sites can

remain within the minimum temperature difference of 20^oC, and nonoperational time intervals are extensive and representative to provide implementation viability of a long-term OTEC plant.

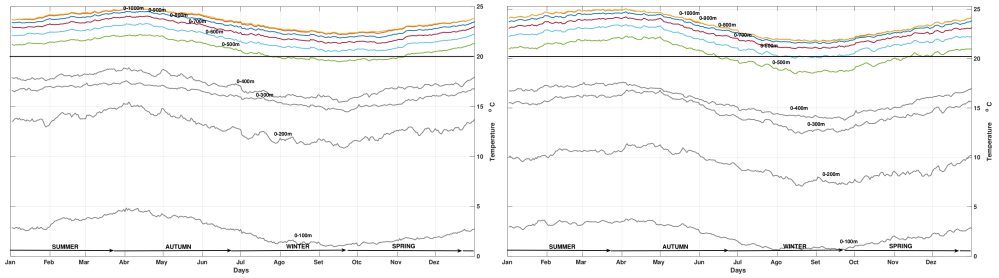

(a) (b)

Figure 10: *Time series of thermal gradients between the surface and depth ranges up to* 1000*m (alternating every* 100*m) in points 1 and 2, referring to thermal gradients isolines of* 23.5^oC *and* 23^oC *shown in Figure 6 and highlighting the solid black line, which marks the minimum operational thermal gradient threshold of Crews [8].*

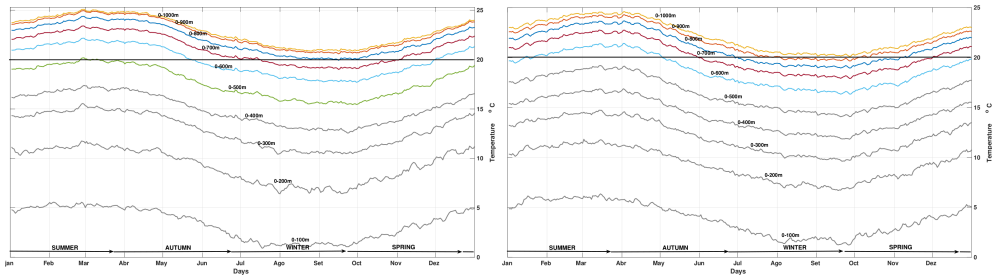

(a) (b)

Figure 11: *Time series of thermal gradients between the surface and the depth ranges up to* 1000*m (alternating every* 100*m) in points 3 and 4, referring to thermal gradients isolines of* 22.5^oC, 22^oC, 21.5^oC *and* 21^oC *indicated in Figure 6 and highlighting the continuous black line, which marks the minimum operational thermal gradient threshold of Crews [8].*

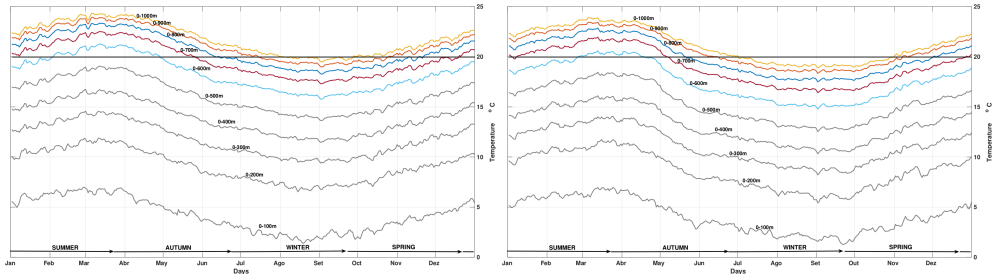

(a) (b)

Figure 12: *Time series of thermal gradients between the surface and the depth ranges up to* 1000*m (alternating every* 100*m) in points 3 and 4, referring to thermal gradients isolines of* 22.5^oC, 22^oC, 21.5^oC *and* 21^oC *indicated in Figure 6 and highlighting the continuous black line, which marks the minimum operational thermal gradient threshold of Crews [8].*

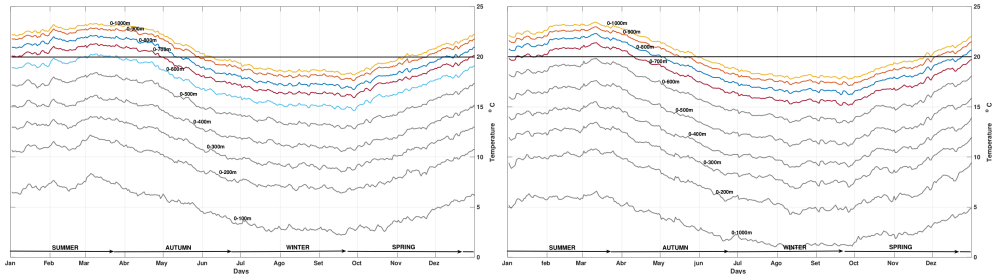

(a) (b)

Figure 13: *Time series of thermal gradients between the surface and depth ranges up to* 1000*m (alternating every* 100*m) in points 7 and 8, referring to thermal gradients isolines of* 20.5^oC *and* 20^oC *indicated in Figure 6 and highlighting the continuous black line, which marks the minimum operational thermal gradient threshold of Crews [8].*

The results of this section indicate the narrowness of operational viability for an OTEC plant at sites 1,2 and 3 of the study area (Figure 6). Figures 10 and 11 a) indicate the variability in the thermal gradients at the depths of interest, showing low seasonal sensitivity and operational thermal gradients throughout the annual sinusoid, and the daily Julian mean at several depths.

5.3.2. Operational depths and latitudinal variability

Based on the three viable sites (points 1, 2 and 3, shown in Figure 14) and the annual average ranges of operating thermal gradients, 23.5^oC, 23^oC and 22.5^oC, throughout the mean Julian daily calendar, it is possible to complete the analysis and present the thermal gradients formed between the surface and depth ranges that are viable for installation of an OTEC plant.

An analysis of the site variability indicated by points 1 and 2 in Figure (10) made it possible to verify the operational viability between the surface and depth levels $600m \leq z \geq 1000m$ m throughout the annual sinusoid. These sites, which are located in the Blue Amazon, contain the largest operational depth ranges, making these the best thermal structures to which to apply the OTEC concept. Site 1 has higher thermal gradients and upper gradient values in the depth bands

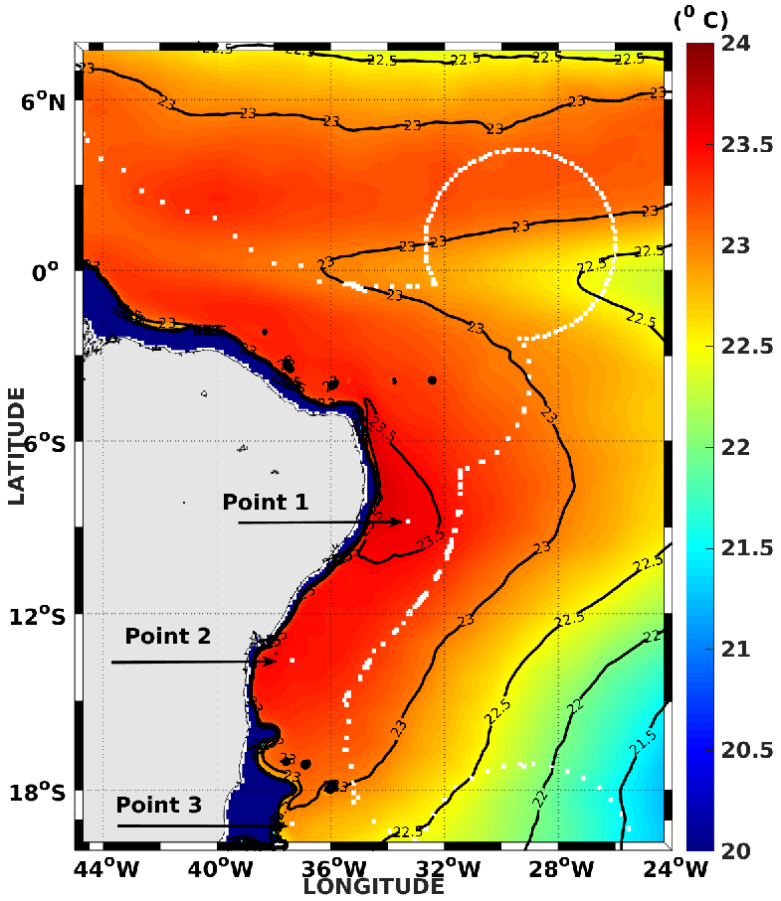

Figure 14: *Region of the south Atlantic Ocean and Blue Amazon, containing the three main Brazilian thermal energy sites, illustrating a future OTEC resource exploration park.*

(comparing the vertical axes in 10 a) and b)) than point 2. This result indicates that site 1 has the highest operational viability.

By observing the site indicated by point 3 and its variability (Figure 11 a)), it is possible to identify the operational viability between the surface and depth levels $900m \leq z \geq 1000m$ throughout the annual average time series. The thermal gradient variation between $900m \leq z \geq 1000m$ is nearly nonexistent, which is a consequence of being below the thermocline base where the temperature vertical profile is nearly constant.

Considering the operation of only three points among the eight points analysed, there is an evident direct relationship between the site characteristics and the latitudinal range that the sites occupy, i.e., we can establish a direct relationships among the amplitude of the thermal gradient (surface and its range of depths), sensitivity to the average daily Julian calendar, and the geographical latitudinal coordinates. In terms of the mean annual thermal gradients in relation to latitude (Figure 15), we can list a directly proportional relationship among latitude, radiation, SST (thermal gradient control variable), depth of the mixing layer and the thermal gradient.

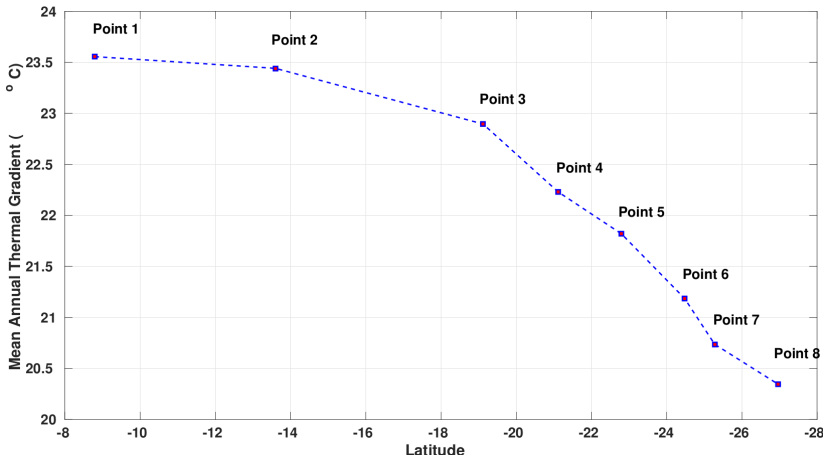

Figure 15: *Annual mean latitudinal variation at points that represent the eight regions of the same thermal gradient in Figure 6.*

6. Conclusions

In nearly the entire Blue Amazon, the average annual thermal gradients are greater than or equal to 20^oC. In this region, nine thermal gradient isolines were identified, with three thermal bands being fully operational throughout the period where the daily Julian average was processed. In these locations, points 1 and 2 have thermal gradient operability between the surface and depth range of $600m \leq z \geq 1000m$ and point 3 between the surface and depth range of $900m \leq z \geq 1000m$. The three vertical thermal structures along the annual average thermal gradient isolines and their point representatives 23.5^oC (PT_1), 23^oC (PT_2), and 22.5^oC (PT_3), represent extraction points of the thermal time series, with high energetic and commercial importance. Point 1 is highlighted, where the highest contents of thermal energy are found, and this area can be converted into its vertical compartments.

Therefore, the results obtained in this study indicate the viability of installing a solar thermal energy extraction facility in the Brazilian Blue Amazon, highlighting the large thermal energy reserve that is contained in a zone of national sovereignty with the potential to contribute strategically to the Brazilian energy matrix for sustainable development. In addition to renewable energy generation, these parks offer the possibility of continuous technological development and the installation of other structures dedicated to the extraction of animal protein (aquaculture farms), such as those that would benefit from the OTEC plant subproducts.

The information and decision-making presented here offer more technical detailed description and planning for all involved scientific environmental apparatus. By allowing a reduction in the semiadiabatic water transport of bottom water (smaller depths), capital losses may occur in numerous oceanographic campaigns at sea, requiring these campaigns to be more precise and of greater scientific impact. When using modelling and Julian signal filters (small time scale) with a high level of confidence in continuous operations, the main difficulty will be the investments; however, along the passage of days, months, seasons, and years, the investment return will certainly occur over a shorter timescale.

The results and definitions of the positions, amplitudes, capture depths, and variability in the

thermal gradients obtained in the present study impact the apparatus configurations for operation of the OTEC technology plant and subsystems. In this context, this study represents evolution of the state-of-the-art knowledge of potential thermal gradient energy exploitation in the oceans and of the technical configuration required for this exploitation. Once this possibility is presented to the market, it may become attractive to private investors and to the national renewable energy policy makers, which is an expectation for the XXI century.

7. Acknowledgements

The authors thank the Federal University of Rio Grande - FURG, and Conselho Nacional de Desenvolvimento Cientifico e Tecnologico (CNPq), for their support and financial aid. We thank CNPq for the research grants Process 88882.182313/2018-01 (RVS) and 308274/2011-3 (EHLF).

8. References

[1] Acha, E.M., Mianzan, H.W., Guerrero, R.A., Favero, M., Bava, J., 2004. Marine fronts at the continental shelves of austral south america: physical and ecological processes. Journal of Marine systems 44, 83–105.

[2] Ascari, M.B., Hanson, H.P., Rauchenstein, L., Van Zwieten, J., Bharathan, D., Heimiller, D., Langle, N., Scott, G.N., Potemra, J., Nagurny, N.J., et al., 2012. Ocean Thermal Extractable Energy Visualization-Final Technical Report on Award DE-EE0002664. October 28, 2012. Technical Report. Lockheed Martin Mission Systems and Sensors.

[3] Bomventi, T.N., Wainer, I.E.K.C., Taschetto, A.S., 2006. Relação entre a radiação de onda longa, precipitação e temperatura da superfície do mar no oceano atlântico tropical. Revista Brasileira de Geofísica 24, 513–524.

[4] Carton, J.A., Cao, X., Giese, B.S., Da Silva, A.M., 1996. Decadal and interannual sst variability in the tropical atlantic ocean. Journal of Physical Oceanography 26, 1165–1175.

[5] Carton, J.A., Zhou, Z., 1997. Annual cycle of sea surface temperature in the tropical atlantic ocean. Journal of Geophysical Research: Oceans 102, 27813–27824.

[6] Castro, B.d., Lorenzzetti, J., Silveira, I.d., Miranda, L.d., 2006. Estrutura termohalina e circulação na região entre o cabo de são tomé (rj) eo chui (rs). O ambiente oceanográfico da plataforma continental e do talude na região sudeste-sul do Brasil. EDUSP, São Paulo , 11–120.

[7] Chelton, D.B., Schlax, M.G., Witter, D.L., Richman, J.G., 1990. Geosat altimeter observations of the surface circulation of the southern ocean. Journal of Geophysical Research: Oceans 95, 17877–17903.

[8] Crews, R., 1997. Otec sites. Aquarius Rising Maldives-An Ocean Research Centre and Eco-tourist Facility 28.

[9] Gordon, A.L., 1989. Brazil-malvinas confluence–1984. Deep Sea Research Part A. Oceanographic Research Papers 36, 359–384.

[10] Hastenrath, S., Greischar, L., 1991. The monsoonal current regimes of the tropical indian ocean: Observed surface flow fields and their geostrophic and wind-driven components. Journal of Geophysical Research: Oceans 96, 12619–12633.

[11] McGregor, G.R., Nieuwolt, S., et al., 1998. Tropical climatology: an introduction to the climates of the low latitudes. Ed. 2, John Wiley and Sons Ltd.

[12] Neshyba, S., 1987. Oceanography: Perspectives on a fluid earth .

[13] Olson, D.B., Podesta, G.P., Evans, R.H., Brown, O.B., 1988. Temporal variations in the separation of brazil and malvinas currents. Deep Sea Research Part A. Oceanographic Research Papers 35, 1971–1990.

[14] Pedlosky, J., 1994. Ridges and recirculations: gaps and jets. Journal of Physical Oceanography 24, 2703–2707.

[15] Piola, A., Matano, R., Steele, J., Thorpe, S., Turekian, K., 2001. Brazil and Falklands (Malvinas) currents. Academic Press, London.

[16] Podestá, G.P., Brown, O.B., Evans, R.H., 1991. The annual cycle of satellite-derived sea surface temperature in the southwestern atlantic ocean. Journal of Climate 4, 457–467.

[17] Schettini, C., Resgalla Jr, C., Pereira Filho, J., Silva, M., Truccolo, E., Rörig, L., 2005. Variabilidade temporal das caracterísiticas oceanográficas e ecológicas da região de influência fluvial do rio itajaí-açu. Brazilian Journal of Aquatic Science and Technology 9, 93–102.

[18] Silva, P, C.M., 1978. Energias do Mar, in: Usos do Mar. Instituto de Estudos do Mar Almirante Paulo Moreira (IEAPM), Marinha do Brasil, Brasilia, p. 137;155.

[19] Skielka, U.T., Soares, J., Oliveira, A.P.d., 2010. Study of the equatorial atlantic ocean mixing layer using a one-dimensional turbulence model. Brazilian Journal of Oceanography 58, 57–69.
[20] de Souza, R.V., Marques, W.C., 2016. Energy budget of the thermal gradient in the southern brazilian continental shelf. Renewable energy 91, 531–539.
[21] Stramma, L., England, M., 1999. On the water masses and mean circulation of the south atlantic ocean. Journal of Geophysical Research: Oceans 104, 20863–20883.
[22] Tarbell, D., et al., 2006. Instream tidal power in north america–environmental and permitting issues.
[23] Vega, L.A., 1992. Economics of ocean thermal energy conversion (otec). Ocean Energy Recovery: The State of the Art, American Society of Civil Engineers, New York .
[24] Weingartner, T.J., Weisberg, R.H., 1991. On the annual cycle of equatorial upwelling in the central atlantic ocean. Journal of Physical Oceanography 21, 68–82.
[25] Yu, K., Wong, A., Yau, K., Wong, Y., Tam, N., 2005. Natural attenuation, biostimulation and bioaugmentation on biodegradation of polycyclic aromatic hydrocarbons (pahs) in mangrove sediments. Marine pollution bulletin 51, 1071–1077.
[26] Zavialov, P.O., Ghisolfi, R.D., Garcia, C.A., 1998. An inverse model for seasonal circulation over the southern brazilian shelf: Near-surface velocity from the heat budget. Journal of Physical Oceanography 28, 545–562.

IV.II Artigo II

Potential for Conversion of Thermal Energy in Eletrical Energy: Highlighting the Brazilian Ocean Thermal Energy Park and the Inverse Anthropogenic Effect

Roberto Valente de Souza[a,], Elisa Helena Leão Fernandes[a,], José Luiz Lima de Azevedo[b,], Mariana dos Santos Passos[c,], Rafaela Martins Corrêa[a,]

[a] *Institute of Oceanography, Laboratory of Coastal and Estuarine Oceanography (LOCOSTE). Federal University of Rio Grande, Carreiros Campus, Av. Itália without number Km 8, CEP 96201-900, Brasil*
[b] *Institute of Oceanography, Laboratory of Ocean Studies and Climate (LEOC) . Federal University of Rio Grande Carreiros Campus, Av. Itália without number Km 8, CEP 96201-900, Brasil*
[c] *Institute of Oceanography, Coastal Management Laboratory . Federal University of Rio Grande Carreiros Campus, Av. Itália without number Km 8, CEP 96201-900, Brasil*

Abstract

Renewable energies as an additional source have become vital in the modern. The search for alternative energy sources has led the scientific community to the oceans, leading to a shift in energetic policies, which must be redefined to favour the development of renewable energy technologies at sea. The goal is to generate electric energy while producing less pollutants or even while using the outputs of human anthropic activities as input for the generation of energy, food, products and for the mitigation of climate change impacts.The present study focuses on one of these technologies, Ocean Thermal Energy Conversion (OTEC), which presents the greatest potential for energy exploitation from the oceans and which generates a range of by-products. The South Atlantic Ocean presents the potential to support OTEC plants, with emphasis on the region of full operation, called the Brazilian Ocean Thermal Energy Park , with a total coverage area of 1.893.216 km^2 and an operating potential of up to 376 OTEC plants. The results of this work indicate that the operation of park in maximum capacity can generate energy at a nominal power is $34.028GW$, and to remove $0,97T\ J/s$ of ocean heat and $0,25\ g/s$ or 681 $tons/year$ of atmospheric CO_2.

Keywords: Renewable energy, thermal energy, OTEC, Ocean Thermal Energy Park, Blue Amazon, Inverse Anthropogenic Effect.

1. Introduction

Renewable energies as an additional source of energy have become vital in modern societies in developed countries. The search for alternative energy sources has led the scientific community to the oceans, as shown by the works of Neshyba [14], Skinner and Turekian [19], Thurman

Email addresses: robertovalente@furg.br (Roberto Valente de Souza), fernandes.elisa@gmail.com (Elisa Helena Leão Fernandes), joseazevedo@furg.br (José Luiz Lima de Azevedo), marianapassos91@gmail.com (Mariana dos Santos Passos), rafsmcorreay@gmail.com (Rafaela Martins Corrêa)

Submitted to Renewable Energy

and Trujillo [23]. Throughout evolution, the adoption of new energy matrices, using technologies based on sustainable development models, is necessary. In recent years, environmental issues have been at the center of the discussions of various segments of society, where the many environmental problems we face today lead us to an instability in all the compartments through which energy circulates, in other words, the atmosphere, oceans and the continents. Problems of climatic nature (atmospheric pollution, greenhouse effect, acid rain and etc), ocean degradation (acidification, heating, raising of the level, presence of plastic and etc) and others generated by radioactive contamination (nuclear waste, plant leaks, exposed reactors and etc) are derived from scenarios caused by man's action in order to generate energy.

All these problems suggest a search for solutions directed to sustainable development, which aims to reduce the use of fossil fuels and a greater use of renewable resources. In light of this scenario, energy policies need to be redefined in order to favor the development of technologies that generate less pollutants or that use them as input for the generation of energy or raw materials of any nature. The focus of this work is the mapping, in a sea of national sovereignty-, of one of these technologies, known worldwide by the name of Ocean Thermal Energy Conversion (OTEC), in other words, a thermal machine that fed by the thermal dipole present in the oceans, vertical thermal gradient, directs these heat packs to the exchangers (evaporator and condenser), where they transfer heat from the ocean to the working fluid that converts them to a mechanical moment, which is transferred to the generator and releases electricity.

2. The sun, oceans and OTEC technology

Several authors, such as Neshyba [14], Avery and Wu [4], Wright [27] and Thurman and Trujillo [23], report the possibility of using seawater as an energy source. Their works highlight the characteristic of the renewal of oceanic energy resources, where such resources would be obtained and used without relevant oceanic and atmospheric pollution. Neshyba [14] points out another quality of the oceans as energy providers for the population, the fact that at a given moment of time, due to their great thermal capacities, they have a greater amount of energy derived from the sun stored in the water column than that contained, in the same situation, in the atmosphere or on the continent.

Avery and Wu [4] postulate that, on average, the heat absorbed daily by surface waters in $2,6$ km^2 of oceanic area is bigger than that produced by the burning of $1,1$ million liters of petroleum. For Vega et al. [25], the amount of annual solar energy absorbed by the oceans is equivalent to at least 4000 times the annual rate of energy consumption in the world, taking as reference the nineties decade. Meisen and Loiseau [13] estimates show that an area of $60x10^6$ km^2, in the tropical seas, absorbs an average amount of solar radiation similar to the heat content of about $39,75x10^12$ liters of petroleum daily.

The ocean, in physical terms, can be seen as a large thermal machine, in which water functions as the working fluid, moving between the surface layer of the tropical oceans (warm source) and the polar and subpolar regions (cold source), where part of it sinks and spreads through the ocean basins [14];[19]. According to Avery and Wu [4] and Wright [27], the higher layers of the tropical oceans behave as a large reservoir of hot water, retaining the average annual temperatures of up to 28^0C, through the balance between the absorption of heat from the sun and the loss of heat through the processes of evaporation, convection and by the emission of long-wave radiation. This temperature remains approximately constant diurnal and month to month.

In regions between latitudes of 15°N and 15°S, for Avery and Wu [4], or between 20°N and 20°S according to Meisen and Loiseau [13], there are stable vertical thermal gradients greater

than or equal to 20°C. Valente et al. [24] demonstrate that temperature differences of at least 20° C between the superficial water and that of 600 to 1000 m of depth can be found in vertical strata of seawater, and in this scenario is therefore possible to implement a plant of ocean thermal energy conversion (OTEC) into electric.

D'Arsonval [9] sugested that certain engineering equipments installed in the oceans could use the surface hot water of the tropical seas to evaporate a working fluid, while the deep cold water would produce its later condensation. Thus, there would be a sufficient pressure difference for an engineering plant to function [7]. The work of Claude [7] introduced the first concrete projects that would lead to the primordial concept of the OTEC plant, having his name associated to one of the types of cycle of this plant.

There are two ways to operate an OTEC plant: (i) through a closed loop cycle (Rankine), where a low-boiling operating fluid, such as ammonia or freon, is vaporized by seawater, at a higher temperature (superficial), when passing through a heat exchanger (evaporator), and the generated steam drives a turbine that produces electricity; (ii) through an open cycle (Claude), where warmer seawater is pumped into a chamber, in which the pressure is reduced through a vacuum pump to a sufficiently low value (about 3% at 1 atm) so the water undergoes a partial evaporation (fast volume evaporation) and soon the generated steam expands, passing through a low pressure turbine, which is connected to an electric generator. In both processes we will have power generation, however, the performance of closed cycles in such generation is significantly higher.

3. OTEC byproducts and the application of artificial resurgence

The potential for OTEC technology is enormous and its byproducts have an important contribution to its economic viability, once some researches are carried out focused on the byproducts of an operating OTEC plant [11]. This is understandable when the interest of research funders is currently directed at these by-products related to clean and renewable energy. This is understandable when the interest ofgiven that research funders is are currently directed interested at thesein by-products related toof clean and renewable energy.

This set of byproducts and services come from the artificial resurgence, rise of bottom water to surface, which can be obtained from an OTEC plant. For some industries, there is a potential market for such products, including beverage, food, pharmaceutical and cosmetic industries [11]. Avery and Wu [4], MacKenzie and Avery [12] and Avery and Berl [3] report the possibility of ocean thermal energy conversion into chemical energy.

As has been seen previously, the open or hybrid cycle, a byproduct of the OTEC system is desalinated water [4]; [25]; [21]. Once the working fluid is seawater and it changes its physical state, through a low pressure chamber, separates the salt from the water, so that it is desalinated and can be used for human and animal watering, in addition to serve for agriculture.

According to Meisen and Loiseau [13], a plant of $2MW$ net power would produce about 4.300 m^3/day of desalinated water. Takahashi [21] reports that a $1MW$ plant could produce up to 3.500 m^3/day. Human communities living on islands are potential candidates for this type of fresh water supply [14]; [25]; [21]. More refined and higher added value applications can also be made from desalinated water. Researches have resulted in the manufacture of mineral water and isotonic drinks [11]. In agriculture, cold seawater can allow the cultivation of crops from temperate zones in tropical areas, diversifying the supply of vegetables in these regions [21].

An OTEC plant can integrate a polyculture operation that combines energy production with protein production [13]. This is possible because the deep water pumped to the surface, which

would characterize an artificial resurgence Kobayashi [11] ; Takahashi [21], is rich in nutrients and relatively free of pathogens. Thus, it is an excellent medium for the growth of plankton, which can sustain the captive breeding of certain fish and shellfish of commercial value, increasing the utility of an installed plant [14]; [13]. As it happens to agriculture, artificial resurgence allows the creation of non-native species from tropical regions inside tanks [13]. Seventy two high value products such as biodrugs and biopigments (for example astaxanthin) can also be obtained from the cultivation of certain microalgae in tanks continuously supplied by the artificial resurgence from an OTEC plant [21].

The cold seawater (at 5^0C after the thermodynamic cycle) provided by an OTEC plant can be used in cooling systems near the plant. The captive bred organisms mentioned above, for example, need, after their removal from the tanks, a correct storage at a suitable temperature to ensure their quality. A cooling system that uses cold seawater could be used for this purpose [13]. This same principle can also be used for air conditioning in buildings [13].

Research made by Johns Hopkins University Applied Physics Laboratory, between 1975 and 1982, demonstrated the technical viability of building OTEC plants, with the help of the electricity generated by itself, to produce chemical substances that could act as fuel [3]. In this plant, through the electrolysis of water, hydrogen and oxygen can be obtained and so, are capable to supply driving systems.

The OTEC plant allows, through the method of electric power generation, to reverse the logic of anthropogeny, in other words, it allows partial withdrawal of the heat content absorbed by the oceans, inserted in the last century by human action and also coming from natural processes. It is remarkable that the increase in the temperature of the oceans is linked to the increase of greenhouse gases, CO_2 concentration, which has exceeded the natural limits (379 $ppmv$ current - 180 a 300 $ppmv$ natural).

The thermodynamic cycle that operates an OTEC plant enables to withdraw high rates of heat content from the ocean by converting the heat difference into electricity through the evaporator (providing heat to the working fluid) and condenser (removing heat of working fluid). In addition, it absorbs large amounts of atmospheric CO_2, via artificial resurgence, forced by vacuum pumps and the cold water collecting pipe which, considering its various conversion possibilities, can reverse, even on a small scale, the acceleration of the greenhouse effect and consequently climate change.

4. The Blue Amazon and the viability of applying the renewable energies of the Sea: the Ocean Thermal Energy Park (OTEP).

Brazil is a country with an extensive coast, about 8.000 km, bathed by the Atlantic Ocean. The fact that about 80% of the Brazilian population lives in an environment surrounding 200 km from the coast defines a scenario in which the conversion of sea's energy potential represents an important contribution to the diversification of the Brazilian electricity generation matrix. The national territory of maritime sovereignty, the Blue Amazon (BA), has $4,4$ million km^2 ($3,5$ million km^2 of continental shelf plus its extension of 911 thousand km^2) and is spatially equivalent to approximately 52% of the Brazilian continental territorial coverage.

Among the main renewable energy sources of the sea are thermal gradient, salinity gradient, ocean currents, tides, waves and wind. As Brazil is a country of continental dimensions, all sources mentioned are contemplated, and there are two large freshwater systems flowing into the ocean, the Amazon River and the Patos Lagoon (salt gradient), a high intensity west contour

current, Brazilian Current (BC), with variations of transported volum from 8 up to 32 Sv (1 Sverdrup = $1x10^6$ m^3/s) and high intensity meanders, associated to its transport (energy of the currents), systems from micro to macro tides (tidal energy), intercalated with frontogenic regions along the coast (wind energy), generating wave regime in the coastal adjacencies (wave energy).

Based on the results obtained by Valente et al. [24], we have defined an oceanic region contained in BA,which meets the minimum values of heat content for the operation of an OTEC plant, in other words, the existence of a vertical thermal gradient (greater or equal to 20^0C) between the surface and 1000 m along the whole passage of the annual calendar. This region, from now on titled as Brazilian Ocean Thermal Energy Park (OTEP) (Figure 1), defined by the operational vertical thermal gradients for an OTEC plant, covers the far north from Espírito Santo (ES) coast (latitude 19^0S), practically all northeast coast and the north portion until half of the Lençóis Maranhenses National Park (excluding the delta region of the Mearin and Amazonas rivers, due to the difficulty of collecting surface and bottom water with high sediment concentration).

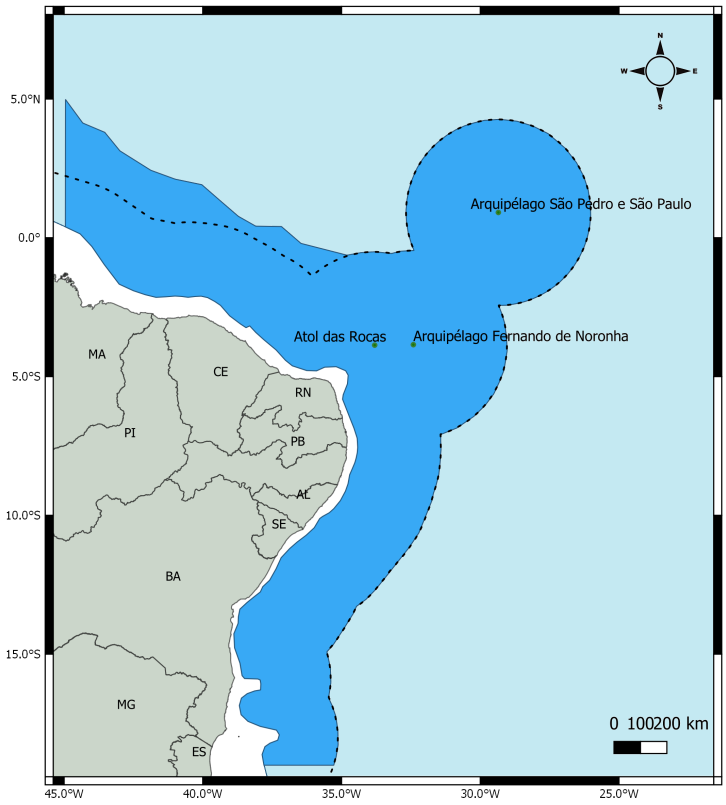

Figure 1: *Delimitation of the Brazilian oceanic region subject to continuous operation of OTEC plants, highlighted in dark blue with its geographical limits (OTEP), where the dashed line delimits the BA and in white the continental shelf.*

It is pointed out the area for the use of OTEC plants within OTEP (Figure 1), which covers all the states of the northeast region of Brazil and the north of the ES state in its coastal portions, including two archipelagos (Arc.), Fernando de Noronha (F. Noronha) and São Pedro and São

Paulo (S.P. and S.P.) and the Rocas Atoll (At.), respectively belonging to the BA, except the most offshore portion in the states of Maranhão (MA), Piauí (PI) and Ceará (CE). We emphasized the region outside the dashed line (Figure 1), not yet included in the Brazilian legal limits of exploration.

The Brazilian government, through its communication portal (`www.itamaraty.gov.br`), decided to architect a revised proposal for these outer limits of its continental shelf in order to respond to the recommendations of the International Commission on the Limits of the Continental Shelf and ensure the approval of the entire area demanded by the country.

The latitudinal and longitudinal bands, bathed by the Atlantic Ocean, including BA and OTEP, receive a large amount of radiation and present intense and stable vertical thermal gradients. The scenarios of all the renewable energies of the sea are interesting, but in this work we wish to contribute to one of the topics of a future renewable energy atlas of the Brazilian ocean, where the energy of the thermal gradient has the highest estimated potential of the oceans [14]; [4]; [24].

This work is organized as follows, after an introduction to the subject and the definition of the OTEP, the methods to simulate a theoretical OTEC matrix will be presented, which lead to the results obtained in several spatial scales (Atlantic Ocean, OTEP, areas of property and punctual isolines), for the input and output parameters, that concomitantly will be discussed in their correlations, variabilities and obtained information to be highlighted. Thus, building the organization of all the results and discussions of outstanding importance, presented in the form of conclusion of the study.

5. Methods and Materials

The methodological organization follows the order: (i) OTEC concept; (ii) presentation of the OTEC Energy Module Teorical (OEMT), its equations, approximations and theoretical assumptions; (iii) the three-dimensional numerical model, the important intrinsic characteristics to evaluate the resources related to the OTEC plants, besides the results used; (iv) the parametrizations, applied functions and mathematical models used, thus demonstrating the construction of the results to be presented in the study.

5.1. OTEC Concept

In this system shown in Figure 2, the working fluid used to produce mechanical work runs through a closed circuit. According to Avery and Wu [4], a low boiling working fluid, such as ammonia, freon or propylene, is vaporized by seawater from the surface (warmer), when passing through a heat exchanger (evaporator), with a moderate expansion of the steam, which drives the generating turbine, producing electricity. Following the thermodynamic circuit, it contacts the other heat exchanger (condenser), and that makes the working fluid to yield heat to the ocean.

Both in the evaporator, as in the condenser, there is no direct contact between the working fluid and seawater. Therefore, after leaving the condenser, the condensed fluid is pumped back to the evaporator to restart the cycle. Thus, a closed circulation is established for the working fluid, which must operate continuously, while an appropriate vertical thermal gradient exists (greater or equal to 20^0C).

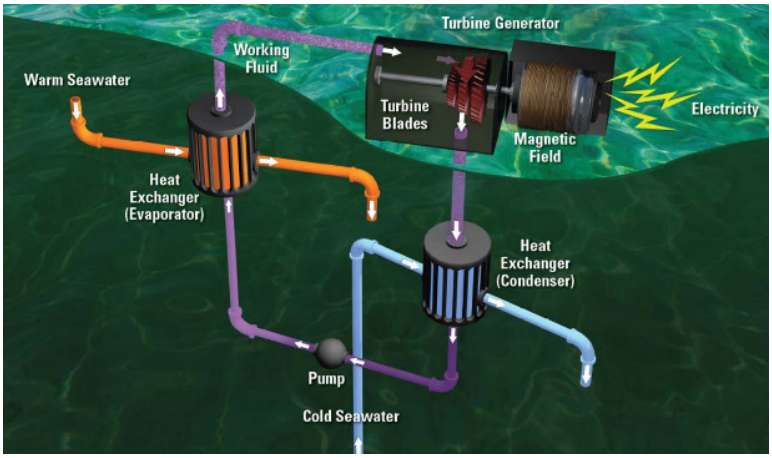

Figure 2: *Thermodynamic and power generation devices of an OTEC plant operating a closed circuit and the optimization of Rankine cycle, adapted from Ascari et al. [1].*

5.2. Theoretical OTEC Energy Module

The analysis of the energy potential of the thermal gradient in BA was carried out using daily, monthly, seasonal and annual Julian averages of the temperature and salinity field, applied to OEMT, obtained from the numerical model [24]. These data were used to indicate, through the thermal gradient analysis, the most favorable regions to the installation and operation of OTEC plants.

A standard OTEC energy conversion system was proposed by Nihous [15], based on the Rankine cycle, for modeling purposes, with a generalization of the loss due to the thermal changes and the devices that consume energy, in order to obtain a simplified optimization.

The parameter and control of a standard OTEC system is the thermal gradient between the surface and deep sea temperature, and its application is distributed among the main components of a simplified power plant Johnson [10]. This thermal gradient is associated with the efficiency of the OTEC plant, represented by the term of thermodynamic efficiency equation, where it is multiplied by the turbine-generator electrical efficiency, as well as being present in the balance of the heat quantification in each operation cycle of the plant.

The thermodynamic efficiency of a standard OTEC cycle is given by:

$$\varepsilon_{otec} = \varepsilon_{tg}\left[\frac{T_h - T_c}{2T_h}\right] \tag{1}$$

Where : ε_{otec} is the efficiency of the standard OTEC plant optimized; ε_{tg} is the efficiency of the turbine-generator; $\Delta T = (T_h - T_c)\,(K)$ is the thermal gradient between hot and cold water; T_h (K) is the input temperature of hot seawater; T_c (K) is the cold water input temperature. Thus, with the vertical thermal gradient minimum values, the efficiency of the generating turbine can reach its highest value of approximately 0.85, for modeling purposes, according to Nihous [15].

In order to obtain the amount of available energy, the equation of the heat flux in the cycle is necessary, so we can write the amounts of heat as:

$$\dot{Q}_h = \dot{m}_h C_{Ph} [T_{hin} - T_{hout}] \tag{2}$$

$$\dot{Q}_c = \dot{m}_c C_{Pc} [T_{cin} - T_{cout}] \tag{3}$$

Where: $\dot{Q}_h$ and $\dot{Q}_c$ (point above the terms indicates the temporal variation) are respectively the heat transfer rate to the system through evaporator and the heat transfer rate of the system to the condenser (J/s); $\dot{m}_h$ and $\dot{m}_c$ (point above the terms indicates the temporal variation) are respectively the mass flow of hot and cold water (kg/s); T_{hin} and T_{cin} are respectively the input temperature of hot and cold seawater (^0C); T_{hout} and T_{cout} are respectively the output temperature of hot and cold seawater (^0C); C_{Ph} and C_{Pc} are respectively the specific heat of hot and cold water (J/kg^0C).

According to [4] and Vega et al. [25], in a large plant $(100MW)$, there is a need for an input of 400 m^3/s ($\dot{v}_h$ flow, the point above indicates the variation of time over the volume) of hot seawater and 200 m3/s ($\dot{v}_c$ flow, the point above indicates the variation of time over the volume) of cold seawater into the system. Based on these input flows, to obtain the amount of water entering the system, the seawater state equations were used to obtain the typical densities of these flows, based on the pressure data, calculated based on the depth, temperature and salinity from the Julian dataset obtained, through statistical treatment, applied to the numerical model [24], in order to obtain realistic values for the density. As described below:

$$\rho_h = f(S_h, T_h, P_0) \tag{4}$$

$$\rho_c = f(S_c, T_c, P_{depth}) \tag{5}$$

$$\dot{m}_h = \rho_h \dot{v}_h \tag{6}$$

$$\dot{m}_c = \rho_c \dot{v}_c \tag{7}$$

Where: ρ_h and ρ_c are the densities of the hot seawater at the gradient limit depth (kg/m^3), depending on the pressure (N/m^2), temperature (^0C) and salinity (psu); $\dot{m}_h$ and $\dot{m}_c$ are the mass flows of oceanic water bodies entering the OTEC plant (kg/s).

The specific heat C_{Ph} and C_{Pc} for hot and cold water to be used in the system is obtained according to Sharqawy et al. [18] (j/kg^oC), which describe C_P through a polynomial for the temperature scale in ^0C, as:

$$C_{Ph} = A + BT_h + CT_h{}^2 + DT_h{}^3 \tag{8}$$

$$C_{Pc} = A + BT_c + CT_c{}^2 + DT_c{}^3 \tag{9}$$

Where T_h and T_c are the water temperatures in the surface and depth at the gradient limit (^0C); A,B,C and D are the coefficients of the specific heat equation (C_{Ph}; C_{Pc}), which will be calculated individually for each heat exchanger in the form:

$$A_h = 4206.8 - 6.6197 * S_h + 1.2288E - 2 * S_h.^2 \tag{10}$$

$$A_c = 4206.8 - 6.6197 * S_c + 1.2288E - 2 * S_c.^2 \tag{11}$$

$$B_h = -1.1262 + 5.4178E - 2 * S_h - 2.2719E - 4 * S_h{}^2 \tag{12}$$

$$B_c = -1.1262 + 5.4178E - 2 * S_c - 2.2719E - 4 * S_c{}^2 \tag{13}$$

$$C_h = 1.2026E - 2 - 5.3566E - 4 * S_h + 1.8906E - 6 * S_h{}^2 \tag{14}$$

$$C_c = 1.2026E - 2 - 5.3566E - 4 * S_c + 1.8906E - 6 * S_c{}^2 \tag{15}$$

$$D_h = 6.8777E - 7 + 1.517E - 6 * S_h - 4.4268E - 9 * S_h{}^2 \tag{16}$$

$$D_c = 6.8777E - 7 + 1.517E - 6 * S_c - 4.4268E - 9 * S_c{}^2 \tag{17}$$

Where: S_h and S_c are the input salinities (psu) of hot and cold water masses and the numerical values are the constants of the terms.

Based on the equations described above and according to the calculations of Vega et al. [25], the available electric power, after one cycle of operation, will be represented by the available power without losses (gross) and about the dissipations, the pump system consumption and the losses or gains of heat in the pipes, varies from 20 to 30% of the power generated in the turbine-generator set. The maximum loss is used, so we will have the following relation for final energy (net), which can be represented by:

$$Pel_{gross} = \varepsilon_{otec}\,(Q_h - Q_c) \tag{18}$$

$$Pel_{net} = (0.7)Pel_{gross} \tag{19}$$

Where: Pel_{gross} and Pel_{net} are, respectively, net and gross electrical power available after one operating cycle ($Watts(W) = J/s$).

5.3. Materials

The equations presented above are supplied with the results of the HYCOM (HYbrid Coordinate Ocean Model - `https://hycom.org`) numerical model. The temperature and salinity results of the model were used in three processing: (i) Julian climatological averages, constituted of the variability along the days, months, seasons and the annual signal; (ii) increase of the heat exchanger rates (output of hot and cold water collection pipes), according to the values tabulated by by Vega et al. [25]; (iii) calculation of the typical densities of the water masses, constituents of the thermal gradients, used for the thermodynamic cycle through the state equation of seawater.

5.4. HYCOM

According to Ascari et al. [2], the HYCOM has a hybrid approach to an ocean of vertical structures, capable to represent more robustly the effects of surface exchange processes, advection on isopycnals and flow due to the bathymetric features. So it represents in a more realistic way the structures of the thermal gradients, that allow a more reliable application of OEMT.

Salinity and temperature outputs of the HYCOM Model derived through, experiments 19.0 and 19.1, were collected on 40 vertical levels, depth up to $6366m$, with horizontal resolution grid of $1/12^0$, between the coordinates (70^0W,0^0W; 39^0S, 10^0N), temporal resolution every 3 hours, between January 1th, 1993 and December 31 *th*, 2012, totalizing 20 years of results.

5.5. Julian Climatology

From the results of temperature and salinity, daily, monthly, seasonal and annual Julian Climatology (JC) was calculated, the method was described in greater detail in the work of Valente et al. [24].

5.6. OEMT's input and output temperatures and salinities

According to the equations presented in the OEMT section, we have subscript indexes that represent the thermohaline characteristics, being the salinity and temperature accompanied by $_h$, (S_h, T_h), when belong to hot water masses and those with index $_c$, (S_c, T_c), to cold water masses of input.

In order to calculate the heat flow in the thermodynamic cycle, we have to obtain the output temperatures of the heat exchangers, in other words, multiply their input values, based on the values tabulated by Vega et al. [25]. The percentage of loss is $8,4\%$ in the evaporator ($_h$), T_h, and $23,6\%$ of gain in the condenser ($_c$), T_c, making it possible to quantize the heat flowing through the OTEC plant.

5.7. Calculation of OEMT's input densities and pressures

In order to calculate the typical densities of the water masses that come in contact with the heat exchangers, input and output of the evaporator and condenser, it was necessary to obtain the pressures at the depth level of the model and their thermohaline identities (S, T). In light of the need for this information, seawater state equations were used.

In the calculation of the typical pressures, we need the depths of seawater collecting (surface and bottom plant pipelines) and the latitude of the matrix grid. Thus, we can create the pressure matrix to be used to calculate the densities. So we obtain the seawater densities in four situations: before and after the passage through the evaporator and condenser, thereby, two matrix grids of seawater densities. In this way, we have all the necessary results to run the OEMT in its matrix form.

6. Results and Discussion

From the annual and daily average climatological results of the temperatures, salinities and other calculated variables, indicated in the methodology, the necessary data to run OEMT are provided. Thus , such values allowed to verify the behavior of the variables, input and output, and their behavior in the entire numerical domain collected from the model and after with the highlight in the OTEP. Based in the work of Ascari et al. [2], the largest depth to be operated by the bottom water collection pipe of the OTEC plant is $1000m$. So, the results initially presented will always be related to the vertical thermal gradients between the surface and the $1000m$ depth.

The results establish a direct relationship with the limits imposed by the theory, that is, an OTEC plant with maximum capacity to generate 100MW. They are organized in a sequence in order to initially contemplate the entire matrix grid collected (70^0W,0^0W; 39^0S, 10^0N), almost all the Atlantic Ocean in the portion covered by the Brazilian coast, the OTEP and a deeper investigation in regions with higher energy content.

6.1. Theoretical OTEC in the South Atlantic Ocean

The potential of the thermal energy of the South Atlantic Ocean (SA) is presented in Figures 3 a efficiency and 3 b power, and is indicated by the power production rates very close to the OEMT operational limit. The results grid represents all the coverage processed in this study. However, the focus of the analysis is on BA, more precisely on the OTEP. Nevertheless the data processing shows the full operating capacity of OTEC plants in several regions that are not part of the objective of the proposed study.

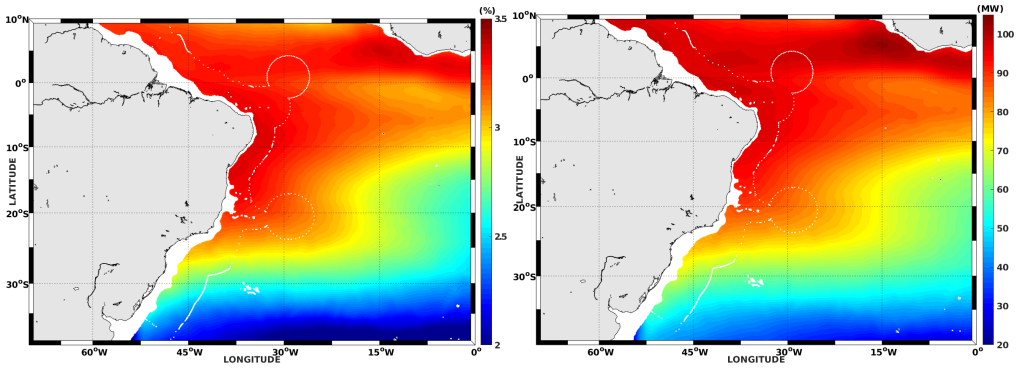

(a) (b)

Figure 3: *Efficiency (%) a) and Power (MW) b) at OEMT's output, including regions outside the Blue Amazon.*

The results indicate that the regions of maximum values of power and efficiency, below the equator line, are in the contour of the Brazilian north coast, contained within the OTEP. Production values close to OEMT's limit value are found, towards the open ocean, but with lower conversion rates in relation to the peaks close to the Brazilian adjacencies.

In order to understand how these thermal energy regions are configured, a synthesis of the water masses that configure this vertical thermal gradient that feeds our OEMT is necessary. According to Cirano et al. [6], the system of superficial marine currents in this area is associated

to the subtropical turn of the south atlantic, resulting from the action of the atmospheric anti-cyclone. Due to the effects of the Equatorial South Current (ESC), which flows east-west and influences the Brazilian Northeast (NE), a bifurcation occurs, originating the Brazil's Current (BC) and the Brazil's North Current (BNC), which through direct observation are closely linked with the regions of greater efficiency and power (Figures 3 a and b).

The BC and BNC can be associated to the flow of the movement of Tropical Water (TW), where the high heat contents are derived from intense radiation and excessive evaporation in relation to precipitation, characteristic of the equatorial atlantic. In this way, the upper portion of the thermal gradient is identified, but it is still necessary to identify the mass that flows in the deepest part and that configures the gradient with the surface. The South Atlantic Central Water (SACW), originated from the confluence of Brazil Malvinas, occupies the position at a lower level than the TW and maximizes the thermal gradient, and its depth interval is between the values of 500m to 1000m, according to the synthesis of water masses published by Stramma and England [20].

In the northernmost region, in the same depth band occupied by SACW in the NE portion of OTEP, we now have the presence of North Atlantic Central Water (NACW) Stramma and England [20], in a region close to Amapá, which, with the contribution of the high heat contents of the intertropical convergence zone, maximizes the values of the thermal gradient over the north region, as indicated by the efficiencies and powers shown in the Figures 3 a and b.

Quantitatively, in terms of power (MW) and efficiency ($\%$) respectively, we see that the peaks are represented by values of $96,5$ to values lower than $90,5MW$ and $3,4\%$ to lower percentages with a value of $3,25\%$ in the Brazilian coast, and the maximums are found in two regions, the first is almost entirely in SA ocean, contained within the OTEP, in the adjacencies of the north and northeast coast. The second region is located on the west coast of Africa, covering almost the entire coast of Liberia where it reaches $100MW$ and $3,5$ of efficiency.

6.2. OEMT in OTEP

According to the results of Valente et al. [24], the OTEP consists of three operational sites, where the vertical thermal gradient shown in Figure 4 c is represented by the limit extracts, that is, for surface temperature (Figure 4 a) and at 1000m of depth (Figure 4 b), based on the unique signal of the Julian average and in the time series of the points sweeping the days of the Julian calendar, where the thermal gradient isolines delimit the three sites, from 23,5º C, 23º C to 22,5º C, that together define the OTEP.

Valente et al. [24] demonstrated that the OTEP region is characterized by the presence of a vertical thermal gradient equal or greater than 20^0C, between the surface and the possible depths between 600 and $1000m$, along the Julian calendar, covering a horizontal extension of $1.893.216km^2$.

The Figure 4 demonstrates the thermal structures to be applied in the OEMT, so that the characteristics contained in Figure 4 a can show a preview of the heat to be inserted in the evaporator (through hot water collection pipe) and the Figure 4 b of the heat to be withdrawn through condenser. However, the OTEC plant operates a thermodynamic cycle that responds throughout its apparatus to its efficiency, then for an estimate of its percentages, the vertical thermal gradient must be observed, Figure 4 c, which provides the terms of its equation 1).

In terms of surface temperature, Figure 4 a), the bands of higher values follow the power and efficiency peak locations indicated in the Figures 3 a and b, demonstrating that the OTEP actually indicates the highest heat content in terms of surface temperature, which is the main control variable of an OTEC plant.

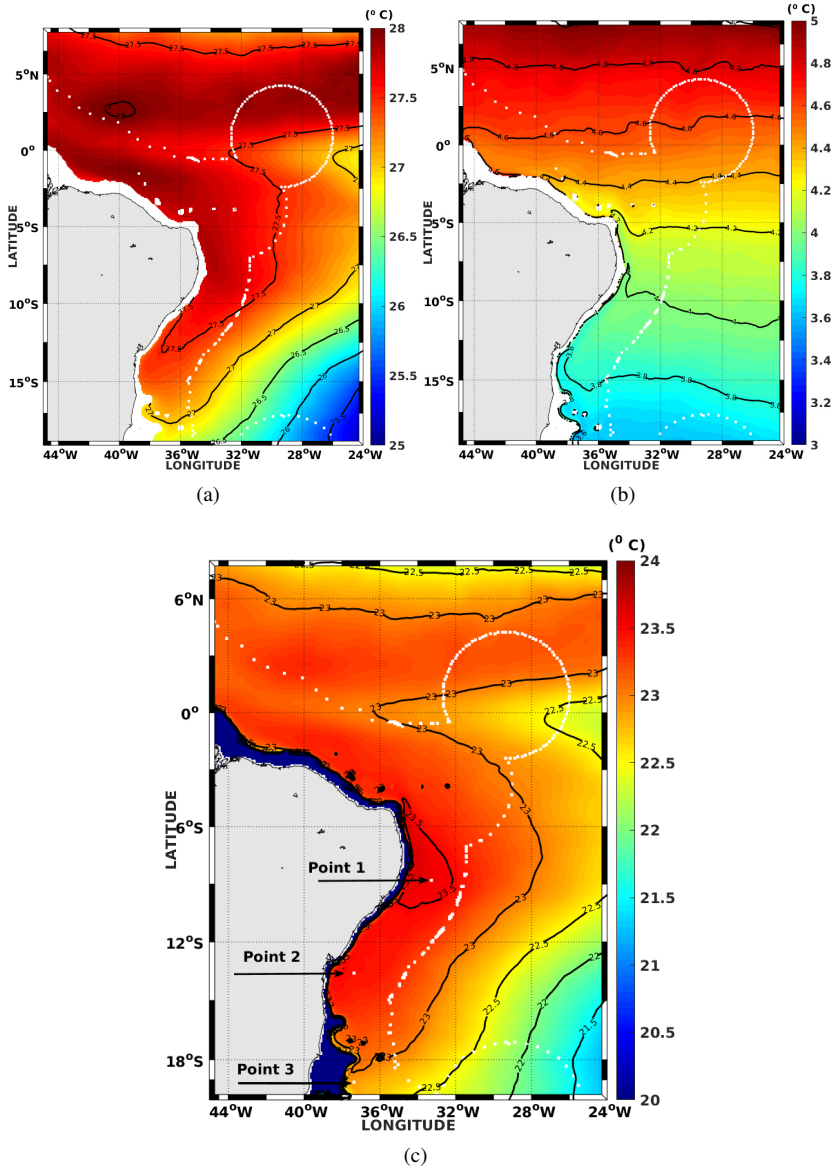

Figure 4: *Superficial temperature (^0C) (evaporator input) a) in* 1000*m (condenser input) b) and the thermal gradient (between the surface and the* 1000*m) c) (obtained by Valente et al. [24], which defines the limits of the OTEP, where the OEMT will be applied.*

Objectively discussing, the surface temperature isotherms in the range of $27,5^0C$, 27^0C and $26,5^0C$ (Figure 4 4 a, within the OTEP, the first due to its proximity to the coast, its high thermal content, and its greater coverage area. Directly elucidating the temperature at $1000m$, Figura 4 b, the isotherms from 4.6^0C to 3.6^0C have their sense of growth from the largest latitudes

to the smallest, approximately linear offshore, but with small intrusive tongues of the isolines, responding to the shape and layout of the continental shelf.

6.2.1. Heat exchangers from OEMT

The results obtained from the evaporator and condenser output are the theoretical application of the percentages of gain and loss described in the methodology. Through the output temperatures of hot water heat exchangers (Figure 5 a) and cold water (Figure 5 b), it is verified the mirroring of the values of the surface input temperature (Figure 4 a) and deep in 1000m (Figure 4 b).

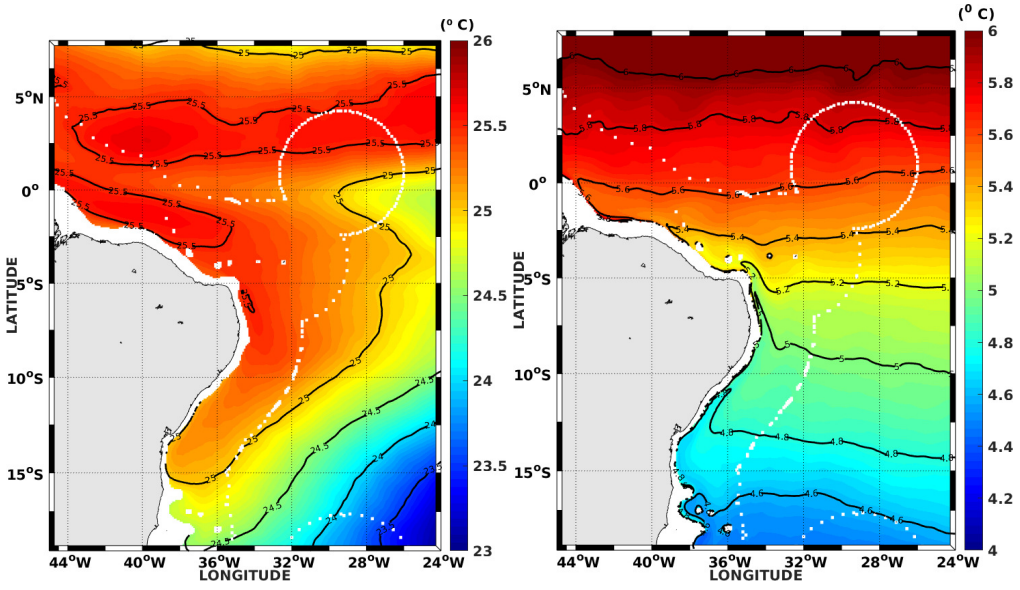

Figure 5: *Superficial temperature (^0C) (evaporador output) a), in 1000m (condenser output) b), at OTEP limits.*

Through the exercise of comparative observation, of directly related variables (Figures 4 4 and 5 a), we verified that the highest heat contents (Figure 6 a) are in the isolines of $3,45GJ$, in other words, in the same positions of the highest values of evaporator inlet and outlet temperature isolines and where the highest heat values can be absorbed by the working fluid of the OTEC plant. These regions are located to the north between the approximate latitudes and longitudes of 0^0 to $2,5^0S$, 43^0 to 36^0W, coastline of the states of MA, PI and CE, besides the extreme northeast of OTEP, between approximately $2,5^0N$ to 4^0N, 32^0 to 26^0W, next to S.P. and S.P Arc.

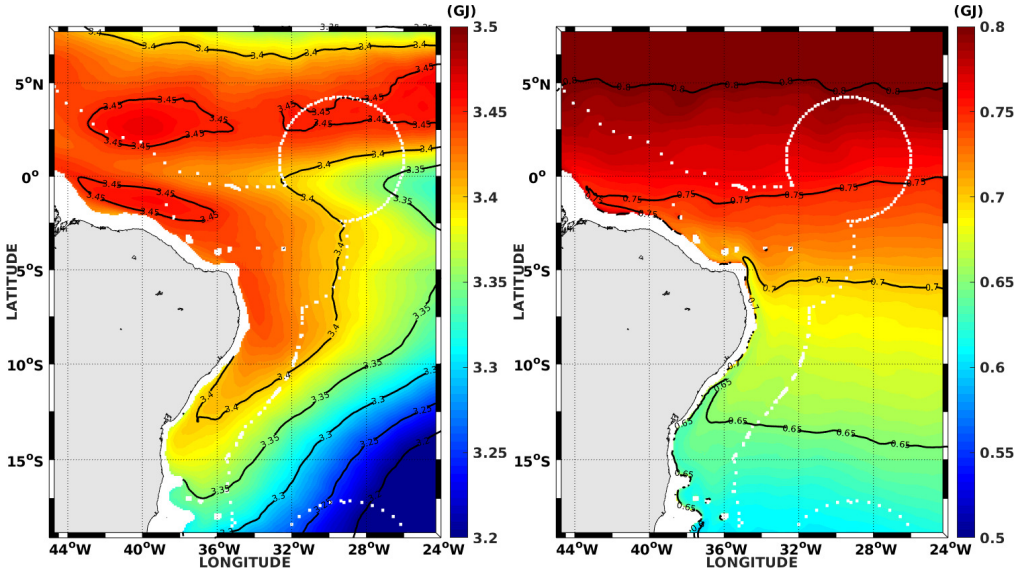

(a) (b)

Figure 6: *Input heat (GJ) through evaporator a) and output heat via condenser b), obtained by OEMT at OTEP.*

Likewise for the values withdrawn from the working fluid through the condenser, a pattern which is repeated in Figure 6 b in relation to the Figures 4 b e 6 b, in other words, latitudinal bands of heat isolines and intrusive tongues in the adjacencies of the continental shelf.

6.2.2. Eficiency and Power of OTEC plant

When approaching the output variables, the main parameters when the objective is to measure the viability of operation of an OTEC plant, are the efficiency and power (matrix application of equations 1 and 19) of operation in OTEP.

Firstly in terms of system efficiency, there is a fluctuation of the isolines between a maximum value of $3,35\%$, up to a minimum value of $3,2\%$. It is emphasized that in Figure 7 a, the efficiency peak, $3,35\%$, is located in the states of Alagoas (AL), Pernambuco (PE), Paraíba (PB) and Rio Grande do Norte (RN) (sweeping latitudinally the coast), with its latitudinal limits (approximately between roughly $5,2^0S$ and $9,4^0S$) to the north of RN and to the south in the coastal half of AL, near the capital Maceió.

The second highlighted isoline, $3,30\%$, includes in its delimitations the northeast states, beginning in the most offshore portion of Baía de São Marcos in MA (44^0W), passing by PI, CE (near the coastal region), RN (on the longitudinal side of the coast), PB and PE (offshore portion), AL, Sergipe (SE), Bahia (BA) and north portion of ES ($18,5^0S$).

Following the efficiency isoline of $3,25\%$, located near the coast of the states MA and PI, being present in the most offshore portion of them and of the states of CE and RN. Two offshore regions, one near the São Pedro and São Paulo Archipelago, north portion, and the other in the south of the OTEP, in the offshore portion of ES.

This region part of the archipelagos mentioned above, also presents an eficiency isoline of $3,2\%$, only in the small portion to the southeast, being almost in its totality dominated by the

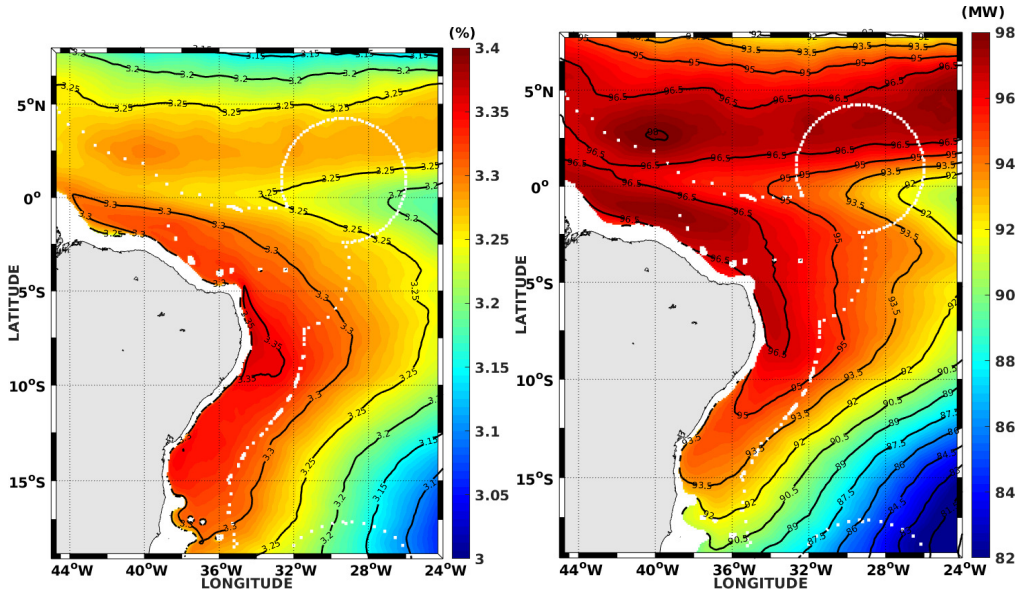

(a) (b)

Figure 7: *Efficiency (%) a) and power (MW) b) of operation, obtained by OEMT at OTEP.*

decreasing efficiency in the direction of this isoline.

After verifying the efficiency behavior, the available power of the theoretical OTEC plant (Figure 7 b) is now studied, being the same variable of greater representativeness about the electricity generation. It is verified that its isolines, delimitations and coverage areas, provide a production map of the annual average of OTEP.

It is important to highlight three ocean regions with higher operating power to be obtained by an OTEC plant within OTEP, correlated with higher efficiency peaks ($96,5MW$ and the range between $3,35\%$ and $3,3\%$). The first region has an approximate coverage area of $371.617km^2$, the largest power region of $96,5MW$, which bathes near the end of the continental shelf, passing through the states of MA, PI, CE, RN, PB and PE, the underestimated total capacity of an instantaneous available network of $7.141\ GW$ or $62.555TWh$ can be obtained.

The second region of $96,5MW$, north of the S.P. and S.P. Arc., shows the efficiency of $3,25\%$ and an area of $131.456km^2$. The third region of same power has an area of $74.123km^2$, corresponding to the most offshore portion of the MA and PI states, whose area exceeds the legal limits of BA.

Such as efficiency, the power is distributed throughout the OTEP, so that the rates decrease radially in offshore direction, subdividing into two regions. Stands out the first power zone with a nominal value between $96,5MW$ and $95MW$, with the largest area, approximately $509.181km^2$, latitudinally distributed in the adjacencies of the continental shelf near the coast of AL and PE, extending through the states of SE, PB, RN, CE, PI and MA, in the more offshore portions, including a small strip that longitudinally sweeps the RN, CE, PI and MA. It is also worth mentioning the presence of Arc. F. Noronha and Rocas At. included within this power range. The

second and smaller region is at north of S.P. e S.P. Arc. with an area of $72.269km^2$.

In the direction of the lowest power rates within the OTEP, there is the power isoline, delimited by the values of 95 to $93,5MW$. Surrounding the São Pedro and São Paulo Archipelago, with the third largest area $216.137km^2$, also passing through the states of AL, SE and much of BA, where its area has a value of $198.029km^2$ (4th largest area).

Between the power isolines of $93,5$ to $92MW$, we have two regions, the first to the southeast of S.P. and S.P. Arc. ($81.868km^2$), and the second to the south of the state of BA ($61.841km^2$).

The isolines which delimit the regions between $92MW$ and $90,5MW$, are located in east-southeast áreas of S.P. and S.P. Arc. ($12.441km^2$) and in south of state of BA ($54.028km^2$). The last power range within the OTEP is in the range of $90.5MW$ to $89MW$, at the south limit of the OTEP, which lies on the northernmost coast of the ES ($22.908Km^2$).

Avery and Wu [4] highlight that for the $100MW$ plants, adopted in the OEMT of this study, the flow rates are in the range of 300 to 500 m^3/s of hot water. The removal of these m^3/s from the surface layer will induce a radial inflow, towards that sink in a dependente pattern on surface currents. However, a flow describing a vortex may develop as a result of surface water sinking, possibly induced by the resulting friction, convective acceleration mixture, Coriolis forces, as well as other terms [4].

Walsh [26] present a vortical flow of standard superficial water of circulation of OTEC from a nearby field, to a cylindrical hot water collection piping project. At any latitude different from those of the equatorial environment, the Coriolis' effects will cause the flow of the surroundings of the sink of an OTEC plant to be like a spiral, where the pressure drop associated with this withdrawal of surface water would cause a slight depression at sea level and the displacement of the isotherms in the upper part of the thermocline. The horizontal pressure of the field, resulting from this rearrangement in the density field, would support a balanced, cyclonic geostrophic flow, characteristic of a cold core swirl.

According to Walsh [26], the models of a vortical flow in a $100MW$ plant, glimpse the same with a radius of 10 to 20 km, where warm water in a layer of $100m$ depth feels s its presence and the thermocline, below the cylindrical pipe, rises about roughly $15m$. The two layer simple model of Walsh [26] assumes that the bottom of the layer is infinitely deep, motionless and has a solid body motion core. Similar models were used to study the circulation flow in a hurricane [4].

The distortions of the thermal field and the increase in the thermocline could, in fact, reduce the surface water temperature, available as a heat source for an OTEC plant. However, calculations by Roels [17] suggest that the drop in hot water temperature, due to circulation, is insignificant for a 100 MW plant, operating on a surface layer of $100m$ depth. If the space between the plants is large enough, this temperature reduction is insignificant.

Based on the information presented in the preceding paragraphs, the maximum radius value of the hot water vortex as $20Km$. Assuming the double of this radius as a damping zone of the thermal and dynamic effects of an OTEC plant, a safe operating area of a plant of $5.026Km^2$ is adopted.

The OTEP coverage area is approximately $1.893.216Km^2$, that is, by dividing this value by the damping area, the OTEP could provide the installation of 376 OTEC plants. Associating the number with the average power value between $96.5MW$ and $95MW$, in the largest area $509.181Km^2$, we could approximate the instantaneous and approximate rate of nominal capacity theoretically available in this area, in a value of $9,67GW$ for 101 plants.

Making a logical estimate, by associating the smaller isoline that passes inside the OTEP, $90,5MW$, and multiply by the maximum of plants, 376, the underestimated total capacity of an

instantaneous available network of 34.028 GW or 298.085TWh can be obtained.

According to the available data Company [8] the northeast region has the consumption in network of 80.147GWh. Assuming that this value, in an instant nominal network is 9.14GW, the OTEP is able to supply the entire northeast, with 101 OTEC plants, considering that 275 are surplus, generating about 24.88GW.

Complementing the information presented at the end of this section, it is highlighted that within the regions presented here, either in the adjacencies of the continental shelf or in the more offshore regions, the type of installation that could be implemented in almost all OTEP, would be in the form of an OTEC plant on a platform (structure similar to a floating platforms described by Valente et al. [24].

Within the domains of OTEP, we have the strategic advantage of having the archipelagos, Fernando de Noronha (between 95MW and 96MW) and São Pedro and São Paulo (between 93MW and 95MW) and also the Rocas Atoll (over the isoline of 96, 5MW). These two archipelagos and the atoll are feasible for the installation of an OTEC plant in its inshore version, with its units built in ground.

It must be highlighted that the São Pedro and São Paulo Archipelago is part of a Program, PROARQUIPÉLAGO, which has a permanent working group for occupation and research, supported and with representation in the Brazilian Navy and other institutions at a Brazilian governmental structure level.

PROARQUIPELAGO is responsible for conducting a continuous and systematic program of scientific research in the region, in the following areas: geology and geophysics, biology, fishing resources, oceanography, meteorology and seismography. Thus, it would facilitate a case study, with open ocean characteristics, and temporal methodological sequence of other studies until the application of a real scale OTEC plant, relating to the mentioned areas, besides covering the research on renewable energy and mitigating the impact of the anthropogenic effect on the oceans.

6.2.3. Inverse Anthropogenic Effect (IAE)

Ocean thermal renewable energy comes from natural conversion cycles of solar radiation and, therefore, is practically inexhaustible. In the current global technology landscape there are several concepts of energy generation with zero carbon emission and low environmental impact. However, in the present configuration, besides the energy production, there is a need to act in an attempt to mitigate our historical anthropogenic effect that presses the global warming and the climate change scenario.

In the section about the applications of artificial resurgence, the IAE concept was presented, in other words, the ability of the OTEC technology to withdraw (through its operation with heat flowtraveling between evaporator and condenser) large amounts of ocean heat (Figure 6), enabling to convert this heat into clean and available electric energy. In addition, it was approached the ability of the system to enable the operation of mariculture farms around the plant, via artificial resurgence (deep water loaded with nutrients in an area with a lot of solar energy), fertilizing the oceans.

At first, through Figure 8 the ability of OTEP to withdraw amounts of anthropogenic heat of less than 2.8GJ and greater than 2.6GJ is quantified. We clearly identify that the region of maximum efficiency (3.35%) and power (96.5MW), Figures 7 a and b, coincides with the maximum IAE, through heat. Located between the south of BA and north of RN (between 13.90^0S and 15.25^0S), is the peak region of heat withdrawal, however we see that the IAE decreases radially

in offshore direction, reaching its smaller values, between the isolines of $2.65GJ$ and $2.60GJ$, in the most NE region of OTEP.

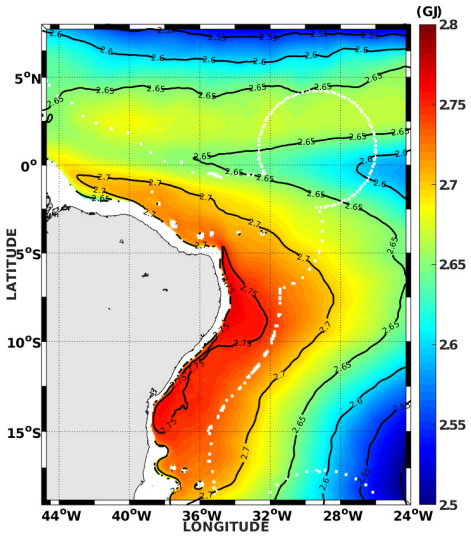

Figure 8: *Heat content (GJ) withdrawn from the ocean via OTEC plant (IAE).*

In possession of the number of OTEC plants, 376, capable to operate within the OTEP coverage area, $1.893.216km^2$, and associating with the smallest IAE isoline of withdrawn heat, $2.6GJ$, in its maximum limit the OTEP, in instantaneous and underestimated rate, could withdraw an approximate value of $0.97TJ$ of heat content.

Installing a mariculture farm, estimate below the possibility [21], in each of the 376 OTEC plants, within the OTEP, and according to Bagni [5] the region has thermohaline characteristics to the creation of Atlantic salmon species. Knowing that for the production of 100 species of it, it is necessary a bottom water renewal flow of $1m^3/s$, and that according to Takahashi et al. [22] and Oschlies et al. [16] 18 $Pg/year$ of carbono are removed by resurgence, corresponding to a flow of $26.4Sv$.

In possession of the information listed in the previous paragraph, taking the focus away from the production of high quality animal protein, it is estimated that the maximum absorption of atmospheric CO^2 in OTEP, in 376 mariculture farms, generating 376 m^3/s of artificial resurgence, underestimated is of approximately $0,25$ g/s or $681ton/year$.

6.3. Featured site within the OTEP

According to the results of section 6.2.2, it is presented a region of average annual peak of efficiency and power, 3.38% and $97.5MW$, where according to Valente et al. [24], the highest thermal energy content along the water column are established. Still according to Valente et al. [24], the vertical thermal gradients that have these power and efficiency values presented here, are operational between the surface and the depth range of $600 \leq z \geq 1000$. Thus, differently from the application of the matrix OEMT, in all results obtained so far, it applies in a punctual form on the region of maximum power (Figure 9 a), obtaining all the parameters greater prominence for an OTEC plant.

Starting from the points indicated in Figure 9 a, the power time series of thermal gradients were withdrawn, established along daily average Julian climatology between the surface ($0m$) and the depths of $600m$, $700m$, $800m$, $900m$ and $1000m$, and their production differences between the indicated levels in points 1 and 2 (Figure 9 b and c).

We emphasize the almost overlapping of the power values for the different gradients capable of operation, throughout the calendar, at both points and that their differences, at both points, never exceed $1.5MW$.

Based on the information obtained, it is stated that, for an OTEC plant, the bottom water collection pipe (semi-adiabatic) is the most expensive apparatus and the most difficult to operate. The regions represented by points 1, 2 and almost all of the OTEP (excluding the part of its area at NE and the range below 18^0S) allow to operate with the thermal gradient between $0m$ and $600m$ and to generate power values with loss percentages, related to the maximum gradient between 0 and $1000m$, of a maximum of 1.5%.

6.3.1. Daily variability of energy conversion (vertical termal gradient between the surface and 600m)

The OEMT is fed by a series of oceanographic parameters between the surface and the considered level of depth, to be inserted in its constitutive equations, such as temperatures, salinity, pressure, density, water specific heat and etc, besides the parameters of the thermodynamic apparatus. So, here are presented the input and output parameters (between 0 and 600m, as set in the previous section), considered control variables of the OTEC plant for points 1 and 2 (Figures 10, 11, 12, 13 and 14), in order to emphasize its variability along the annual senoidal (solar Julian calendar) and its seasonal plots.

Highlighting the variability between points 1 and 2, with a latitudinal difference of 5.1^0, we see that the annual average (continuous line) is 27.64^0C and 27.84^0C, respectively, that is, a difference of 0.2^0C. So, observing the averages by seasons (dotted lines), we noticed that the averages are very close during summer (27.87^0C and 27.94^0C) and the autumn (28.60^0C and 28.64^0C), and their differences are smaller than the annual value. However in the winter (26.93^0C and 27.15^0C, higher by 0.02 of the anual difference), and mainly in spring (26.97^0C e 27.48^0C, higher by 0.51 of the annual average difference), the averages are different and higher than the annual value.

Based on the results highlighted in the previous paragraph, it can be stated that the latitudinal difference interferes directly in the winter and spring seasons, forcing the annual average of point 1 to the lowest value. Thus, a direct relationship of the obtained values for the input heat in an OTEC plant through evaporator is established, which will present similar fluctuation of the total average and the seasonal influence.

It is verified that the fluctuation of the temperature in the depth of $600m$ in points 1 and 2 (highlighted in Figure 10) is different from the surface temperature, where it configures due to the difference in the thermal energy input that, through its stratification in the water column, reaches the analyzed depth.

It should be noted that the higher values in the annual mean and in all seasons, Figure 11, do not have a disturbance of the seasonal influence, once the differences between the seasons are approximately equal. Thus, the same behavior is expected for values obtained for the output heat of an OTEC plant through condenser, which will present a similar annual average variation and absence of seasonal influence.

The efficiency of points 1 and 2, Figure 12 a and b, due to the annual average values of their time series have a very small difference and very similar fluctuations, it was necessary to express

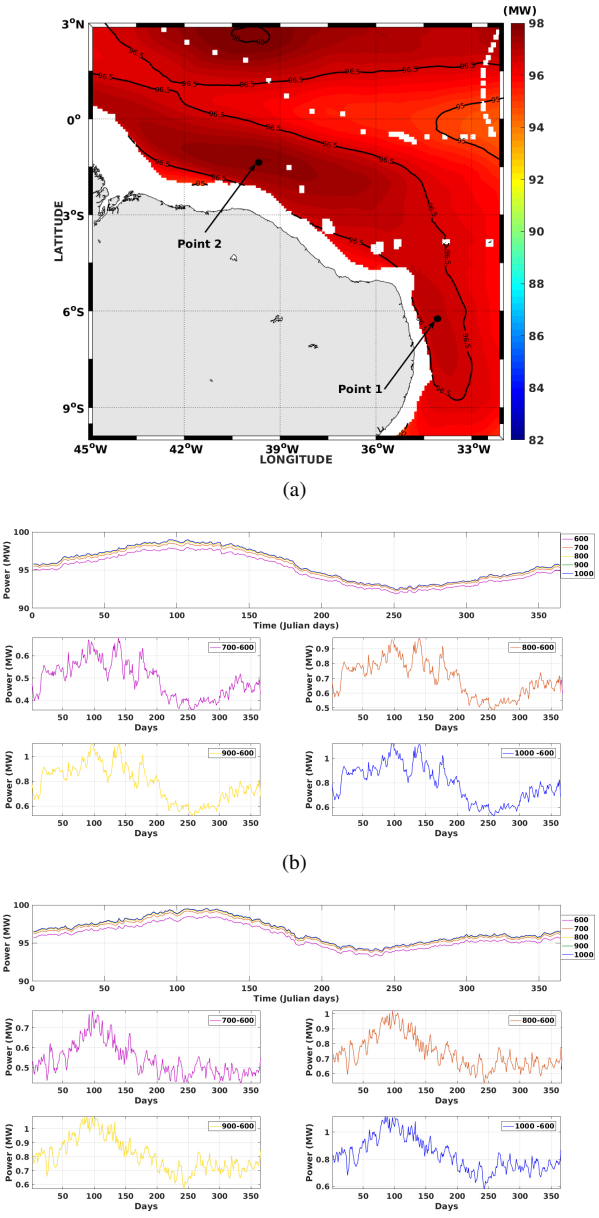

Figure 9: *Anual average power (MW) and points of maximum value a), produced power (MW) between the surface and the depths of* 600, 700, 800, 900 *and* 1000*m, and the available power differences between the levels of the specific depths identified by the colors, point 1 b) and point 2 c).*

the graphs in different figures, making possible the comparative of their behaviors.

This behavior parity is due to the surface and bottom temperatures maintaining a stable and

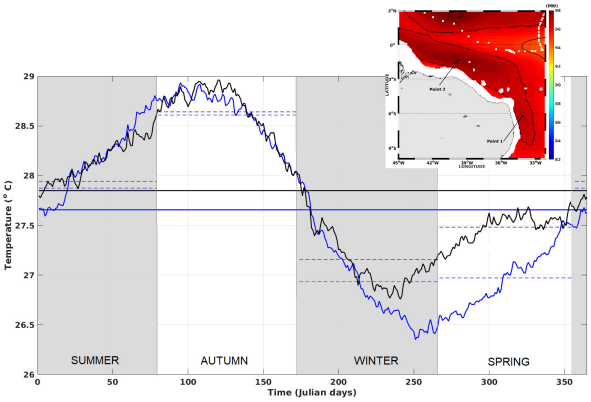

Figure 10: *Daily average Julian climatology of surface temperature to the points* 1 *(black) and* 2 *(blue), where the continuous line represents the annual average and the dotted line represents the seasons averages, represented by the contrast between shaded and non-shaded areas, highlighting the interval of the Julian days of the seasons of summer (357-079), autumn (*080 – 142*), winter (*143 – 265*) and spring (*266 – 356*). In the upper right corner the location of points 1 and 2 is shown to ease the reader.*

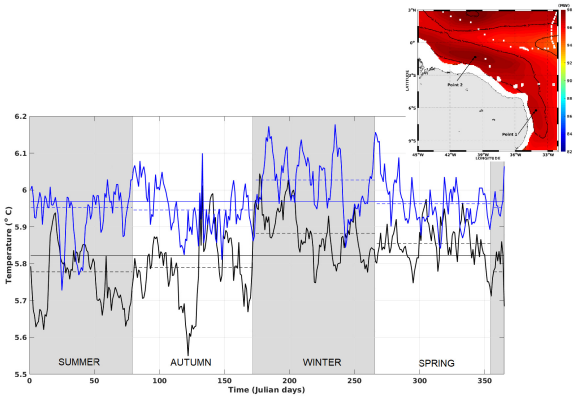

Figure 11: *Daily average Julian climatology at depth of* 600*m to the points* 1 *(black) and* 2 *(blue), where the continuous line represents the annual average and the dotted line represents the seasons averages, represented by the contrast between shaded and non-shaded areas, highlighting the interval of the Julian days of the seasons of summer (*357 – 079*), autumn (*080 – 142*), winter (*143 – 265*) and spring (*266 – 356*). In the upper right corner the location of points* 1 *and* 2 *is shown to ease the reader.*

continuous vertical gradient, when applied in the efficiency equation (Equation 1). We can notice a small influence of the seasonality, when realizing that in the summer the point 1 and in the spring the point 2, both move minimally in a positive way in relation to the annual average, making possible to say that they end up balancing the effect on the total average.

The behavior of the surface temperatures and in 600m, Figures 10 and 11, represent in a mirrored way the heat fluxes through evaporator, condenser and the efficiency behavior through

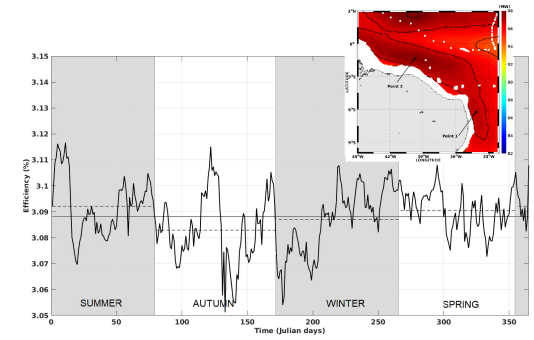

(a)

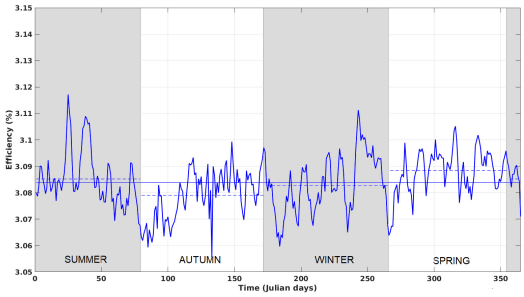

(b)

Figure 12: *Daily average Julian climatology of efficiency, between the surface and the depth of* 600*m, to the points* 1 *(black) a) and* 2 *(blue) b), where the continuous line represents the annual average and the dotted line represents the seasons averages, represented by the contrast between shaded and non-shaded areas, highlighting the interval of the Julian days of the seasons of summer (*357 – 079*), autumn (*080 – 142*), winter (*143 – 265*) and spring (*266 – 356*). In the upper right corner the location of points* 1 *and* 2 *is shown to ease the reader.*

equation 1. The heat flux and the efficiency with which it is converted, allows to glimpse the nominal power, Figure 13, through equations 18 and 19. In this way the prediction of a seasonality, coming from the signal of the surface temperature, control variable of the OTEC plant, for the winter and spring period, due to the latitudinal difference.

In quantitative terms we highlight the variability between points 1 and 2, of the anual average power of $94.96MW$ and $95.88MW$, that is, a difference of $0.92MW$. Thus, observing the averages by seasons, it is observed that during the summer ($95.50MW$ and $96.11MW$) and autumn ($97.21MW$ and 97.75) the differences are smaller than the annual average. However, in the winter (93.22 and 94.22) and mainly in spring (93.33 and 95.028), the values of the differences are higher than the annual average, that is, there will be the production of lower nominal values of electricity in point 1.

The latitudinal difference interferes directly in the seasons of winter and spring, forcing the annual average of point 1 to the lowest value. Thus, the direct relationship with the surface temperature behavior, in terms of its influence on the oscillation of the power signal, demonstrates that the positive fluctuation in this variable is a direct influence of the higher thermal energy

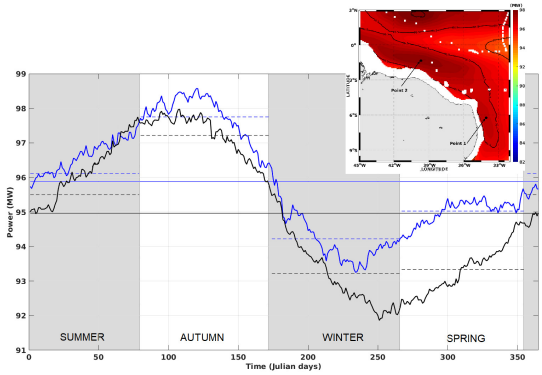

Figure 13: *Daily average Julian climatology of available nominal power, of the vertical thermal gradient between the surface and the depth, to the points* 1 *(black) and* 2 *(blue), where the continuous line represents the annual average and the dotted line represents the seasons averages, represented by the contrast between shaded and non-shaded areas, highlighting the interval of the Julian days of the seasons of summer (*357 – 079*), autumn (*080 – 142*), winter (*143 – 265*) and spring (*266 – 356*). In the upper right corner the location of points 1 and 2 is shown to ease the reader.*

content received by point 2, that is, its proximity to the equator, Intertropical Convergence Zone and consequently the zones with the higher incidence rates of solar radiation.

Based on the results obtained by the OEMT matrix for the IAE, it is verified that in the area of $371.617 Km^2$ the points 1 and 2 are inserted (Figure 8 a). From these points, we now obtain the time series of heat withdrawn from the oceans, Figure 14, thus verifying the variability of the anthropogenic effect and the closing of the obtained results.

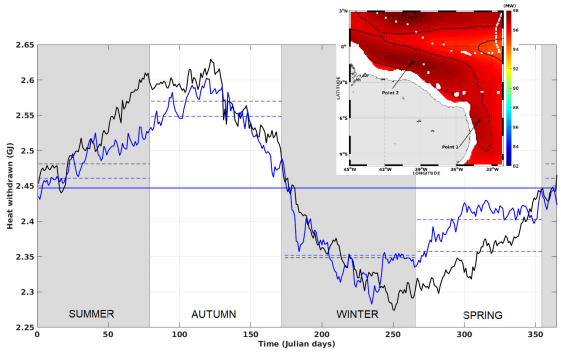

Figure 14: *Daily Julian climatology of the heat content withdrawn from the oceans, between the surface and the depth of* 600*m, to the points* 1 *(black) and* 2 *(blue), where the continuous line represents the annual average and the dotted line represents the seasons averages, represented by the contrast between shaded and non-shaded areas, highlighting the interval of the Julian days of the seasons of summer (*357 – 079*), autumn (*080 – 142*), winter (*143 – 265*) and spring (*266 – 356*). In the upper right corner the location of points* 1 *and* 2 *is shown to ease the reader.*

It can be seen that the annual average of the heat content withdrawn from the ocean is exactly equal to the value of $2.44 GJ$, thus demonstrating that the highest heat rates withdrawn in the

seasons of summer and autumn at point 1 are fully compensated, when the seasonal influence on it, in the spring, leads to significant losses.

It is concluded that due to the behavior shown for both points, related to OEMT input and output parameters, they have very close values to the installed theoretical capacity, $100MW$, of electricity production. It must be evidenced that the gradients mentioned in this subsection refer to those between the surface and 600m of depth.

Both points represent the second largest area within the OTEP ($371.617Km^2$), close to the continental shelf and the coast, and capable to withdraw large amounts of heat and CO_2 from the ocean. We emphasize both as fully qualified to perform the IAE, to generate electricity and to obtain other byproducts not deepened in this study.

7. Conclusion

An OTEC plant generates electricity from vertical thermal gradients present in the ocean water column. The installation of such plants is conditioned to the presence of a vertical gradient of at least 20^0C and that the maximum depth for the establishment of this gradient does not exceed $1000m$. The present study proposed to test the viability of the conditions imposed by the literature for an OTEC plant to operate in the Brazilian territorial sea (BA). The obtained results demonstrate the tecnical viability of operation of this type of plant along a vast region, here called the Ocean Thermal Energy Park, where the high heat content and converted electric energy are highlighted.

The region of sovereignty of the thermal resources of the Brazilian ocean called OTEP, where there is the viability of operating OTEC plants, in its offshore version, in the molds of adapted petroleum platforms, and inshore, verifying the possibility of interacting with the archipelagos of Fernando de Noronha and São Pedro and São Paulo, in order to collect information on the variables of the plant in places with open sea characteristics. The OTEP has a total coverage area of $1.893.216km^2$ and potential for the operation of up to 376 OTEC plants, each with a damping radius of thermal and dynamic effects of $40km$ or an area of $5.026Km^2$.

Around the oceanic islands of the northeast coast, in the section between MA and RN, is the region with the highest power contents possible to implement OTEC plants, where its extension is distributed by the main states and cities in the northeast, Fortaleza (CE), Natal (RN), João Pessoa (PB) and Recife (PE), with the second largest coverage area, $371.617Km^2$, within the OTEP and delimited by the largest power isoline $96.5MW$, and and capable of generating of 7.141 GW or $62.555TWh$. In addition, in this region the narrowing of the northeast portion of the Brazilian continental shelf allows the lowest possible distance between the point of implementation of the plant and the coastline in the area of study. This leads to a significant drop in the costs about sending energy for the continent, as well as facilitating the transport of technicians to the operation and maintenance of the plant. Thus, this is the prominent area for the installation of OTEC plants, in small scale, for the analysis of oceanographic parameters of the OTEP.

We found that the operation of 101 OTEC plants, underestimated, would be sufficient to meet the energy demand of the northeast region, with $9.14GW$ of instantaneous nominal power of consumption. In addition, about the economic issue, using water collection piping deeper than $600m$ would not be necessary, since the power produced by the a OTEC plant has a derisory gain, approximately 1%, when the pipe advances to larger depths.

The OTEC technology attenuates human anthropic action in relation to ocean warming and CO_2 withdrawal from the atmosphere, through artificial resurgence. At OTEP, the maximum

capacity, 376 plants in operation to generate renewable energy at a nominal power is 34.028GW or 298.085TWh, withdraw 0.97TJ/s of ocean heat and 21.5 g/s or 681 $ton/year$ of atmospheric CO_2.

The OTEC plant provides a range of byproducts from its two cycles (Claude and Rankine) or hybrid, where the most known and important are potable water, sea salt, animal and vegetable protein (mariculture), the conditioning of temperature, clean electric energy, and the possibility, realizthe IAE through the withdrawal of heat of the oceans and CO_2 of the atmosphere, to realize the IAE. We also emphasize that, although they are not included in the present study, the inherent impacts of any engineering structure operating on an oceanic region have to be taken into account, such as changes in the local environment, where several oceanic species inhabit, due to thermodynamic changes in the system.

The analysis of the time series of production testifies the viability and stability of the operation OTEC plants, installed in OTEP, throughout the Julian calendar. This fact demonstrates the level of reliability that renewable energies need to provide for the safety of a firm and convinced step of tecnical operation, energy and environmental viability (IAE).

8. Acknowledgements

The authors thank the Federal University of Rio Grande - FURG, and Conselho Nacional de Desenvolvimento Cientifico e Tecnologico (CNPq), for their support and financial aid. We thank CNPq for the research grants Process 88882.182313/2018-01 (RVS) and 308274/2011-3 (EHLF).

9. References

[1] Ascari, M. B., Hanson, H. P., Rauchenstein, L., Van Zwieten, J., Bharathan, D., Heimiller, D., Langle, N., Scott, G. N., Potemra, J., Nagurny, N. J., et al., 2012. Ocean thermal extractable energy visualization-final technical report on award de-ee0002664. october 28, 2012. Tech. rep., Lockheed Martin Mission Systems and Sensors.

[2] Ascari, M. B., Hanson, H. P., Rauchenstein, L., Van Zwieten, J., Bharathan, D., Heimiller, D., Langle, N., Scott, G. N., Potemra, J., Nagurny, N. J., et al., 2012. Ocean thermal extractable energy visualization-final technical report on award de-ee0002664. october 28, 2012. Tech. rep., Lockheed Martin Mission Systems and Sensors.

[3] Avery, W. H., Berl, W. G., 1997. Solar energy from the tropical oceans. Issues in Science and Technology 14 (2), 41–44.

[4] Avery, W. H., Wu, C., 1994. Renewable energy from the ocean: a guide to OTEC. Oxford University Press.

[5] Bagni, M., 2005. Fao fisheries & aquaculture-cultured aquatic species information programme—dicentrarchus labrax (linnaeus, 1758). FAO Fisheries and Aquaculture Department [online].

[6] Cirano, M., Mata, M. M., Campos, E. J., Deiró, N. F., 2006. A circulação oceânica de larga-escala na região oeste do atlântico sul com base no modelo de circulação global occam. Revista Brasileira de Geofísica 24 (2), 209–230.

[7] Claude, G., 1930. Power from the tropical seas. Mechanical Engineering 52 (12), 1039–1044.

[8] Company, E. R., 2017. National energy balance 2017: Base year 2016. Rio de Janeiro: EPE.

[9] D'Arsonval, J.-A., 1881. Utilization des forces naturelles, avenir de l'electricite. Le Revenue Scientifique 17, 370–372.

[10] Johnson, F., 1992. Closed-cycle ocean thermal energy conversion (otec). Ocean Energy Recovery, 70–108.

[11] Kobayashi, H., 2002. "water" from the ocean with otec. In: Forum on Desalinatio n using Renewable Energy.

[12] MacKenzie, J. J., Avery, W. H., 1996. Ammonia fuel: the key to hydrogen-based transportation. Tech. rep., Inst. of Electrical and Electronics Engineers, Piscataway, NJ (United States).

[13] Meisen, P., Loiseau, A., 2009. Ocean energy technologies for renewable energy generation. Global Energy Network Institute.

[14] Neshyba, S., 1987. Oceanography: Perspectives on a fluid earth.

[15] Nihous, G., 1989. Conceptual design of a small open-cycle otec plant for the production of electricity and fresh water in a pacific island. In: Proc. of Int. Conf. on Ocean Energy Recovery.

[16] Oschlies, A., Pahlow, M., Yool, A., Matear, R. J., 2010. Climate engineering by artificial ocean upwelling: Channelling the sorcerer's apprentice. Geophysical Research Letters 37 (4).
[17] Roels, O., 1980. From the deep-sea-food, energy, and fresh-water. Mechanical Engineering 102 (6), 36–43.
[18] Sharqawy, M. H., Lienhard, J. H., Zubair, S. M., 2010. Thermophysical properties of seawater: a review of existing correlations and data. Desalination and water treatment 16 (1-3), 354–380.
[19] Skinner, B. J., Turekian, K. K., 1988. The man and the ocean. São Paulo, Editora Edgard Blücher Ltda.
[20] Stramma, L., England, M., 1999. On the water masses and mean circulation of the south atlantic ocean. Journal of Geophysical Research: Oceans 104 (C9), 20863–20883.
[21] Takahashi, P., 2004. Energy from the Sea: The Potential and Realities of Ocean Thermal Energy Conversion (OTEC). UNESCO.
[22] Takahashi, T., Sutherland, S. C., Wanninkhof, R., Sweeney, C., Feely, R. A., Chipman, D. W., Hales, B., Friederich, G., Chavez, F., Sabine, C., et al., 2009. Climatological mean and decadal change in surface ocean pco2, and net sea–air co2 flux over the global oceans. Deep Sea Research Part II: Topical Studies in Oceanography 56 (8-10), 554–577.
[23] Thurman, H., Trujillo, A., 2004. Introductory oceanography, (upper saddle river).
[24] Valente, R. d. S., Fernandes, E. H., Azevedo, J. L. L., Corrêa, R. M., 2019. No prelo. Thermal energy sites in the south atlantic ocean: The potential of the brazilian blue amazon. Renewable energy.
[25] Vega, L., et al., 1999. Ocean thermal energy conversion (otec). OTEC News-Clean Energy, Water and Food.
[26] Walsh, J., 1981. Potential environmental consequences of ocean thermal energy conversion (otec) plants. a workshop. Tech. rep., Brookhaven National Lab., Upton, NY (USA).
[27] Wright, J., 1995. Seawater: its composition, properties, and behaviour. Vol. 2. Pergamon.

V.**Capítulo:** Síntese da Discussão e Conclusões

V.I Síntese das Discussões

Os resultados obtidos nos dois manuscritos são totalmente dependentes entre si, ou seja, as informações obtidas no primeiro viabilizam a metodologia do segundo e seus resultados e informações. Desta forma, vamos apresentar sua síntese de maneira sequencial, destacando os principais aspectos e conectando suas conclusões.

No manuscrito I, a partir dos resultados climatológicos das temperaturas médias mensais, sazonais e anual, foram obtidos os mapas de gradiente térmico, tais valores permitiram verificar a variabilidade dos ciclos. Foram

selecionados os gradientes térmicos entra a superfície e a profundidade de 1000 m, pois esta representa a tubulação mais profunda da captação da água fria no Sistema OTEC.

Os resultados mostraram que os campos médios julianos dos gradientes térmicos têm variabilidade temporal e espacial, diferenciada para as regiões equatorial e sudeste-sul do Oceano Atlântico Sul. Os resultados estabelecem uma relação direta com os limites impostos pela teoria, onde foram observadas as temperaturas ao longo da coluna de água, além das ferramentas de análise responsáveis por indicar a manutenção e configuração do reservatório oceânico de energia térmica.

Foram selecionados os filtros julianos para os ciclos, em ordem metodológica, mensal, sazonal, anual e diária. De forma a poder identificar os sítios de viabilidade em termos de gradiente e logo após aplicar a variabilidade diária no intuito de verificar a manutenção desta viabilidade ao longo dos dias e suas características solares.

Da observação dos ciclos mensal, sazonal e anual, foi verificado oito faixas de gradiente térmico superiores a 20^0C. Porém destes foi verificado, através da variabilidade diária que apenas três sítios são viáveis. Identificados pelas faixas médias anuais de gradiente térmico operacionais, 23.5^0C, 23^0C e 22.5^0C.

Observando cada um dos sítios individualmente, vemos que o de menor conteúdo térmico, 22.5^0C, e de menor cobertura na AA. Identificamos sua viabilidade de operação entre a superfície e os níveis de profundidade 900m <= z <= 1000m, ao longo de todo a série média anual. Sendo os de maiores

conteúdos térmicos operacionais ao longo de todo calendários, entre a superfície e os níveis de profundidade de 600m <= z <= 1000m.

Tendo em vista a operacionalidade de apenas três faixas dentre os oito analisados, fica evidente que existe uma relação direta entre as características do sítio e a faixa latitudinal que ele ocupa. De forma que os três sítios operacionais supracitados, ocupam as faixas de menores latitudes do domínio e com cobertura da AA em sua porção Sudeste (pequena faixa e de menor conteúdo térmico), Nordeste e Norte.

No manuscrito II, a partir dos resultados obtidos no I, vamos aplicar o Módulo de Energia OTEC Teórica (MEOT) nos sítios e em suas áreas de cobertura. Definimos então uma região, do extremo norte do litoral do Espírito Santo (ES) (latitude 19^0S) e praticamente todo litoral nordeste e a parcela norte até a metade dos Parque Nacional dos Lençóis Maranhenses (excluindo a região dos deltas dos rios Mearin e Amazonas, devido à dificuldade da coleta de água em superfície e fundo com alta concentração de sedimentos), intitulada pelo autor, no título desta seção, como Parque de Energia Renovável Térmica Oceânica (PERTO). Brasileira.

Porém antes de focar no PERTO, foi aplicado em grande parte do AS o MEOT, dando destaque para a faixa próxima ao equador e da Zona de Convergência Intertropical. Destacando de forma quantitativa, em termos de potência e eficiência respectivamente, os picos estão representados pelos valores de 96,5 até valores inferiores à 90,5MW e inferiores à 3,4%, sendo que estes máximos são encontrados em duas regiões, a primeira, encontra-se em

quase sua totalidade no Oceano AS, contida dentro da PERTO, nas adjacências da costa norte e nordeste. A segunda região encontra-se na costa oeste da África, abrangendo praticamente todo o litoral da Libéria onde chega aos valores de 100MW e 3,5 de eficiência.

Destacamos três regiões oceânicas de maior potência passíveis de implementação de uma planta OTEC, correlacionadas com maiores picos de eficiência (96,5MW e o intervalo entre 3.35% e 3.3%). Suas localizações geográficas cobrem, de maneira aproximada, a área de 371.617 Km^2, segunda em área e a maior da região de potência 96,5MW, que banham as proximidades do fim da PC, passando pelos estados do MA, PI, CE, RN, PB e uma parcela mais offshore da costa de PE.

A segunda região de 96.5MW, ao norte do arquipélago São Pedro e São Paulo, destacando sua eficiência de 3,25% e área de 131.456km^2. A terceira região de mesma potência possui área 74.123km^2, corresponde a porção mais offshore nos estados do MA e PI, esta área extrapola os limites legais da AA.

Assim como a eficiência a potência se distribui ao longo do PERTO, de forma que as taxas decrescem de forma radial em direção offshore. Podemos destacar zonas de potência com valor nominal entre 96,5MW à 95MW, com a maior área, aproximada, de 509.181 km^2, distribuída latitudinalmente nas adjacências da PC próxima a costa de AL e PE. Se estendendo pelos estados do SE, PB, RN, CE, PI e MA, mas nas porções mais offshore, exceto por uma pequena faixa que varre longitudinalmente o RN, CE, PI e MA onde está apresenta uma área de 54.777 km^2 com 95MW de potência.

A área de cobertura da PERTO é aproximadamente de 1.893.216 Km^2, ou seja, dividindo este valor pela área de amortecimento (valor máximo de raio do vórtice de água quente como 20Km, assumindo o dobro deste raio como uma zona de amortecimento dos efeitos térmicos e dinâmicos OTEC), o parque poderia operar 376 plantas OTEC.

Associando o número ao valor médio de potência entre 96.5MW a 95MW, na maior área cobertura (509.181 Km^2). Poderíamos aproximar a taxa, instantânea e aproximada, de uma capacidade nominal teoricamente disponível 9,67GW.

A capacidade da PERTOB de retirar quantidades de calor antropogênico inferiores a o 2.8GJ e superiores 2.6GJ Identificamos claramente que a região de máxima eficiência (3.35%) e potência (96.5MW), identificada nas Figuras 6 a) e b), coincide com a região de máxima retirada do EIA via calor. Sendo assim, localizado no sul do BA e norte do RN (entre 13.90^0S e 15.25^0S). Através da observação direta, verificamos que a retirada do EIA via calor decresce de forma radial em direção offshore, atingindo seus menores valores, entre as isolinhas de 2.65GJ e 2.60GJ, na região da NE.

Sabendo toda a área de cobertura da PERTO poderia operar 376 plantas OTEC em suas delimitações. Associando o número de possíveis plantas de operação pela menor isolinha de EIA (2.6GJ). Destacamos então que seu limite máximo a PERTO, em taxa instantânea e subestimada, pode retirar de conteúdo de calor no valor de aproximadamente 0.977TJ.

Tendo como base as informações apresentadas, supomos uma fazenda de

maricultura por planta OTEC, 376 fazendas. Sabendo que, um tanque de produção de salmão do atlântico, para produção de 100 espécies. Seria necessária uma vazão de renovação de água de fundo 1m^3/s para superfície no valor de $24m^2$ [FAO.2019]. Segundo Oschlies et al.[2010], é de 18 Pg/ano de absorção de co_2, para uma vazão de 26.4 sv (1sv = 10^6 m^3/s), em ressurgência., equivalente a quase metade da taxa de absorção de co_2 do oceano global [Takahashi et al., 2009], podemos estimar que temos a absorção em máxima operação da PERTO de 681Gg, ou 681 toneladas, de carbono em um ano.

Em uma planta OTEC, onde a tubulação de coleta de água de fundo (semi adiabáticas) são de alto custo e dificuldade de operação, que quase a totalidade do PERTO (excluindo uma pequena parte da região NE e a parcela do PERTO abaixo de 18^0S) podemos trabalhar com o gradiente térmico entre 0 e 600m e gerar valor de potência com percentuais de perda, em relação ao máximo gradiente entre 0 e 1000m, de aproximadamente 1%. Podemos obter aproximadamente as mesmas taxas, perda de 1%, para todos os parâmetros citados, com menor custo, melhoria da operação do sistema e menores perda devidos as bombas de vácuo.

V.II Síntese das Conclusões

As informações e tomadas de decisões, aqui apresentadas, tem como finalidade um afunilamento técnico e planejamento de todo aparato científico de operação de uma usina OTEC. Possibilitando a diminuição das tubulações semi-adiabáticas de transporte de água de fundo (menores profundidades),

perdas de capital com inúmeras campanhas oceanográficas em alto mar, tornando-os mais precisas e de maior impacto científico, se utilizando através de modelagem e de filtros de sinal juliano (pequena escala temporal), e principalmente alto nível de confiança da operação ser continua, principal dificuldade de investimento, ao longo da passagem dos dias, meses, estações e anos, ou seja, certeza de que o retorno do investimento acontecerá em uma escala de tempo menor.

Na AA, em quase na sua totalidade, os gradientes térmicos médios anuais são superiores ou iguais a 20^0C, onde foram identificadas isolinhas de gradiente térmico, sendo destas três totalmente operacionais ao longo de todo o período onde a média juliana diária foi processada. Nestes três locais ainda foi constatado que duas faixas, possuem operacionalidade do gradiente entre a superfície e a faixa de 600m<=z=<1000 m de profundidade, e a faixa menor entre a superfície e 900m<= z =<1000m. Demonstrando três estruturas térmicas verticais de alto valor energético e comercial.

O planeta e sociedade, juntos como ecossistema vivo devem abandonar comportamentos de uma revolução industrial que não atende nossas necessidades atuais;

A tecnologia OTEC fornece um aparato de subprodutos, oriundos dos seus dois ciclos (Claude e Rankine), água potável, sal marinho, proteína animal e vegetal (maricultura), condicionamento de temperatura para as plantas offshore e onshore, energia elétrica limpa e a possibilidade de viabilizar o EIA, retirada de calor dos oceanos e CO_2 da atmosfera;

Foi definida neste trabalho uma região de soberania dos recursos térmicos do oceano denominada de PERTO, onde corrobora uma tentativa da Marinha do Brasil junto a Organizações das Nações Unidas, via direito Marítimo de agregar uma região além das 200 m.n, demonstrando a importância e valor energético que o Brasil pode explorar.

Dentro dos domínios do PERTO, existe a viabilidade de operação de plantas OTEC, em sua versão offshore, nos moldes de plataformas de petróleo adaptadas ao conceito OTEC, e inshore, verificando a possibilidade de interagir com os arquipélagos de Fernando de Noronha e de São Paulo e São Pedro, de forma a coletar informações sobre as variáveis da planta OTEC em locais com características de mar aberto;

O PERTO tem uma área total de cobertura de 1.893.216 km^2 e potencial para operação de até 376 plantas OTEC, sendo cada uma com um raio de amortecimento, dos efeitos térmicos e dinâmicos, de 40 Km ou uma área radial no entorno da planta de 5.026 Km^2.

É importante destacar a região com maior potencial para implantação de sistemas OTEC, dentro do OTEP, correlacionada com picos de maior eficiência (96; 5MW eentre 3; 35% e 3; 3%). A região tem uma área de cobertura aproximada de 371: 617km2, que banha todo o contorno da plataforma continental em sua parcela mais curta, passando pelos estados de MA, PI, CE, RN, PB e PE, podendo operar 74 usinas OTEC e com capacidade total, subestimada, de um rede instantânea disponível de 7: 141 GW ou 62:555 TWh.

O estreitamento da porção nordeste da plataforma continental Brasileira, de modo com a menor distância possível entre o ponto de implantação da usina e a linha de costa na área em estudo. Diminui os custos com o envio de energia para o continente, além de facilitar o transporte dos técnicos para a operação e manutenção da usina. Desta maneira, essa área é a mais com maior destaque propícia para implantação de sistemas OTEC pilotos.

Sabendo que a operação de 101 plantas OTEC, de forma subestimada, seriam suficientes para atender a demanda energética da região do Nordeste com 9,14GW de potência nominal instantânea de consumo ou 80.147GWh de energia.

A tecnologia OTEC na PERTO, em sua capacidade máxima subestimada, é capaz de gerar energia renovável numa potência nominal por segundo 34.028GW ou 298.08TWh, retirar no mesmo intervalo de tempo 0,977TJ de calor do oceano e converter 681 toneladas de co_2 atmosférico por ano.

Não vale a pena, no que se refere ao viés econômico, usar tubulação de coleta de água mais profunda que 600m apontada neste estudo, uma vez que os parâmetros de saída da planta OTEC tem um ganha irrisório, menos de 1% quando a tubulação avança para maiores profundidades.

Sendo as séries temporais de produção, demonstrativos da viabilidade e estabilidade ao longo de todo o calendário juliano. De forma que o nível de confiabilidade que as energias renováveis precisam oferecer, para a segurança de passo firme e convicto da viabilidade financeira, energética, ambiental (EIA)

e de estarmos na linha do tempo de nossa evolução e responsáveis pela vida que nos circunda em todos os aspectos.

VI. **Capítulo:** Limitações do Estudo e Sugestões para Trabalhos Futuros

Ao finalizar este estudo, percebemos as limitaçoes dos resultados obtidos, que várias análises podem ser realizadas e que outras formas de viabilidades devem ser exploradas para trabalhos futuros. A seguir constam algumas limitações do estudo e sugestões para trabalhos futuros que devem ser ressaltadas.

VI.I Limitações do Estudo

O estudo indica a viabilidade de operação de usinas OTEC, dentro dos limites da Amazônia Azul, indicando os gradientes térmicos verticais e sua conversão em energia elétrica e outros parâmetros de funcionamento, via módulo de energia teórica OTEC. Entretanto, a viabilidade não depende apenas de capacidade operacional, único foco deste estudo, dependendo de fatores econômicos de sua implementação e operação, além do impacto inerente ao seu funcionamento. Ressaltando que a operação de uma usina OTEC gera impactos térmicos e dinâmicos nos extratos oceânicos, verticais e horizontais, podendo afetar o ecossistema natural e as características genuínas do local.

Neste estudo são utilizados dados do modelo HYCOM que possui uma

grade de resolução horizontal de 1/12º, ou seja, sua flutuabilidade é de aproximadamente de 9km. Isto acarreta incertezas nas coordenadas geográficas obtidas, de forma que a confirmação das posições e dos gradientes térmicos verticais destes locais necessitaria de comparativo com dados de campo para sua validação, apesar do modelo ser de alta confiabilidade na comunidade científica.

Os dados utilizados no estudo, foram mediados para variabilidade diária via climatologia juliana, aplicada aos 20 anos de dados de 3 em 3h. O parâmetro principal utilizado no estudo é a temperatura, superficial e ao longo da distribuição vertical, destacando que sua variabilidade pode apresentar fenômenos em escala temporal no contemplada nos dados ou filtrada pelo processamento da climatologia.

VI.II Sugestões Trabalhos Futuros

Construir um modelo teórico de viabilidade econômica, estabelecendo os custos dos aparatos operacionais e de suas performances técnicas, estimando o custo de instalação, operação e transmissão dos recursos obtidos, ao longo de todo o OTEP.

Identificar, via modelo teórico de impacto, os padrões hidrodinâmicos e termodinâmicos do oceano no entorno do ponto a ser aplicado a usina OTEC, com e sem a presença da mesma, com finalidade de verificar as alterações pertinentes ao ecossistema marinho local. Associando os parâmetros obtidos, com as alterações biológicas passiveis aos organismos originários do bioma marinho.

Utilizar uma fonte de dados com alta resolução especial e temporal, permitindo uma analise mais fiel do real comportamento das variáveis e dos fenômenos de pequena escala de tempo. Além disso, a realização de campanhas oceanográficas de validação dos resultados obtidos, com o objetivo de aumentar a confiabilidade dos resultados.

Atualizar o modulo oceânico teórico OTEC, para as versão de ciclos termodinâmicos mais atuais, incluindo um ciclo hibrido onde operem os dois ciclos simultaneamente, fechado e aberto. Com a finalidade de obter percentuais maiores de eficiência e potencia, além de mensurar os inúmeros subprodutos inerentes a operação de uma usina OTEC.

Analise do gradiente térmico vertical nas regiões próximas ao talude da plataforma continental, local de possível ressurgência em baixa profundidade devido a topografia, possibilitando a indicação dos melhores locais para os teste de protótipos e de uma futura usina piloto, ou seja, locais mais próximos da costa, com tubulações de coleta água fria menos profundas e com menores consumo do sistema de bombas (menores perdas de energia).

VII. **Capítulo:** Referências Bibliográficas

VII.I - Referências Tese

Ascari, M. B., Hanson, H. P., Rauchenstein, L., Van Zwieten, J., Bharathan, D., Heimiller, D., Jansen, E. *Ocean Thermal Extractable Energy Visualization-Final Technical Report on Award DE-EE0002664. October 28,(2012*),(No. DOE/EE0002664-1)., Lockheed Martin Mission Systems and Sensors.

Armines, Edited Thierry Ranchin, Centre for Energy and Processes., (2006), CRNS Ecole des Mines de Paris.

Avery, W.H. and Wu, C. Renewable energy from the ocean: a guide to OTEC, (1994), Oxford: Oxford University Press, 450p.

Béguery, M. A exploração dos oceanos: a economia do futuro., (1979), São Paulo: DIFEL/ Difusão Editorial S.A. 137p.

Beavis, A.; Charlie , R. C. and Meye, C. De. On-shore siting of OTEC plants, In: OCEANS, (1986), Whasington DC Institute of Electrical and Electronics Engineers (IEEE)., IEEE publications, vol 18, p.174 - 179.

Bharathan, D., Staging Rankine cycles using ammonia for OTEC power production, (2011), National Renewable Energy Laboratory., Technical Report NREL/TP-5500-49121.

Brow E. Seawater: its composition properties and behavior. (1995) 2.ed. Oxford: Pergmon Press, (Série The Oceanography Course Team). 168p.

Castro, B. D., Lorenzzetti, J. A., Silveira, I. D., & Miranda, L. D. Estrutura termohalina e circulação na região entre o Cabo de São Tomé (RJ) e o Chuí (RS). (2006)., *O ambiente oceanográfico da plataforma continental e do talude na região sudeste-sul do Brasil. EDUSP, São Paulo*, 11-120.

Cirano, M., Mata, M. M., Campos, E. J., Deiró, N. F. A circulação oceânica de larga-escala na região oeste do Atlântico Sul com base no modelo de circulação global OCCAM., (2006.), *Revista Brasileira de Geofísica*, *24*(2), 209-230,

Claude. G., “Power from Tropical Seas”, (1930), Mechanical Engineering. Vol. 52, No. 12, pp, 1039-1044.

Clausius, R. Über die bewegende Kraft der Wärme und die Gesetze, welche sich daraus für die Wärmelehre selbst ableiten lassen., (1850), *Annalen der Physik*,*155*(3), p368-397.

Cheng, L., Abraham, J., Hausfather, Z., & Trenberth, K. E. How fast are the oceans warming?. (2019). *Science*, vol *363*(6423), p128-129.

Crews, R. "OTEC sites."., (1997), *Aquarius Rising Maldives-An Ocean Research Centre and Eco-tourist Facility,* 28p.

Castell, J. P., and Krug, L. C., (2015), *Introdução às ciências do mar*. Editora Textos., Captulo 5 – Propriedades Físicas da agua do mar., Osmar Olinto Möller Jr. e Carla Rosana de Castro Aseff .

Christopherson, R. W., Byrne, M. L., and Aitken, A. E., *Geosystems: an introduction to physical geography,* (2009), Upper Saddle River, New Jersey: Pearson/Prentice Hall

Da Rosa, A. V., Fundamentals of renewable energy processes., (2012), Academic Press.

D'Arsonval. A; "Utilization des forces naturelles, ivenirde l'electricire., (1881), Revue, Vol 17, 372p.

De Souza, A.G.Q, Estrutura e variabilidade das águas modais na termoclina do oceano Atlântico Sul, (2015), Dissertação (Mestrado), Instituto de Oceanografia, Universidade Federal do Rio Grande, Rio Grande:, FURG.

FAO, Food and Agriculture Organization of the United Nations (FAO), (2019) available in http://www.fao.org/fishery/culturedspecies/Salmo_salar/en.

Friedrich,H.B., and Krause,P.F.Internal vibrational mode sand hydrogen bonding in mixed crystals of HCN and DCN., (1973), The Journal of Chemical Physics, 59(9), 49424948.

Fröhlich, C. and Lean, L. "The Sun's total irradiance: Cycles, trends and related climate change uncertainties since 1976, (1998), *Geophysical Research Letters, vol* 25.23,p 4377-4380.

Iqbal, M., *Introduction to Solar radiation.*, (1983), Academic press, Londres, Reino Unido.

Kennett, J. P. Paleo-oceanography: Global ocean evolution., (1983), *Reviews of Geophysics*, vol *21* (5), p 1258-1274.

Luiou, K.N., An introduction to atmospheric radiation., (2002), Elsevier.

Stocker, T. F., Qin, D., Plattner, G. K., Tignor, M., Allen, S. K., Boschung, J., and Midgley, P. M. Climate change , (2013), The physical science basis.

Meisen, P.L.A. Ocean energy technologies for renewable energy generation., (2009), Global Energy Network Institute.

Mémery, L., M. Arhan, X. A. Alvarez-Salgado, M. J. Messias, H. Mercier, C. G. CastroandA.F.Rios. The water masses along the western boundary of the south and equatorial Atlantic., (2000.), Progress in Oceanography, 47, 69-98.

Neshiba,S., Oceanography: perspectives on fluid Earth., (1989) - New York, John Wiley and Sons, Inc.

Rau, G.H.; Baird, J.R. Negative-CO2-emissions ocean thermal energy conversion. (2018), Renewable and Sustainable Energy Reviews, v. 95, p. 265-272.

Sears, M. and Merriman, D. (Ed.) .Oceanography: ThePast., (1980), Springer-Verlag. New York, 812p.

Skinner, B.J.; Tukerian, K.K. Man and the ocean, (1988), Foundations of earth sciences series, Publish by Prentice hall

Stramma, L., and England, M. On the water masses and mean circulation of the South Atlantic., (1999), Ocean *Journal of Geophysical Research: Oceans*,v*104*(C9),p 20863-20883.

Silva, P. C. M. in: Oceanografia Física: O sol e o mar, (1975), Instituto de Estudos do Mar Almirante Paulo Moreira (IEAPM), Marinha do Brasil, Brasilia.

Silva, P. C. M. in: Usos do Mar, (1978), Instituto de Estudos do Mar Almirante Paulo Moreira (IEAPM), Marinha do Brasil, Brasilia.

Silva, A. C, An analysis of water properties in the western tropical Atlantic using observed data and numeric model results.(2006) 135 f. Tese (Doutorado em Oceanografia) – Centro de Tecnologia e Geociências, Universidade Federal de Pernambuco, Recife.

Sverdrup, H. U., M. W. Johnson, and R. H. Fleming, (1942). The oceans: Their physics, chemistry, and general biology. Englewood Cliffs, N.J.: Prentice-Hall.

Takahashi T, Sutherland SC, Wanninkhof R, Sweeney C, Feely RA, Chipman DW, Hales B, Friederich G, Chavez F, Sabine C, Watson A, Bakker DCE, Schuster U, Metzl N, Yoshikawa-Inoue H, Ishii M, Midorikawa T, Nojiri Y, Körtzinger A, Steinhoff T, Hoppema M, Olafsson J, Arnarson TS, Tilbrook B, Johannessen T, Olsen A, Bellerby R, Wong CS, Delille B, Bates NR, de Baar HJW. Climatological mean and decadal change in surface ocean pCO2, and net sea–air CO2 flux over the global oceans., (2009), Deep-Sea Res. II; v56,p554–777.

Thomson, W. T., and Trent, H. M. Laplace Transformation. *American.* (1951). *Journal of Physics*, v*19*, p 391-392.

Thurman, H.V.; Trujillo, A.P. Introductory ocenography., (2004), New Jersey: Pearson Prentice Hall, 10 ed, 608p.

Twidell, J. and Weir, T., Renewable energy resources., (2015), Routledge.

Thurman, H. V. Essentials of Oceanography. (1986) Merrill Publishing Company, Columbus, 370p.

Valente, R. S and Marques, W. C., Energy budget of the thermal gradient in the Southern Brazilian continental shelf, (2016), Renewable Energy, v91, p531–539.

Vega, L.A. Ocean Thermal Energy Conversion (OTEC), (1999),Technical report, University of Hawaii, Hawaii, USA.